



Search for a light CP-odd Higgs boson decaying into a pair of τ -leptons in proton–proton collisions at $\sqrt{s} = 13$ TeV with the ATLAS detector

The ATLAS Collaboration

This paper reports a search for a light CP-odd scalar resonance with a mass of 20 GeV to 90 GeV in 13 TeV proton–proton collision data with an integrated luminosity of 140 fb^{-1} collected with the ATLAS detector at the Large Hadron Collider. The analysis assumes the resonance is produced via gluon–gluon fusion and decays exclusively into a $\tau^+\tau^-$ pair which decays into a fully leptonic $\mu^+\nu_\mu\bar{\nu}_\tau e^-\bar{\nu}_e\nu_\tau$ or $e^+\nu_e\bar{\nu}_\tau\mu^-\bar{\nu}_\mu\nu_\tau$ final state. No significant excess of events above the predicted Standard Model background is observed. The results are interpreted within a flavour-aligned two-Higgs-doublet model, and a model-independent cross-section interpretation is also given. Upper limits at 95% confidence level between 3.0 pb and 68 pb are set on the cross-section for producing a CP-odd Higgs boson that decays into a $\tau^+\tau^-$ pair.

Contents

1	Introduction	2
2	ATLAS detector	4
3	Data and simulated event samples	5
3.1	Selection of data events	5
3.2	Monte Carlo event simulation	5
4	Event reconstruction	7
5	Signal selection	7
6	Background estimation	9
6.1	Background with prompt leptons	9
6.2	Background with non-prompt leptons	10
6.3	Event yields	12
7	Systematic uncertainties	13
7.1	Experimental uncertainties	13
7.2	Theoretical uncertainties	15
8	Statistical model and results	18
9	Conclusion	23

1 Introduction

The discovery of a Higgs boson [1, 2] at the Large Hadron Collider (LHC) [3] has provided important insight into the mechanism of electroweak symmetry breaking. Experimental studies of the Higgs boson [4, 5] demonstrate consistency with Standard Model (SM) predictions. However, the discovered particle could still be part of an extended scalar sector motivated by several theoretical arguments [6, 7]. One such extension of the SM is the flavour-aligned two-Higgs-doublet model (2HDM), which introduces a second SU(2) doublet [8]. The couplings of the two doublets to fermions are aligned in flavour space such that one doublet obtains Yukawa couplings like those in the SM, while the second has Yukawa couplings proportional to the former ones, which prevents flavour-changing neutral currents. The proportionality constants between the two diagonalised Yukawa matrices are the fermionic coupling parameters ζ_f . Within this model, five physical Higgs bosons arise, of which two are neutral and CP-even (h, H), one is neutral and CP-odd (A), and the remaining two are charged (H^\pm). The model thus incorporates a Higgs boson h with SM properties, while allowing the presence of an additional CP-odd A boson with a mass m_A smaller than the mass of the h boson. A search for a light CP-odd A boson hence provides further insights into the scalar sector and may shed light on its particle multiplicity.

Further interest in the search for a light A boson originates from the anomalous magnetic moment of the muon, a_μ , which has been a topic of discussion because of an observed discrepancy of up to 5σ between the experimental measurement and SM predictions [9–11]. While the theoretical situation is

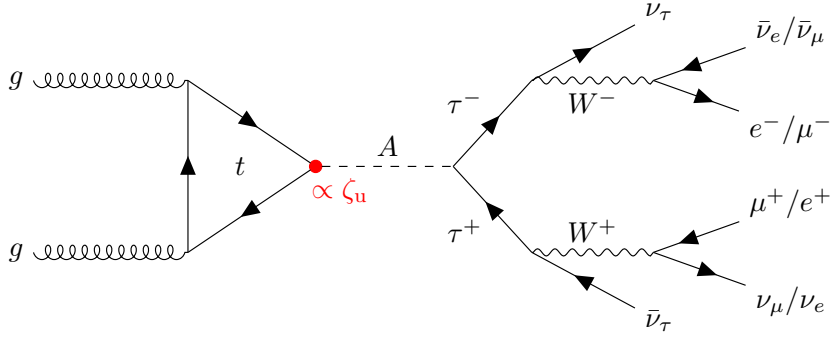


Figure 1: Leading-order Feynman diagrams of the processes $gg \rightarrow A \rightarrow \tau^+\tau^- \rightarrow \mu^+\nu_\mu\bar{\nu}_\tau e^-\bar{\nu}_e\nu_\tau$, $e^+\nu_e\bar{\nu}_\tau\mu^-\bar{\nu}_\mu\nu_\tau$ within the flavour-aligned 2HDM with large A boson couplings to τ -leptons and top quarks, and suppressed couplings to down-type quarks. The vertex in red describes the coupling of the A boson to up-type quarks and scales with ζ_u .

unclear due to contradictory calculations of the hadronic contributions [12–15], the apparent discrepancy motivates searches for physics beyond the SM. The flavour-aligned 2HDM predicts additional contributions to a_μ and can therefore significantly impact the level of agreement with experimental measurements [9, 16]. In particular, fermionic two-loop contributions of the Barr–Zee type [17] involving τ -lepton and top-quark loops coupling to Higgs bosons and to the external photon are important [18–22]. However, it was shown that near-maximal contributions may be required to explain the observed value of a_μ [16, 23]. For neutral and charged Higgs bosons with masses $m_H = m_{H^\pm}$ in the range of 150 GeV to 250 GeV, the a_μ contributions are maximised if the CP-odd Higgs boson A is light, with a mass between 5 GeV and 105 GeV. While loop contributions to a_μ involving the A boson are dominated by its large couplings to τ -leptons and top quarks, the A boson coupling to down-type quarks is suppressed [16, 23]. This motivates the search for CP-odd Higgs bosons A produced in proton–proton (pp) collisions at the LHC via gluon–gluon fusion involving a top-quark loop, with exclusive decay into a pair of τ -leptons: $gg \rightarrow A \rightarrow \tau^+\tau^-$. Within the flavour-aligned 2HDM, subject to the constraints described above, the cross-section for this production process scales with the square of the up-type quark coupling parameter ζ_u . The current upper limit at 95% confidence level (CL) on $|\zeta_u|$ is 0.5 [16].

In the analysis presented here, A boson masses from 20 GeV to 90 GeV are considered. Previous searches for neutral Higgs bosons produced by gluon–gluon fusion in pp collisions and with decays into τ -lepton pairs were performed by the ATLAS and CMS collaborations and focused on m_A ranges above a starting value of 60 GeV to 100 GeV [24–28]. The mass range from 20 GeV to 60 GeV is thus explored here for the first time for this production and decay mode.

Since the τ -leptons have transverse momentum values of $p_T \approx m_A/2$, the final-state hadrons, electrons, and muons from the τ -lepton decays are in a transverse momentum range below $p_T \approx 45$ GeV. Because of the large background from QCD-induced processes in pp collisions, the trigger p_T thresholds for hadronically decaying τ -leptons are typically well above these values. Electron–muon dilepton triggers, however, apply lower p_T thresholds and are better suited for the light A boson search. Therefore, and also to suppress background from $Z \rightarrow e^+e^-$ and $Z \rightarrow \mu^+\mu^-$ decays, the analysis focuses on the fully leptonic signal process with exactly one electron and one muon in the final state, $gg \rightarrow A \rightarrow \tau^+\tau^- \rightarrow \mu^+\nu_\mu\bar{\nu}_\tau e^-\bar{\nu}_e\nu_\tau$ or $gg \rightarrow A \rightarrow \tau^+\tau^- \rightarrow e^+\nu_e\bar{\nu}_\tau\mu^-\bar{\nu}_\mu\nu_\tau$, as shown in Figure 1. These final states correspond to 6.2% of all possible $\tau^+\tau^-$ final states [29]. The CP-odd nature of the A boson and its decay kinematics are exploited to further reduce the background.

2 ATLAS detector

The ATLAS detector [30] at the LHC covers nearly the entire solid angle around the collision point.¹ It consists of an inner tracking detector surrounded by a thin superconducting solenoid, electromagnetic and hadronic calorimeters, and a muon spectrometer incorporating three large superconducting air-core toroidal magnets.

The inner-detector system (ID) is immersed in a 2 T axial magnetic field and provides charged-particle tracking in the range $|\eta| < 2.5$. The high-granularity silicon pixel detector covers the vertex region and typically provides four measurements per track, the first hit generally being in the insertable B-layer (IBL) installed before Run 2 [31, 32]. It is followed by the SemiConductor Tracker (SCT), which usually provides eight measurements per track. These silicon detectors are complemented by the transition radiation tracker (TRT), which enables radially extended track reconstruction up to $|\eta| = 2.0$. The TRT also provides electron identification information based on the fraction of hits (typically 30 in total) above a higher energy-deposit threshold corresponding to transition radiation.

The calorimeter system covers the pseudorapidity range $|\eta| < 4.9$. Within the region $|\eta| < 3.2$, electromagnetic calorimetry is provided by barrel and endcap high-granularity lead/liquid-argon (LAr) calorimeters, with an additional thin LAr presampler covering $|\eta| < 1.8$ to correct for energy loss in material upstream of the calorimeters. Hadronic calorimetry is provided by the steel/scintillator-tile calorimeter, segmented into three barrel structures within $|\eta| < 1.7$, and two copper/LAr hadronic endcap calorimeters. The solid angle coverage is completed with forward copper/LAr and tungsten/LAr calorimeter modules optimised for electromagnetic and hadronic energy measurements, respectively.

The muon spectrometer (MS) comprises separate trigger and high-precision tracking chambers measuring the deflection of muons in a magnetic field generated by the superconducting air-core toroidal magnets. The field integral of the toroids ranges between 2.0 and 6.0 T m across most of the detector. Three layers of precision chambers, each consisting of layers of monitored drift tubes, cover the region $|\eta| < 2.7$, complemented by cathode-strip chambers in the forward region, where the background is highest. The muon trigger system covers the range $|\eta| < 2.4$ with resistive-plate chambers in the barrel, and thin-gap chambers in the endcap regions.

The luminosity is measured mainly by the LUCID-2 [33] detector that records Cherenkov light produced in the quartz windows of photomultipliers located close to the beampipe.

Events are selected by the first-level trigger system implemented in custom hardware, followed by selections made by algorithms implemented in software in the high-level trigger [34]. The first-level trigger accepts events from the 40 MHz bunch crossings at a rate below 100 kHz, which the high-level trigger further reduces in order to record complete events to disk at about 1 kHz.

A software suite [35] is used in data simulation, in the reconstruction and analysis of real and simulated data, in detector operations, and in the trigger and data acquisition systems of the experiment.

¹ ATLAS uses a right-handed coordinate system with its origin at the nominal interaction point (IP) in the centre of the detector and the z -axis along the beam pipe. The x -axis points from the IP to the centre of the LHC ring, and the y -axis points upwards. Polar coordinates (r, ϕ) are used in the transverse plane, ϕ being the azimuthal angle around the z -axis. The pseudorapidity is defined in terms of the polar angle θ as $\eta = -\ln \tan(\theta/2)$ and is equal to the rapidity $y = \frac{1}{2} \ln \left(\frac{E+p_z}{E-p_z} \right)$ in the relativistic limit. Angular distance is measured in units of $\Delta R \equiv \sqrt{(\Delta y)^2 + (\Delta \phi)^2}$.

3 Data and simulated event samples

3.1 Selection of data events

The search presented in this paper uses the full pp collision dataset recorded by the ATLAS detector between 2015 and 2018 (Run 2), with the LHC operating at a centre-of-mass energy of $\sqrt{s} = 13$ TeV and a bunch spacing of 25 ns. In this period, the LHC delivered colliding beams with a peak instantaneous luminosity of $L = 2.1 \times 10^{34} \text{ cm}^{-2}\text{s}^{-1}$, achieved in 2018, and an average number of pp interactions per bunch crossing $\langle\mu\rangle$ of 13, 25, 38, and 36 for 2015, 2016, 2017, and 2018 data, respectively [36]. After applying beam, detector, and data-quality criteria the total integrated luminosity of the data is 140 fb^{-1} . The data were recorded using three partially overlapping electron–muon dilepton triggers [37, 38] that applied identification criteria based on shower shapes in the electromagnetic calorimeter. The first trigger required lepton transverse momenta of $p_{\text{T}}^e > 17 \text{ GeV}$ and $p_{\text{T}}^\mu > 14 \text{ GeV}$, while the other two triggers covered the lower p_{T} ranges, with either $p_{\text{T}}^e > 7 \text{ GeV}$ and $p_{\text{T}}^\mu > 24 \text{ GeV}$ or $p_{\text{T}}^e > 24 \text{ GeV}$ and $p_{\text{T}}^\mu > 8 \text{ GeV}$, respectively. These trigger requirements have an efficiency of 72% to 92%, depending on the final state and the dataset, for signal events passing the final signal-region selections.

3.2 Monte Carlo event simulation

All signal and background processes were modelled using Monte Carlo (MC) simulations, with the exception of backgrounds with fake or non-prompt leptons, which were estimated from data (see Section 6.2).

Each sample was passed through the full GEANT4 [39, 40] simulation of the ATLAS detector and reconstructed with the same software as used for data. The only exceptions are the signal samples, for which the fast simulation ATLFast-II [41] was used, where the GEANT4 simulation of calorimeter showers is replaced by a parameterised simulation. The gluon–gluon fusion signal-production process for this analysis, $gg \rightarrow A \rightarrow \tau^+\tau^-$, was simulated with PYTHIA 8.2 [42], using leading-order (LO) matrix elements (ME) for A bosons with masses of 20 GeV to 90 GeV in steps of 10 GeV, as well as for 25 GeV, 75 GeV and 85 GeV. Both τ -leptons were forced to decay leptonically. The parton shower, hadronisation, and underlying event were modelled with parameter values set according to the A14 tune and with the NNPDF2.3LO set of parton distribution functions (PDF) [43]. The signal’s production cross-section was calculated at N³LO with ggHiggs [44–55] version 4.0, setting the coupling parameter of the A boson to up-type quarks to $\cot\beta = \zeta_{\text{u}} = 1$, where $\cot\beta$ is the ratio of the vacuum expectation values of the two Higgs doublets and is used by ggHiggs to parameterise the fermionic coupling parameter. The cross-section values are shown in Table 1 for the relevant mass range.

The MC-simulated background processes considered in this analyses include those with vector bosons (diboson and V +jets, where $V = W, Z$), top quarks ($t\bar{t}$, s - and t -channel single-top, and associated production of a top quark and a W boson (tW)), and SM Higgs bosons, which are all modelled differently.

The V +jets processes were simulated with the SHERPA 2.2.1 [56] generator, with next-to-leading-order (NLO) MEs for up to two partons and LO MEs for up to four partons. The diboson background processes were simulated with NLO MEs for up to one parton and LO MEs for up to three partons, using the SHERPA 2.2.1 [56] or SHERPA 2.2.2 [56] generator, depending on the process. The top-quark-related backgrounds were modelled using the POWHEG BOX v2 [57–60] generator at NLO accuracy in QCD with the NNPDF3.0NLO PDF set [61]. Both the tW and s -channel single-top events were generated using the five-flavour scheme. However, a four-flavour scheme was used for t -channel single-top events. For the

Table 1: N³LO prediction of the cross-section for A boson production, $\sigma(pp \rightarrow A + X)$, via gluon–gluon fusion in the relevant mass range. Values were calculated with ggHiggs [44–55] version 4.0, setting the fermionic coupling strength parameters of the A boson to $\cot\beta = \zeta_u = \zeta_\ell = 1$. The product of the signal acceptance $\mathcal{A}_{\text{signal}}$ and efficiency $\varepsilon_{\text{signal}}$ is the fraction of events generated for gluon–gluon fusion production of the CP-odd Higgs boson A (which is forced to decay into a leptonically decaying $\tau^+\tau^-$ pair) that are reconstructed in the detector and accepted by the analysis event selection described in Section 5.

m_A [GeV]	20	25	30	40	50	60	70	75
$\sigma(pp \rightarrow A + X)$ [pb]	1854	1394	1090	722	514	385	299	266
$\mathcal{A}_{\text{signal}} \times \varepsilon_{\text{signal}}$ [%]	0.017	0.038	0.060	0.094	0.10	0.091	0.077	0.20

m_A [GeV]	80	85	90
$\sigma(pp \rightarrow A + X)$ [pb]	239	215	195
$\mathcal{A}_{\text{signal}} \times \varepsilon_{\text{signal}}$ [%]	0.20	0.19	0.18

$t\bar{t}$ sample, a value of $1.5 m_t$ was assigned to the resummation damping factor h_{damp} , which controls the matching of the POWHEG ME to the parton shower and thus effectively regulates the high- p_T radiation against which the $t\bar{t}$ system recoils.

In order to model the parton shower, hadronisation, and underlying event, the top-quark background events were interfaced to PYTHIA 8.230 with parameter values set according to the A14 tune [62], while the SHERPA parton shower [63], using the MEPS@NLO prescription [64–67] and the set of tuned parameters developed by the SHERPA authors, was applied to W/Z +jets and diboson background events. The NNPDF2.3LO PDF set was used for both types of background.

SM Higgs boson production was simulated using POWHEG BOX v2 [58–60, 68, 69], interfaced with PYTHIA 8 for parton showering and non-perturbative effects. The PDF4LHC15NLO PDF set [70] and the AZNLO tune [71] of PYTHIA 8 were used. SM Higgs boson production via gluon–gluon fusion and via vector-boson fusion was simulated at next-to-next-to-leading-order (NNLO) and NLO accuracy in QCD, respectively. The POWHEG prediction is accurate to NLO for Vh boson plus one-jet production. The loop-induced $gg \rightarrow Zh$ process was generated separately at LO. The normalisation of all SM Higgs boson samples accounts for the decay branching ratio calculated with HDECAY [72–74] and PROPHECY4F [75–77]. The MC prediction for SM Higgs boson production via gluon–gluon fusion was normalised to the cross-section calculated to N³LO in QCD with NLO electroweak (EW) corrections [51, 52, 54, 78–85], while that for production via vector-boson fusion was normalised to the cross-section calculated to approximate-NNLO in QCD with NLO EW corrections [86–88]. The MC predictions for $q\bar{q}/qg \rightarrow Vh$ and $gg \rightarrow Zh$ were normalised to the cross-section calculated to NNLO in QCD with NLO EW corrections or to NLO and next-to-leading-logarithm accuracy in QCD, respectively [89–95].

To model additional pp interactions in the same or neighbouring bunch crossings (pile-up), the hard-scattering events were overlaid with a set of minimum-bias interactions generated using PYTHIA 8.186 [96] and the NNPDF2.3LO PDF set with the A3 set of tuned parameters [97]. Finally, all simulated events are reweighted to match the instantaneous luminosity spectrum in data.

4 Event reconstruction

Charged-particle tracks measured in the ID are used to reconstruct interaction vertices [98], and the one with the highest sum of squared transverse momenta $\sum p_T^2$ of the associated tracks is selected as the primary vertex of the hard interaction.

Electrons are reconstructed from topological clusters of energy deposits in the electromagnetic calorimeter which are matched to a track reconstructed in the ID and are required to satisfy *Loose* identification and *Loose* isolation criteria [99], based on track and shower-shape discriminants.

Muons are reconstructed from signals in the muon spectrometer matched to tracks inside the ID. They are also required to satisfy *Loose* identification and *Loose* isolation criteria based on track information [100].

Jets are reconstructed from particle-flow objects [101] using the anti- k_t with radius parameter $R = 0.4$. This algorithm uses noise-suppressed positive-energy topological clusters in the calorimeter after subtracting energy deposits associated with primary-vertex-matched tracks and including the momenta of those tracks in the clustering instead, thereby improving the jet energy measurement. The jet energy scale is calibrated to the particle level using simulation and further corrected with in-situ methods [102]. Cleaning criteria are used to identify jets arising from non-collision backgrounds or noise in the calorimeters [103]. A dedicated jet-vertex-tagger algorithm [104] is used to remove jets within $|\eta| < 2.5$ that are identified as not being associated with the primary vertex of the hard interaction. Similarly, a dedicated algorithm is used to suppress such ‘pile-up’ jets, arising from additional softer pp interactions, in the forward region [105].

Jets containing b -hadrons are identified using the DL1r [106] b -tagging algorithm. A jet is classified as a b -tagged jet if the DL1r score is above a certain threshold, referred to as an ‘operating point’. In this analysis, the operating point is chosen to obtain an average expected efficiency of 85% for b -jet identification, as determined in simulated $t\bar{t}$ events.

Since the different physical objects are reconstructed independently, multiple objects may be reconstructed from the same detector signal, whereas a signal rarely has contributions from multiple objects. To achieve orthogonality, an overlap removal procedure is performed on objects with small angular separation ΔR to remove the object with lower signal purity. Muons are favoured over electrons if one lies within a $\Delta R = 0.2$ cone around the other, and leptons are favoured over jets if their angular separation is $\Delta R < 0.4$.

The missing transverse momentum \vec{p}_T^{miss} (with magnitude E_T^{miss}) is reconstructed as the negative vector sum of the transverse momenta of leptons, visible hadronic τ -lepton decay products ($\tau_{\text{had-vis}}$) [107], jets, and a ‘soft term’. The ‘soft term’ is calculated as the vector sum of the p_T of tracks matched to the primary vertex but not to reconstructed leptons, $\tau_{\text{had-vis}}$ candidates, or jets [108].

An advanced likelihood-based algorithm named the Missing Mass Calculator (MMC) [109, 110] is used to estimate the invariant mass, m_{MMC} , of the τ -lepton pair.

5 Signal selection

This analysis focuses on final states with exactly one electron and one muon with opposite charges and p_T greater than 10 GeV. Events are required to have been accepted by at least one of the electron–muon triggers that were active during the data-taking periods (see Section 3). The leptons firing the trigger must match the two reconstructed leptons with the highest p_T in the event. The matching is performed according

Table 2: Overview of the selection criteria for the most important regions: the low-mass and high-mass signal regions (SR), the top control region (TCR), the $Z \rightarrow \tau^+\tau^-$ control region (ZCR) and the fake-lepton validation region (FVR). For the final results of the analysis, *Medium* identification and *Tight* isolation criteria are used [99, 100]. For the fake-lepton background estimation, *Loose* criteria are used additionally.

	SR		TCR	ZCR	FVR
	Low-mass	High-mass			
$ \eta_e $	[0, 1.37] \cup [1.52, 2.47]		[0, 1.37] \cup [1.52, 2.47]		[0, 1.37] \cup [1.52, 2.47]
$ \eta_\mu $	[0, 2.7]		[0, 2.7]		[0, 2.7]
$ \eta_j $	[0, 4.5]		[0, 4.5]		[0, 4.5]
p_T^ℓ	> 10 GeV		> 10 GeV		> 10 GeV
p_T^j	> 20 GeV		> 20 GeV		> 20 GeV
E_T^{miss}	> 50 GeV	> 30 GeV	> 30 GeV	–	–
m_T^{tot}	< 45 GeV	< 65 GeV	< 65 GeV	< 65 GeV	< 65 GeV
$\Delta R_{\ell\ell}$	< 0.7	< 1.0	< 1.0	> 1.4	> 1.4
m_{MMC}	> 0 GeV	> 35 GeV & < 130 GeV	> 0 GeV	> 0 GeV	> 0 GeV
$q_e \times q_\mu$	–1	–1	–1	–1	1
$n_{b\text{-jets}}$	0	0	≥ 2	0	0

to the angular distance ΔR between the trigger signature and the reconstructed lepton, requiring $\Delta R < 0.07$ for electrons and $\Delta R < 0.1$ for muons. Furthermore, the selected electron or muon candidates are required to satisfy *Medium* identification and *Tight* or *Tight_VarRad* isolation criteria [99, 100], respectively, in order to increase the signal region’s purity in true reconstructed leptons. Additionally, events with leptons satisfying the *Loose* criteria are used in the fake-lepton estimation.

The signal region (SR) definition depends on the probed A mass value: masses from 20 to 75 GeV are examined in the low-mass SR, and masses from 75 to 90 GeV are examined in the high-mass SR. A common requirement for both SRs is that the number of b -tagged jets, $n_{b\text{-jets}}$, must be zero. This significantly reduces the background from top quarks. In order to optimise the signal sensitivity, the low-mass SR and the high-mass SR have individualised selection criteria for E_T^{miss} , the total transverse mass defined as $m_T^{\text{tot}} = \sqrt{(p_T^e + p_T^\mu + E_T^{\text{miss}})^2 - (\vec{p}_T^e + \vec{p}_T^\mu + \vec{p}_T^{\text{miss}})^2}$, the angular distance between the charged leptons $\Delta R_{\ell\ell}$, and m_{MMC} . The selection criteria are summarised in Table 2. The m_T^{tot} criterion primarily removes diboson events and events with top quarks. The requirement on $\Delta R_{\ell\ell}$ reduces the $Z \rightarrow \tau^+\tau^-$ background, motivated by the mass, spin and CP properties of the A boson signal, and requires the emitted leptons to have a small angular separation. This kinematic configuration also enhances the fraction of A bosons produced with sizeable transverse momentum p_T^A . Thus, the p_T^A distribution starts at approximately 100 to 200 GeV, depending on the mass hypothesis. Therefore, hadronic jets are emitted in the opposite direction to conserve transverse momentum, meaning the process $pp \rightarrow A + \text{jets}$ is preferred for this topology (considering only the gluon–gluon fusion production mode as suggested by the flavour-aligned 2HDM).

6 Background estimation

There are two primary sources of background events associated with the event selection described in Section 5: events with electrons and muons produced in W , Z/γ^* , Higgs boson or top-quark decays (prompt leptons) and events that have at least one lepton arising from another source (fake and non-prompt leptons). In the latter case, electrons and muons originate from improper reconstruction of other physics objects such as hadronic jets, heavy-flavour hadron decays or photon conversions. All processes associated with the prompt-lepton background are predominantly well modelled by simulation and therefore estimated from MC event samples, described in Section 3.2. Two control regions, enriched in top-quark (TCR) and $Z \rightarrow \tau^+\tau^-$ (ZCR) events, are designed to control and validate the major backgrounds modelled by MC simulation. The fake-lepton validation region (FVR) is designed and used to estimate and validate the fake/non-prompt-lepton background using a data-driven method. A summary of the requirements for all regions is given in Table 2.

6.1 Background with prompt leptons

The ZCR is used to control the main background in this analysis, which originates from $Z \rightarrow \tau^+\tau^-$ decays. The requirements for this region are to have an abundance of $Z \rightarrow \tau^+\tau^-$ decays, to be orthogonal to the SR, and to have low contamination from signal events while being kinematically close to the SR. This is achieved by having selection criteria similar to those for the SR, but requiring $\Delta R_{\ell\ell} > 1.4$ because the two leptons originating from the Z boson are well separated. Additionally, the $E_{\text{T}}^{\text{miss}}$ criterion is dropped in order to obtain a large sample of $Z \rightarrow \tau^+\tau^-$ decays with low signal contamination.

The distributions of some variables in the ZCR showed mismodelling of $Z \rightarrow \tau^+\tau^-$ events. In particular, the event count with the number of jets, n_{jets} , equal to 0 is underestimated in simulation and increasingly overestimated for $n_{\text{jets}} > 1$. Also, for high values of the transverse momentum of the ditau system,² $p_{\text{T}}^{\tau\tau} > 50$ GeV, and for $E_{\text{T}}^{\text{miss}}$ between 50 and 100 GeV a surplus of background events is observed. This region is especially important for this analysis because the high-mass SR (low-mass SR) requires $E_{\text{T}}^{\text{miss}} > 30$ (50) GeV, and $Z \rightarrow \tau^+\tau^-$ events are the main background in the SR. Therefore, a data-driven reweighting method, similar to the one used in Ref. [111], is chosen to obtain better agreement between the prediction and data in the ZCR. The weights are calculated as the ratio of the expected number of $Z \rightarrow \tau^+\tau^-$ events to the simulated number in the ZCR and binned in the number of jets. The expected number of events is obtained from data by subtracting the predicted number of other simulated background events, which do not originate from $Z \rightarrow \tau^+\tau^-$. The fake-lepton background (see Section 6.2) must also be taken into account, so the efficiencies for the ‘matrix method’ described in the next section must be determined prior to the calculation of the $Z \rightarrow \tau^+\tau^-$ weights. The weights range from 0.8 to 1.12 with a tendency to be closer to unity for a smaller number of jets. The reweighting not only resolves the mismodeling of n_{jets} but also improves the data-to-background agreement of the $p_{\text{T}}^{\tau\tau}$ and $E_{\text{T}}^{\text{miss}}$ distributions in the ZCR.

The TCR is constructed to control the background resulting from processes involving top quarks, which produce one of the largest backgrounds in this analysis. It has almost the same requirements as the high-mass SR, but at least two b -tagged jets are required. Requiring $n_{b\text{-jets}} \geq 1$ was also tested, but the contamination from signal events was too large. Furthermore, a small improvement to the modelling is incorporated by reweighting each $t\bar{t}$ sample so that its top-quark p_{T} distribution matches that calculated to

² The transverse momentum of the ditau system is defined as the magnitude of the vector sum of the transverse momenta of the electron and the muon and of the missing transverse momentum: $p_{\text{T}}^{\tau\tau} = |\vec{p}_{\text{T}}^e + \vec{p}_{\text{T}}^{\mu} + \vec{p}_{\text{T}}^{\text{miss}}|$

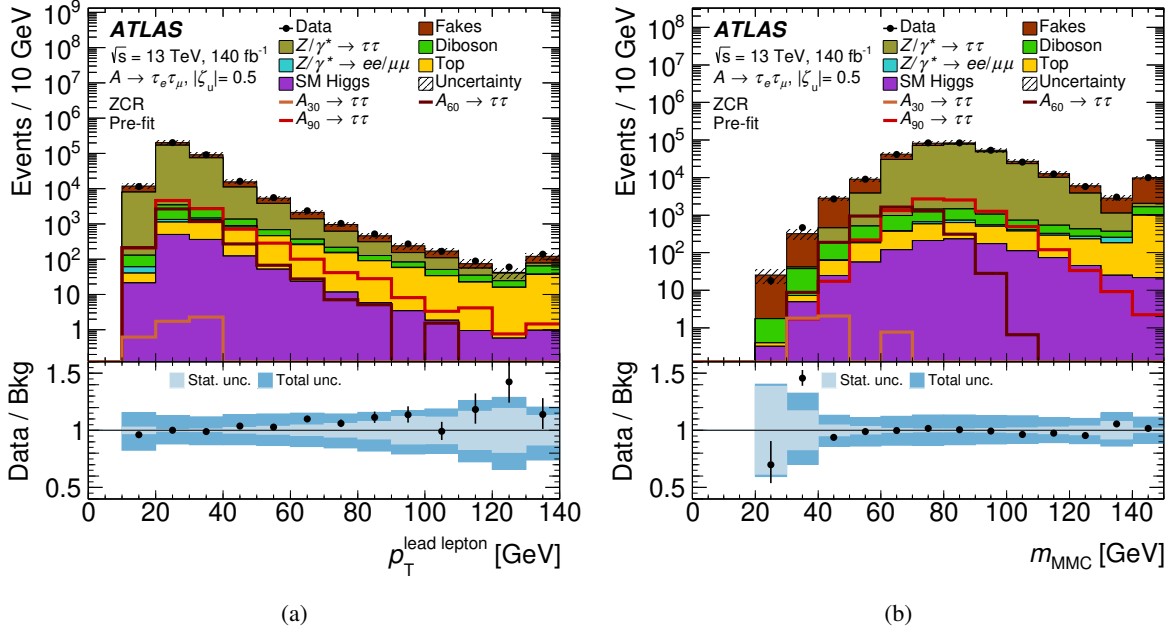


Figure 2: Pre-fit variable distributions in the ZCR after applying all selection criteria: (a) leading-lepton p_T and (b) m_{MMC} mass estimator. The background is estimated by using MC samples and data-driven methods (see text for details). The expected signal contributions for the mass hypotheses $m_A = 30, 60$ and 90 GeV are shown assuming $|\zeta_u| = 0.5$. Events with values exceeding the x -axis range are shown in the last bin of each distribution. The dark blue band in the ratio plot shows the total uncertainty from statistical and systematic sources. The statistical uncertainty band is overlaid in light blue.

NNLO in QCD with NLO EW corrections [112]. Figure 2 and Figure 3 show the validation of Z+jets and top-quark backgrounds, respectively. In both cases, the observed data agrees well with the estimated background within their respective uncertainties.

6.2 Background with non-prompt leptons

The FVR is constructed to perform and validate the fake-lepton estimation in a region enriched in non-prompt leptons. It has the same requirements as the ZCR, except that the two leptons are required to have the same charge. This region can be used for a closure test of the fake-lepton estimation, and systematic uncertainties can be extracted.

To estimate the total contribution of events with fake or non-prompt leptons, as well as leptons with misidentified charge (hereinafter collectively referred to as fake-lepton background), a data-driven matrix method [113] is used, which is especially useful in cases where events with either zero, one, or two fake leptons are expected. Two categories of events are selected, satisfying baseline (*Loose* isolation and *Loose* identification) and tight (*Tight* isolation and *Medium* identification) lepton selection requirements as described in Section 5. The efficiencies for fake leptons, $\varepsilon_{\text{fake}}^\ell$, and for real leptons, $\varepsilon_{\text{real}}^\ell$, that meet the tight criteria are used to estimate the rate of events with fake leptons from the numbers of tight and non-tight

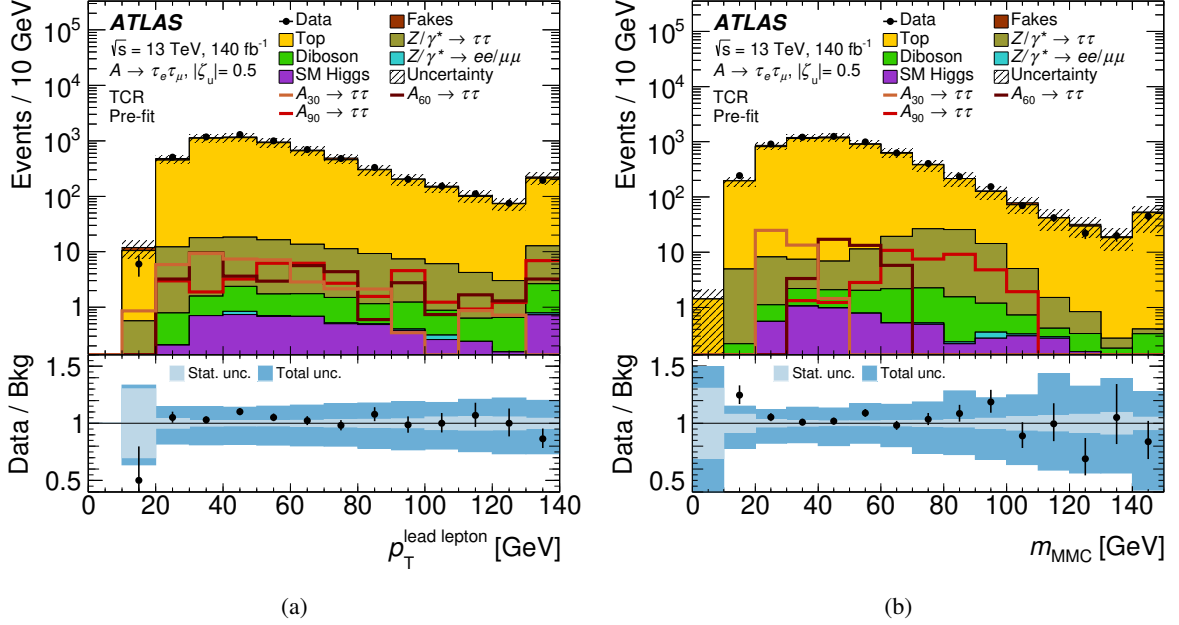


Figure 3: Pre-fit variable distributions in the TCR after applying all selection criteria: (a) leading-lepton p_T and (b) m_{MMC} mass estimator. The background is estimated by using MC samples and data-driven methods (see text for details). The expected signal contributions for the mass hypotheses $m_A = 30, 60$ and 90 GeV are shown assuming $|\zeta_u| = 0.5$. Events with values exceeding the x -axis range are shown in the last bin of each distribution. The dark blue band in the ratio plot shows the total uncertainty from statistical and systematic sources. The statistical uncertainty band is overlaid in light blue.

events passing the baseline selection. This is done by inverting the equation

$$\begin{pmatrix} N_{XX}^{\text{TT}} \\ N_{XX}^{\text{T}\bar{\text{T}}} \\ N_{XX}^{\text{T}\bar{\text{T}}} \\ N_{XX}^{\text{T}\bar{\text{T}}} \end{pmatrix} = \begin{pmatrix} \varepsilon_{\text{real}}^e \varepsilon_{\text{real}}^\mu & \varepsilon_{\text{real}}^e \varepsilon_{\text{fake}}^\mu & \varepsilon_{\text{fake}}^e \varepsilon_{\text{real}}^\mu & \varepsilon_{\text{fake}}^e \varepsilon_{\text{fake}}^\mu \\ \varepsilon_{\text{real}}^e \bar{\varepsilon}_{\text{real}}^\mu & \varepsilon_{\text{real}}^e \bar{\varepsilon}_{\text{fake}}^\mu & \varepsilon_{\text{fake}}^e \bar{\varepsilon}_{\text{real}}^\mu & \varepsilon_{\text{fake}}^e \bar{\varepsilon}_{\text{fake}}^\mu \\ \bar{\varepsilon}_{\text{real}}^e \varepsilon_{\text{real}}^\mu & \bar{\varepsilon}_{\text{real}}^e \varepsilon_{\text{fake}}^\mu & \bar{\varepsilon}_{\text{fake}}^e \varepsilon_{\text{real}}^\mu & \bar{\varepsilon}_{\text{fake}}^e \varepsilon_{\text{fake}}^\mu \\ \bar{\varepsilon}_{\text{real}}^e \bar{\varepsilon}_{\text{real}}^\mu & \bar{\varepsilon}_{\text{real}}^e \bar{\varepsilon}_{\text{fake}}^\mu & \bar{\varepsilon}_{\text{fake}}^e \bar{\varepsilon}_{\text{real}}^\mu & \bar{\varepsilon}_{\text{fake}}^e \bar{\varepsilon}_{\text{fake}}^\mu \end{pmatrix} \cdot \begin{pmatrix} N_{\text{RR}}^{\text{LL}} \\ N_{\text{RF}}^{\text{LL}} \\ N_{\text{FR}}^{\text{LL}} \\ N_{\text{FF}}^{\text{LL}} \end{pmatrix},$$

where $\bar{\varepsilon}_{\text{real/fake}}^\ell = 1 - \varepsilon_{\text{real/fake}}^\ell$. The indices of the event yields N are to be read as follows. The upper indices describe the tightness of the leptons, where T means that the lepton is required to be tight, $\bar{\text{T}}$ that it has to be non-tight, and L that the lepton is part of the baseline selection without further requirements on the tightness. The lower indices indicate whether an event comes from data or from MC simulation, and in the latter case whether the lepton is real (R), fake (F), or without a requirement on a certain ‘truth’ state (X) in the MC event record. The first index always describes the electron, the second one the muon. For example, $N_{\text{RX}}^{\text{LT}}$ is the number of MC events with a real electron that passes the baseline selection and a tight muon, and $N_{\text{Data}}^{\text{T}\bar{\text{T}}}$ is the number of data events with a tight electron and a non-tight muon. The total fake-lepton background is then the sum of the fake-electron, fake-muon, and double-fake-lepton backgrounds

$$N_{\text{fake}}^{\text{TT}} = \varepsilon_{\text{real}}^e \varepsilon_{\text{fake}}^\mu N_{\text{RF}}^{\text{LL}} + \varepsilon_{\text{fake}}^e \varepsilon_{\text{real}}^\mu N_{\text{FR}}^{\text{LL}} + \varepsilon_{\text{fake}}^e \varepsilon_{\text{fake}}^\mu N_{\text{FF}}^{\text{LL}}.$$

The real-lepton (fake-lepton) efficiency is defined as the ratio of the number of real (fake) leptons satisfying the tight selection to the number of real (fake) leptons satisfying the baseline selection. The real-lepton

efficiencies are estimated using the ‘truth particle’ classification from the MC event record, while the fake-lepton efficiencies are estimated from data after subtracting the MC-estimated prompt-lepton background. Assuming that the electron efficiencies are independent of the muon produced in the same event and vice versa, the conventional matrix method is valid. In this analysis, however, it was observed that the fake-lepton efficiencies are not entirely independent of the other (fake) lepton in the event. To account for this, a parameterisation of the real- and fake-lepton efficiencies, based on the tightness of the other lepton, is introduced such that the electron efficiencies depend on the muon’s tightness and vice versa:

$$\varepsilon_{\text{real}}^e(\mu) = \begin{cases} \frac{N_{\text{RX}}^{\text{TT}}}{N_{\text{RX}}^{\text{LT}}}, & \mu \text{ tight} \\ \frac{N_{\text{RX}}^{\text{TT}}}{N_{\text{RX}}^{\text{LT}}}, & \mu \text{ non-tight} \end{cases}, \quad \varepsilon_{\text{real}}^\mu(e) = \begin{cases} \frac{N_{\text{XR}}^{\text{TT}}}{N_{\text{XR}}^{\text{TL}}}, & e \text{ tight} \\ \frac{N_{\text{XR}}^{\text{TT}}}{N_{\text{XR}}^{\text{TL}}}, & e \text{ non-tight} \end{cases},$$

$$\varepsilon_{\text{fake}}^e(\mu) = \begin{cases} \frac{N_{\text{Data}}^{\text{TT}} - N_{\text{RX}}^{\text{TT}}}{N_{\text{Data}}^{\text{LT}} - N_{\text{RX}}^{\text{LT}}}, & \mu \text{ tight} \\ \frac{N_{\text{Data}}^{\text{TT}} - N_{\text{RX}}^{\text{TT}}}{N_{\text{Data}}^{\text{LT}} - N_{\text{RX}}^{\text{LT}}}, & \mu \text{ non-tight} \end{cases}, \quad \varepsilon_{\text{fake}}^\mu(e) = \begin{cases} \frac{N_{\text{Data}}^{\text{TT}} - N_{\text{XR}}^{\text{TT}}}{N_{\text{Data}}^{\text{TL}} - N_{\text{XR}}^{\text{TL}}}, & e \text{ tight} \\ \frac{N_{\text{Data}}^{\text{TT}} - N_{\text{XR}}^{\text{TT}}}{N_{\text{Data}}^{\text{TL}} - N_{\text{XR}}^{\text{TL}}}, & e \text{ non-tight} \end{cases}.$$

Additionally, the efficiencies are binned in lepton p_T as shown in Figure 4, revealing that the fake-lepton efficiencies depend on the tightness of the accompanying lepton for low p_T , while the real-lepton efficiencies are statistically compatible.

When considering real-lepton efficiencies in events with a tight accompanying lepton, it is possible to extract them directly from the SR, as it contains a sufficient number of well-modelled real leptons from prompt-lepton MC background events. Also, different real-lepton efficiencies are calculated for the high-mass SR and low-mass SR, with the E_T^{miss} criterion removed in the latter to increase the event yield. The real efficiencies for events with a non-tight accompanying lepton are calculated in the ZCR because it has more events than the SR. To calculate the fake-lepton efficiencies, one needs a region close to the SR but enriched in fake leptons, conditions best satisfied with enough events by the FVR. Figure 5 shows the validation of the fake-lepton estimate in the FVR, where the fake-lepton efficiencies are measured. In both the $p_T^{\text{lead lepton}}$ and the m_{MMC} distributions, the observed data agrees well with the estimated background within their respective uncertainties.

6.3 Event yields

Table 3 and Table 4 summarise the event yields for the signal and background predictions, respectively, in the different regions in comparison with those observed in data. Due to the $Z \rightarrow \tau^+\tau^-$ reweighting the data-to-background ratio in the ZCR equals 1 by definition. In the other control regions, the expected yield is in agreement with the observed number of events within the total uncertainty. The systematic uncertainties are described and estimated in the following section. The purity of the $Z \rightarrow \tau^+\tau^-$, top-quark and fake-lepton backgrounds reaches 79%, 94% and 97% in the ZCR, TCR and FVR, respectively. No signal is expected in the FVR and it is negligible in both the ZCR and TCR. The purity of the signal in the SR depends on the mass hypothesis, and reaches 60% for masses lower than 60 GeV when scaled according to the cross-sections in Table 1 multiplied by 0.25, the highest currently allowed value of $|\zeta_u|^2$ [16].

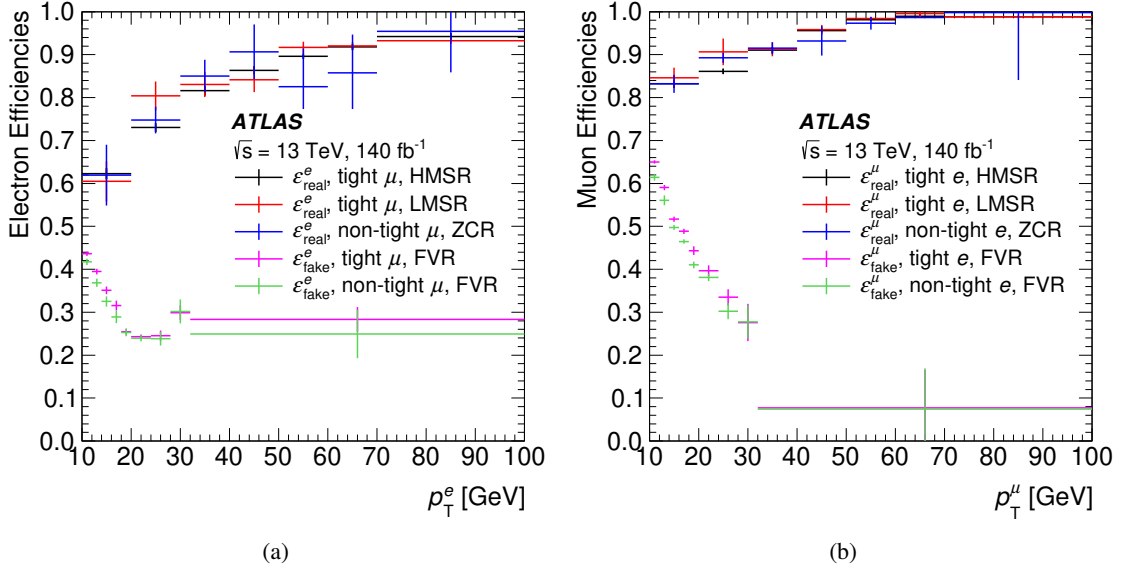


Figure 4: Fake- and real-lepton efficiencies (ϵ_{fake} and ϵ_{real}) for (a) electrons and (b) muons with a tight or non-tight accompanying (a) muon and (b) electron, binned in p_T^e and p_T^μ , respectively. Real-lepton efficiencies with a tight accompanying lepton are calculated in the high-mass and low-mass SRs (HMSR and LMSR), real-lepton efficiencies with a non-tight accompanying lepton are calculated in the ZCR, and fake-lepton efficiencies are calculated in the FVR.

7 Systematic uncertainties

Systematic uncertainties are categorised into those arising from the measurements (experimental uncertainties) and those due to the modelling of various processes (theoretical uncertainties), where the latter are specific to a single process or a group of processes. In contrast, the experimental uncertainties depend on simulations of the detector and reconstruction of objects, and are therefore independent of the process. A nuisance parameter (NP) with a Gaussian prior is assigned to each systematic uncertainty. Additionally, smoothing and pruning procedures are used to reduce the impact of statistical fluctuations and remove the smallest systematic uncertainties evaluated by performing various ‘systematic variations’. The shape and normalisation components of the systematic uncertainties are dropped if they do not exceed 0.5% for a given process (in the case of the shape uncertainties, if no bin shows an effect greater than 0.5%).

7.1 Experimental uncertainties

The uncertainty in the combined 2015–2018 integrated luminosity³ is 0.83% [36], obtained using the LUCID-2 detector [33] for the primary luminosity measurements. A systematic uncertainty is assigned to the reweighting procedure, based on the mean number of pp interactions per bunch crossing, used to correct the pile-up profile in MC simulation to match the data. For leptons, systematic uncertainties are assigned to the scale factors applied to correct for all differences between data and simulation that come from the electron and muon identification, reconstruction, isolation and trigger performance [37,

³ The luminosity uncertainty is only included in the limit calculation and not in the variables’ distribution plots.

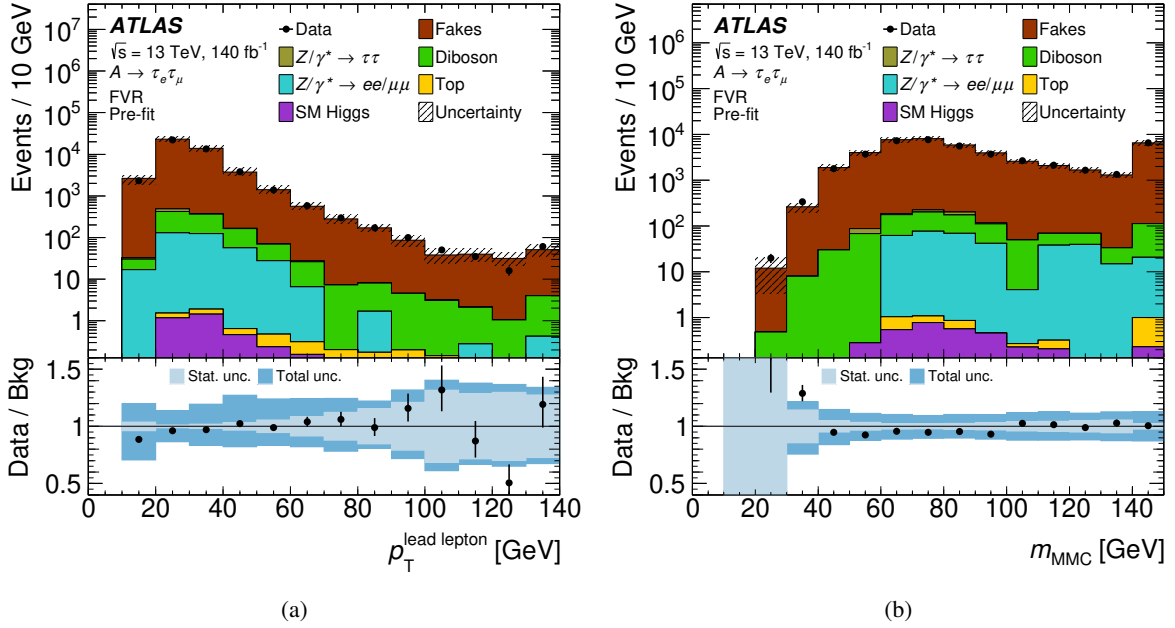


Figure 5: Pre-fit variable distributions in the FVR after applying all selection criteria: (a) leading-lepton p_T and (b) m_{MMC} mass estimator. The background is estimated by using MC samples and data-driven methods (see text for details). Events with values exceeding the x -axis range are shown in the last bin of each distribution. The dark blue band in the ratio plot shows the total uncertainty from statistical and systematic sources. The statistical uncertainty band is overlaid in light blue.

[38, 99, 100] or from the lepton momentum scale and resolution. For jets, systematic uncertainties from the mismodelling of jet energy scale and resolution effects [102], jet vertex-tagging efficiencies [104], and jet flavour-tagging efficiencies [114–116] are considered. For the missing transverse momentum, uncertainties from the scale and resolution of the track-based ‘soft term’ are considered [108]. The latter are one-sided variations. For the E_T^{miss} ‘hard terms’, uncertainties are already covered by electron, muon and jet uncertainties.

Other kinds of uncertainties are considered for the fake- and non-prompt-lepton backgrounds. First, the statistical uncertainties of the real- and fake-lepton efficiencies for electrons and muons are propagated as a single systematic uncertainty for each p_T bin. Also, the dependence of the efficiencies on variables other than the lepton p_T need to be accounted for. However, due to the limited number of data events, it is not possible to split the efficiencies into more components, so systematic uncertainties for the unaccounted dependencies of the efficiencies are included by parameterising them in η , n_{jets} and E_T^{miss} . For the η dependence, three different bins of absolute η values are introduced: $[0, 0.8)$, $[0.8, 1.7)$ and $[1.7, 2.7)$. The dependence of the efficiencies on the number of jets, n_{jets} , is also modelled, using four n_{jets} values $\{0, 1, 2, \geq 3\}$ for the fake-lepton efficiencies and $\{1, 2, 3, \geq 4\}$ for the real-lepton efficiencies, as there are no events without jets in the signal regions. For the E_T^{miss} dependence, four different bins of E_T^{miss} values are used: $[0, 10)$ GeV, $[10, 20)$ GeV, $[20, 30)$ GeV and $[30, \infty)$ GeV. For all those parameterisation uncertainties, the weighted standard deviations of the efficiencies are calculated and used as systematic uncertainties. Furthermore, the region where the efficiencies are measured and the SR could have different compositions. To account for this difference, a composition uncertainty is included by calculating the efficiencies in regions with the same requirements as the signal regions, but with the leptons having the

Table 3: Pre-fit signal yields in the different analysis regions. The numbers correspond to an integrated luminosity of 140 fb^{-1} . The quoted uncertainties are the statistical uncertainties which arise from the finite number of generated events in the simulated samples. No signal is expected in the FVR. The signal cross-sections are calculated to N³LO, as summarised in Table 1. These cross-section values are multiplied by $0.25 = |\zeta_u|^2 = \cot^2 \beta$, which is the highest not-already-excluded value of $|\zeta_u|^2$ [16].

m_A [GeV]	ZCR	TCR	Low-mass SR	High-mass SR
20	0.0 ± 0.0	15.4 ± 3.0	1355 ± 27	-
25	0.3 ± 0.3	30.8 ± 3.3	2326 ± 28	-
30	4.7 ± 1.8	39.6 ± 5.3	2865 ± 44	-
40	314 ± 17	59.4 ± 7.6	2940 ± 52	-
50	1706 ± 43	51.2 ± 7.5	2293 ± 51	-
60	4396 ± 71	39.6 ± 7.1	1516 ± 43	-
70	7242 ± 91	53.6 ± 8.1	1002 ± 35	-
75	8083 ± 75	53.9 ± 6.5	774 ± 23	2312 ± 41
80	8520 ± 96	49.9 ± 7.5	-	2011 ± 47
85	8706 ± 76	39.1 ± 5.4	-	1771 ± 35
90	8710 ± 93	39.6 ± 6.3	-	1512 ± 39

same charge. Also, the m_{MMC} and $E_{\text{T}}^{\text{miss}}$ criteria are omitted to increase the number of events, as the $E_{\text{T}}^{\text{miss}}$ parameterisation is already accounted for by a dedicated uncertainty. Both the parameterisation and composition uncertainties are decorrelated across the regions for the fit because the regions use independent data, and allowing correlations would overly constrain the corresponding NPs. In some cases, a systematic uncertainty may arise from the uncertainty in the MC-event subtraction when calculating the fake-lepton efficiencies. For this analysis, the MC-event contamination in the FVR, where the fake-lepton efficiencies are measured, is only 3%. Thus, the uncertainties coming from the MC-event contamination are not considered in this analysis.

The most significant experimental uncertainties stem from the fake-lepton background estimation, flavour tagging, and muon efficiencies and calibration.

7.2 Theoretical uncertainties

Systematic uncertainties of the signal and background production cross-sections arise from various sources: missing higher-order (MHO) corrections, the PDFs, and the chosen input parameter values. The relative uncertainties in the inclusive cross-sections for backgrounds are 1.9% (5%) [117] for $Z \rightarrow \tau^+ \tau^-$ with $m_{\ell\ell}$ above (below) 66 GeV, 4.4% [43, 118–121] for top-quark processes (dominated by $t\bar{t}$), and an envelope of 7.1% [122–124] for diboson processes. The relative uncertainties in the signal cross-sections are only taken into account for the model-dependent interpretation, with the estimated values ranging from 6.5% to 11.2%.

Table 4: Pre-fit background event yields in the different analysis regions. The numbers correspond to an integrated luminosity of 140 fb^{-1} . The quoted uncertainties are the statistical uncertainties which arise from the finite number of generated events in the simulated samples and from the statistical uncertainties of the measured data as input for the fake-lepton background. The values in parentheses represent the fraction of the corresponding background relative to the total background in each region. For the $Z/\gamma^* \rightarrow \ell^+\ell^-$ background, $\ell^+\ell^-$ includes e^+e^- and $\mu^+\mu^-$.

	ZCR	FVR	TCR	Low-mass SR	High-mass SR
Fakes	$59\,680 \pm 690$ (18%)	$44\,850 \pm 430$ (97%)	213 ± 50 (3.5%)	316 ± 45 (17%)	495 ± 55 (9.0%)
$Z/\gamma^* \rightarrow \tau^+\tau^-$	$262\,700 \pm 1800$ (79%)	82 ± 27 (0.18%)	116.1 ± 4.0 (1.9%)	1210 ± 36 (63%)	3701 ± 46 (67%)
Diboson	4552 ± 26 (1.4%)	747.3 ± 7.4 (1.6%)	10.82 ± 0.50 (0.18%)	139.1 ± 2.4 (7.3%)	449.2 ± 4.4 (8.2%)
$Z/\gamma^* \rightarrow \ell^+\ell^-$	468 ± 71 (0.14%)	354 ± 68 (0.77%)	0.28 ± 0.12 ($< 0.1\%$)	4.0 ± 1.7 (0.21%)	9.8 ± 3.3 (0.18%)
Top	3327 ± 22 (1.0%)	2.02 ± 0.51 ($< 0.1\%$)	5653 ± 28 (94%)	162.9 ± 4.7 (8.5%)	611.4 ± 9.3 (11%)
SM Higgs	1108.7 ± 2.6 (0.33%)	3.63 ± 0.18 ($< 0.1\%$)	5.79 ± 0.23 (0.097%)	76.86 ± 0.79 (4.0%)	227.4 ± 1.3 (4.1%)
Total background	$331\,800 \pm 2000$	$46\,040 \pm 440$	5999 ± 57	1908 ± 58	5494 ± 73
Data	331 797	44 587	6227	1987	6119

Generator systematic uncertainties for $Z \rightarrow \tau^+\tau^-$ and diboson processes arise mainly from the renormalisation and factorisation scales (μ_R and μ_F), as well as α_s uncertainties, PDF parameter value choices, and uncertainties in the resummation (QSF) and CKKW matching scales. The related event samples were produced using SHERPA 2.2.1 and 2.2.2, respectively. Systematic uncertainties associated with renormalisation and factorisation scale, PDF and α_s variations are assessed using corresponding event weights. All uncertainties are calculated in the high-mass SR and ZCR. The latter are applied in the ZCR and FVR. In all other regions, the ones calculated in the high-mass SR are used. For the QCD scale uncertainties, a 7-point variation is performed by varying μ_R and μ_F by factors of 2 and 0.5 in different combinations. For each bin, the uncertainty is given by the maximum positive and negative changes due to the variations. The scale uncertainty for the $Z \rightarrow \tau^+\tau^-$ process is decorrelated between the regions because of its largely different structure in the high-mass SR and the ZCR and to account for potential problems in the extrapolation of n_{jets} weights from the ZCR described in Section 6.1. Using the baseline PDF, NNPDF3.0_{NNLO} with a strong coupling value of $\alpha_s(m_Z) = 0.118$, as the nominal one, the standard deviation of 100 PDF variations is determined and taken as a symmetric uncertainty. Also, α_s is varied from 0.118 by ± 0.001 . The CT14_{NNLO} [125] and MMHT2014_{NNLO} PDF sets with associated 68% confidence-level uncertainty bands [126] are compared with the baseline PDF to cross-check the results. Uncertainties corresponding to CKKW and QSF scale variations are evaluated only for $Z \rightarrow \tau^+\tau^-$, via a parameterisation method. For the CKKW matching, the nominal scale used in calculations of the overlap between jets from

the ME and parton shower is 20 GeV and is varied between 15 GeV and 30 GeV. The soft-gluon emission resummation scale is varied by factors of 0.5 and 2 from its nominal value. All of the $Z \rightarrow \tau^+\tau^-$ and diboson generator uncertainties are calculated in bins of m_{MMC} .

Additional systematic uncertainties are included for the $Z \rightarrow \tau^+\tau^-$ reweighting, described in Section 6.1, by propagating the statistical uncertainties of MC events and data events, as well as experimental and generator systematic uncertainties of MC events, to the weights. The resulting uncertainties cover a reweighting value of unity in most n_{jets} bins. The NPs are decorrelated across the regions to avoid double-counting the propagation of effects from the ZCR (where the weights were determined) to the SR.

The uncertainty in the modelling of top-quark processes has contributions from different sources. The uncertainties from each source are estimated by comparing the nominal sample (POWHEG BOX v2 at NLO with NNPDF3.0_{NLO} and $h_{\text{damp}} = 1.5 m_{\text{top}}$; PYTHIA 8.230 with the A14 tune and NNPDF2.3_{LO}; and EVTGEN 1.6.0) with multiple variations. The uncertainties are evaluated in a modified TCR. Compared to the nominal TCR, the requirement on the number of b -tagged jets is loosened to ≥ 1 b -tagged jet in order to accept more events.⁴ The impact of using a different parton shower and hadronisation model is evaluated by replacing PYTHIA with HERWIG 7.13 [127, 128] and the MMHT2014_{LO} PDF set; for the impact of using different ME generation and matching to the parton shower, MADGRAPH5_AMC@NLO 2.6.0 [129] is used in place of POWHEG BOX; and to estimate the impact of changing the h_{damp} parameter value, a sample with $h_{\text{damp}} = 3 m_{\text{top}}$ is used. Separate alternative datasets were simulated for each of the above variations. Initial-state radiation (ISR) uncertainties are estimated by halving and doubling μ_{R} and μ_{F} , and using the A14 tune's Var3cUp and Var3cDown variations corresponding to the variation of α_{s} for ISR. For final-state radiation (FSR), halving and doubling the renormalisation scale for parton shower emissions gives an estimate of the relevant uncertainty. These α_{s} and scale variations use alternative event weights recorded in the nominal simulation datasets. All of the top-quark generator uncertainties are calculated in bins of m_{MMC} .

Uncertainties in signal modelling arise from the following sources: MHO corrections, the PDFs, the colour reconnection parameters and α_{s} . Furthermore, uncertainties from the modelling of ISR and FSR, multi-parton interactions (MPI), parton showers and hadronisation are considered. They are estimated from ratios of nominal-sample event acceptance to variation-sample event acceptance, binned in p_{T}^{A} . Uncertainties arising from the modelling of ISR, FSR, MPI and colour reconnection are estimated by adding in quadrature the effects of the Var1, Var2, Var3a, Var3b and Var3c up and down eigenvariations of PYTHIA 8's A14 tune. The scale uncertainties due to MHO corrections are determined from event weights given for 7-point combinations of different μ_{R} and μ_{F} values [78]. Analogously, the PDF and α_{s} uncertainties are estimated from variations given in the form of event weights, with the NNPDF2.3_{LO} PDF as the baseline, for two α_{s} values 0.119 and 0.130, and for 100 variations of the PDF set. For every m_{A} value and each systematic variation, about 5 million events were generated to reduce statistical effects. Finally, a smoothing algorithm is applied, taking into account neighbouring mass hypotheses, to reduce remaining statistical fluctuations.

⁴ Systematic variations are performed using simulated top-quark processes only and are thus not affected by a possible signal contamination in an extended TCR.

8 Statistical model and results

The signal strength μ , defined as a multiplicative factor to the cross-section of the hypothetical signal, is obtained from the statistical analysis of the data using a binned likelihood function based on a product of Poisson probability terms. Signal and background predictions depend on systematic uncertainties, which are parameterised as NPs and constrained using Gaussian functions. Normalisation factors for the $Z \rightarrow \tau^+\tau^-$ and top-quark backgrounds are also included but are not constrained. The binned likelihood function is constructed in bins of m_{MMC} . The binning was chosen in a way that ensures the statistical uncertainty per bin does not exceed 10% and that there are at least ten background events per bin, while requiring a minimum bin width of 2 GeV. Additionally, at least one fake-lepton event per bin is required. This is technically necessary in order to avoid having bins with negative expected background contributions or background expectations close to zero with large uncertainties in the statistical analysis. The fit model consists of three regions: the low-mass or high-mass SR, depending on the mass hypothesis, and the two control regions, TCR and ZCR. The two control regions allow the extraction of a normalisation factor for the top-quark and $Z \rightarrow \tau^+\tau^-$ backgrounds and constrain some of the systematic uncertainties. To account for shape effects in the TCR and ZCR, the regions are split into five and six m_{MMC} bins, respectively. The FVR is not used in the fit. The statistical uncertainties of the simulated background and signal, and those of the fake-lepton background histograms, are modelled by dedicated NPs, which use Poisson constraint terms. They are introduced separately for the signals and the combined backgrounds.

The fit is performed separately for each signal mass hypothesis. The final m_{MMC} distributions after the fit are shown in Figure 6 for the 20 GeV mass hypothesis from the low-mass SR and for the 90 GeV mass hypothesis from the high-mass SR, including both the statistical and systematic uncertainties. Although the signal contributions to the control regions are negligible, they are taken into account properly in the fit.

The largest uncertainties in the SR, measured by their grouped impact on the fit result are listed in Table 5. The dominant systematic uncertainties originate from the fake-lepton estimation, the $Z \rightarrow \tau^+\tau^-$ modelling, the $Z \rightarrow \tau^+\tau^-$ reweighting and the $Z \rightarrow \tau^+\tau^-$ MC sample size. Data statistical uncertainties play only a minor direct role; however, they play an important indirect role through the statistical uncertainties of the fake-lepton estimate.

The compatibility of the observed m_{MMC} spectrum with the background-only hypothesis, for a given A boson mass hypothesis, is assessed with a local p_0 -value based on the profile-likelihood-ratio test statistic [130]. No significant deviation from the background-only hypothesis is observed. The largest local excess of events is 1.8σ , observed for an A boson mass of 20 GeV, followed by a 1.3σ excess for the 85 GeV mass hypothesis.

The observed and expected 95% CL exclusion limits are calculated using a modified frequentist approach, the CL_s method [131], with the asymptotic approximation to the test-statistic distribution [130]. Limits are set on the signal strength μ and translated into limits on the gluon–gluon fusion production cross-section $\sigma(gg \rightarrow A)$ times the branching ratio for A boson decay into two τ -leptons, $\mathcal{B}(A \rightarrow \tau\tau)$. The observed and expected upper limits are shown in Figure 7 and include all systematic uncertainties detailed in Section 7 except for the signal cross-section uncertainties. The observed limits range from 68 pb for $m_A = 20$ GeV to 3.0 pb for $m_A = 60$ GeV, increasing to 43 pb at $m_A = 90$ GeV due to the reduced sensitivity near the Z -boson resonance.

In addition, this analysis provides an upper limit on the absolute value of the up-type quark coupling parameter $|\zeta_u|$ within the flavour-aligned 2HDM model. For this, the uncertainties in the cross-sections are

Table 5: Breakdown of the relative contributions to the uncertainty of the extracted signal strength μ in the likelihood fit to data. The contributions are obtained by fixing the relevant NPs to their post-fit values in the likelihood fit. The relative impact is determined as the square-root of the difference of the squares of the nominal uncertainty and the obtained uncertainty, divided by the nominal uncertainty. The sum in quadrature of the individual components differs from the total uncertainty because of correlations between uncertainties in the different groups. The uncertainty from data statistical uncertainties is determined from fits with all NPs fixed to their post-fit values. The background statistical uncertainty includes the statistical uncertainty of the fake-lepton background determination and uncertainties due to background MC statistics. Only NP groups with a relative impact larger than 5% are listed.

$m_A = 20 \text{ GeV}$		$m_A = 90 \text{ GeV}$	
Category	Relative contribution to $\Delta\mu$	Category	Relative contribution to $\Delta\mu$
Data statistical	42%	Data statistical	10%
Systematic	91%	Systematic	99%
Background statistical	81%	Background statistical	67%
$Z \rightarrow \tau^+\tau^-$ statistical	75%	$Z \rightarrow \tau^+\tau^-$ statistical	48%
Fake-lepton statistical	30%	Fake-lepton statistical	47%
Other background statistical	7%	Other background statistical	8%
Fake-lepton systematic	37%	$Z \rightarrow \tau^+\tau^-$ reweighting	55%
Signal modelling	11%	Signal statistical	51%
$Z \rightarrow \tau^+\tau^-$ modelling	10%	Fake-lepton systematic	47%
Muon efficiencies	8%	$Z \rightarrow \tau^+\tau^-$ modelling	45%
Diboson modelling	8%	$Z \rightarrow \tau^+\tau^-$ and $t\bar{t}$ normalisation	34%
Flavour tagging	5%	$t\bar{t}$ modelling	14%
Signal statistical	5%	Flavour tagging	14%
		Muon calibration	13%
		E_T^{miss}	9%
		Diboson modelling	7%
		Electron calibration	6%

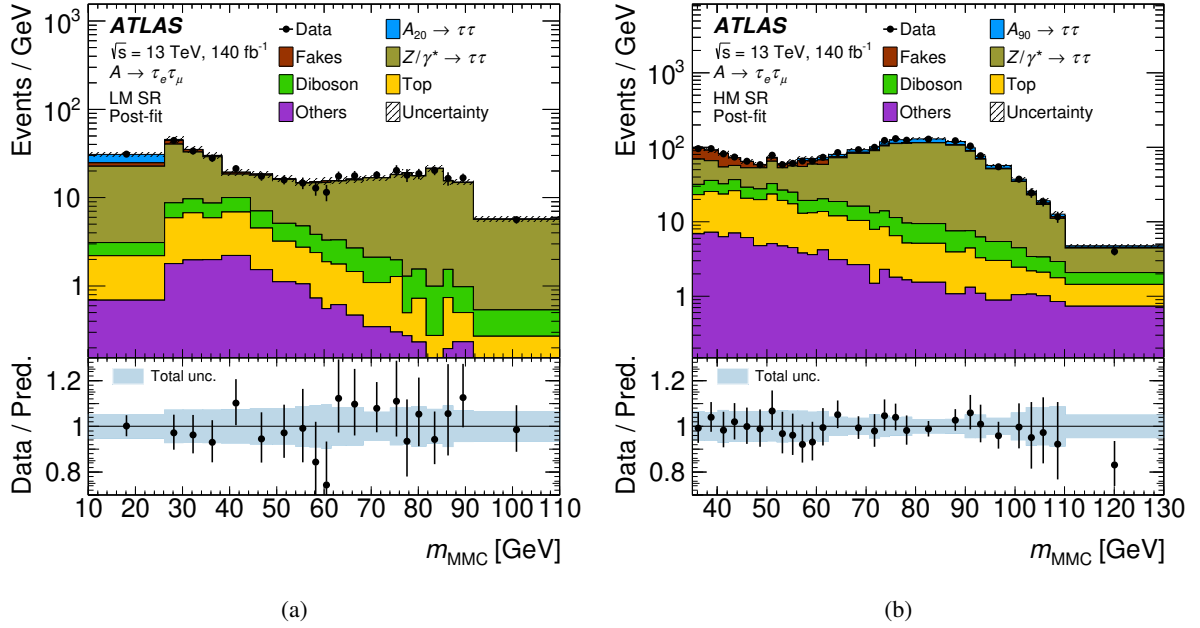


Figure 6: Post-fit m_{MMC} distributions in (a) the low-mass SR for the $m_A = 20$ GeV signal mass hypothesis and (b) the high-mass SR for the $m_A = 90$ GeV signal mass hypothesis. The fits are performed under the signal-plus-background hypothesis using the signal with the respective m_A . Processes contributing to the ‘Others’ background are $Z/\gamma^* \rightarrow \ell^+\ell^-$ and SM Higgs production. In (a), events with values below or above the x -axis range are shown in the first or last bin of the distribution, respectively. The band in the ratio plot shows the total uncertainty of the background estimate.

added to the fit. Since only gluon–gluon fusion production of A bosons via top-quark loops is considered and $\mathcal{B}(A \rightarrow \tau\tau) = 1$ is assumed, the obtained limits σ_{fit} can be transformed into limits on $|\zeta_{\text{u}}|$ via

$$|\zeta_{\text{u}}| = \sqrt{\frac{\sigma_{\text{fit}}}{\sigma_{\text{ref}}}},$$

where σ_{ref} is the cross-section calculated with `ggHiggs` [44–55] for each of the A boson mass hypotheses. The calculated observed and expected upper limits are displayed in Figure 8. As a consequence of the higher production cross-sections for lower A boson masses, the upper limits are more stringent for the lower signal-mass hypotheses around 40 GeV and rise with increasing mass. The quadratic $|\zeta_{\text{u}}|$ dependence attenuates this effect slightly.

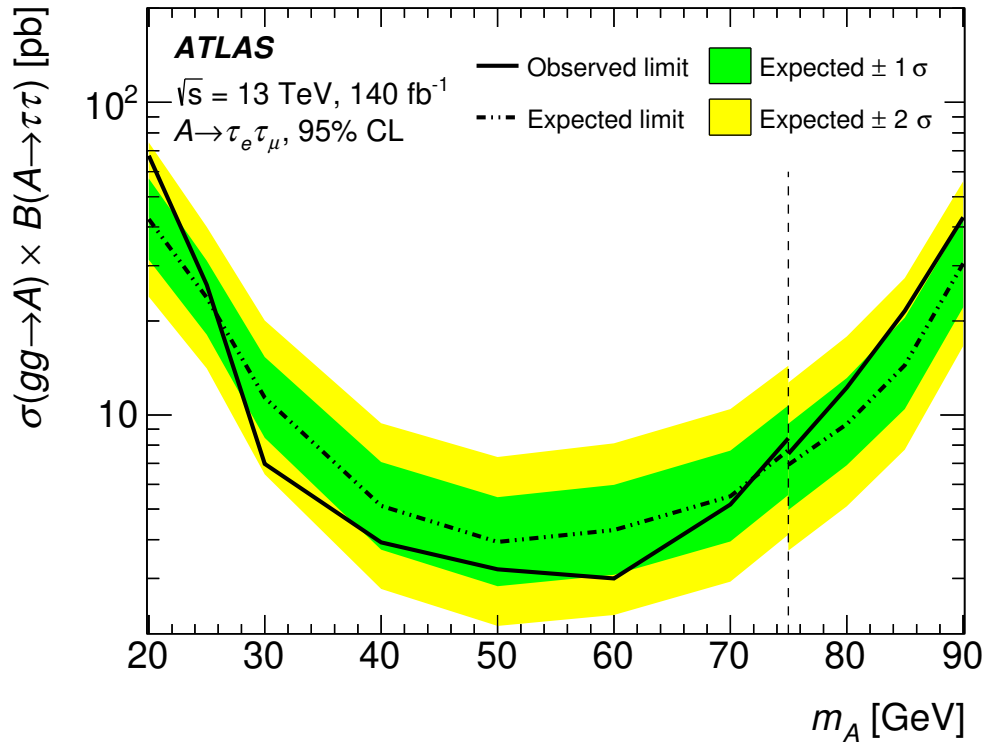


Figure 7: Expected and observed upper limits on the $gg \rightarrow A$ production cross-section times the branching ratio for A boson decay into two τ -leptons, for A boson masses from 20 to 90 GeV. The dash-dotted line shows the expected limit with its 1σ and 2σ uncertainty bands in green and yellow. The solid line shows the observed limit. The vertical dashed line indicates the splitting of the SR: the mass hypotheses on the left side are analysed within the low-mass SR and the ones on the right side in the high-mass SR.

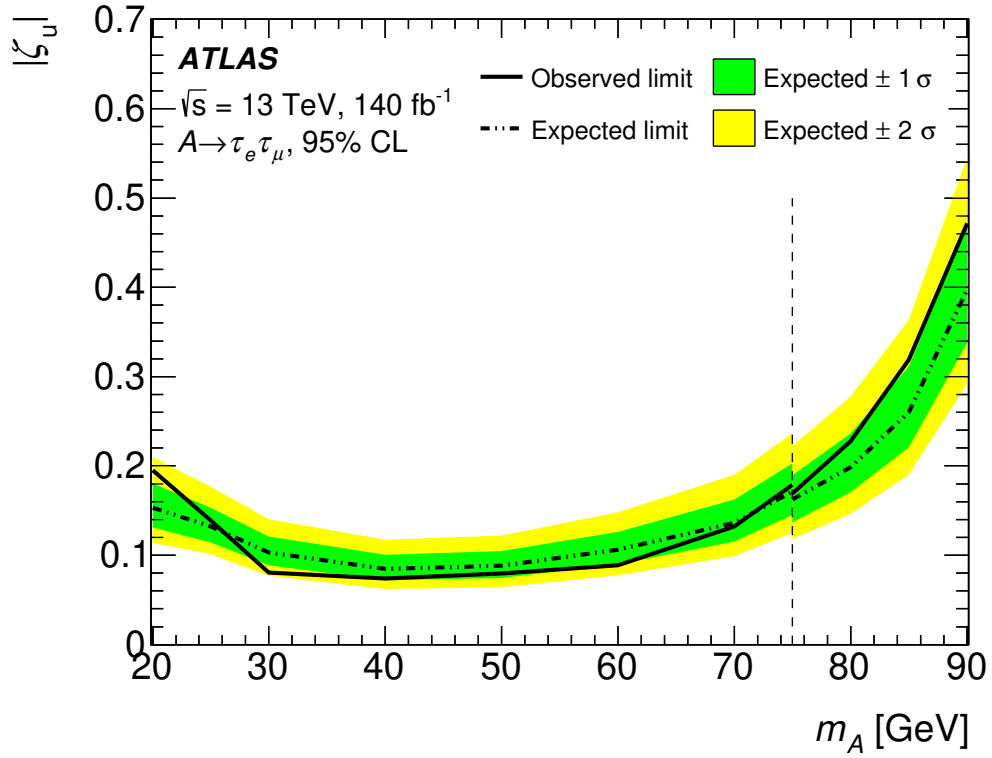


Figure 8: Expected and observed upper limits on the absolute value of the up-type quark coupling parameter $|\zeta_u|$ for masses of the A boson ranging from 20 to 90 GeV. The dash-dotted line shows the expected limit with its 1σ and 2σ uncertainty bands in green and yellow. The solid line shows the observed limit. The vertical dashed line indicates the splitting of the SR: the mass hypotheses on the left side are analysed within the low-mass SR and the ones on the right side in the high-mass SR.

9 Conclusion

A search for a light CP-odd Higgs boson, A , produced in proton–proton collisions at a centre-of-mass energy of 13 TeV during Run 2 of the LHC has been carried out, using the 140 fb^{-1} dataset collected with the ATLAS detector. Results are reported for the decay channels $A \rightarrow \tau^+ \tau^- \rightarrow \mu^+ \nu_\mu \bar{\nu}_\tau e^- \bar{\nu}_e \nu_\tau$ and $A \rightarrow \tau^+ \tau^- \rightarrow e^+ \nu_e \bar{\nu}_\tau \mu^- \bar{\nu}_\mu \nu_\tau$. The search is performed separately in low-mass and high-mass signal regions in order to optimize the signal sensitivity. A data-driven matrix method is applied to estimate the background of fake and non-prompt leptons. Other background expectations are determined by MC simulations. The m_{MMC} variable is used as an estimator of the invariant mass of the τ -lepton pair. Its distributions in the low-mass and high-mass signal regions are utilised in the statistical interpretation of the data. No significant excess of events above the SM background prediction is observed. The 95% CL upper limits placed on the gluon–gluon fusion production cross-section for a CP-odd Higgs boson decaying into the $\tau^+ \tau^-$ final state vary between 3.0 pb and 68 pb in the A boson mass range between 20 GeV and 90 GeV. The mass range below 60 GeV had not been probed before. An interpretation of the results in the context of the flavour-aligned two-Higgs-doublet model is also given. Upper limits between 0.074 and 0.47 at 95% CL are set on the absolute value of the up-type quark coupling parameter $|\zeta_u|$, improving on previous limits on this parameter [16].

Acknowledgements

We thank CERN for the very successful operation of the LHC and its injectors, as well as the support staff at CERN and at our institutions worldwide without whom ATLAS could not be operated efficiently.

The crucial computing support from all WLCG partners is acknowledged gratefully, in particular from CERN, the ATLAS Tier-1 facilities at TRIUMF/SFU (Canada), NDGF (Denmark, Norway, Sweden), CC-IN2P3 (France), KIT/GridKA (Germany), INFN-CNAF (Italy), NL-T1 (Netherlands), PIC (Spain), RAL (UK) and BNL (USA), the Tier-2 facilities worldwide and large non-WLCG resource providers. Major contributors of computing resources are listed in Ref. [132].

We gratefully acknowledge the support of ANPCyT, Argentina; YerPhI, Armenia; ARC, Australia; BMWFW and FWF, Austria; ANAS, Azerbaijan; CNPq and FAPESP, Brazil; NSERC, NRC and CFI, Canada; CERN; ANID, Chile; CAS, MOST and NSFC, China; Minciencias, Colombia; MEYS CR, Czech Republic; DNRF and DNSRC, Denmark; IN2P3-CNRS and CEA-DRF/IRFU, France; SRNSFG, Georgia; BMBF, HGF and MPG, Germany; GSRI, Greece; RGC and Hong Kong SAR, China; ISF and Benozziyo Center, Israel; INFN, Italy; MEXT and JSPS, Japan; CNRST, Morocco; NWO, Netherlands; RCN, Norway; MNiSW, Poland; FCT, Portugal; MNE/IFA, Romania; MSTDI, Serbia; MSSR, Slovakia; ARIS and MVZI, Slovenia; DSI/NRF, South Africa; MICIU/AEI, Spain; SRC and Wallenberg Foundation, Sweden; SERI, SNSF and Cantons of Bern and Geneva, Switzerland; NSTC, Taipei; TENMAK, Türkiye; STFC/UKRI, United Kingdom; DOE and NSF, United States of America.

Individual groups and members have received support from BCKDF, CANARIE, CRC and DRAC, Canada; CERN-CZ, FORTE and PRIMUS, Czech Republic; COST, ERC, ERDF, Horizon 2020, ICSC-NextGenerationEU and Marie Skłodowska-Curie Actions, European Union; Investissements d’Avenir Labex, Investissements d’Avenir Idex and ANR, France; DFG and AvH Foundation, Germany; Herakleitos, Thales and Aristeia programmes co-financed by EU-ESF and the Greek NSRF, Greece; BSF-NSF and MINERVA, Israel; NCN and NAWA, Poland; La Caixa Banking Foundation, CERCA Programme Generalitat de

Catalunya and PROMETEO and GenT Programmes Generalitat Valenciana, Spain; Göran Gustafssons Stiftelse, Sweden; The Royal Society and Leverhulme Trust, United Kingdom.

In addition, individual members wish to acknowledge support from Armenia: Yerevan Physics Institute (FAPERJ); CERN: European Organization for Nuclear Research (CERN PJA5); Chile: Agencia Nacional de Investigación y Desarrollo (FONDECYT 1230812, FONDECYT 1230987, FONDECYT 1240864); China: Chinese Ministry of Science and Technology (MOST-2023YFA1605700), National Natural Science Foundation of China (NSFC - 12175119, NSFC 12275265, NSFC-12075060); Czech Republic: Czech Science Foundation (GACR - 24-11373S), Ministry of Education Youth and Sports (FORTE CZ.02.01.01/00/22_008/0004632), PRIMUS Research Programme (PRIMUS/21/SCI/017); EU: H2020 European Research Council (ERC - 101002463); European Union: European Research Council (ERC - 948254, ERC 101089007), European Union, Future Artificial Intelligence Research (FAIR-NextGenerationEU PE00000013), Italian Center for High Performance Computing, Big Data and Quantum Computing (ICSC, NextGenerationEU); France: Agence Nationale de la Recherche (ANR-20-CE31-0013, ANR-21-CE31-0013, ANR-21-CE31-0022, ANR-22-EDIR-0002); Germany: Baden-Württemberg Stiftung (BW Stiftung-Postdoc Eliteprogramme), Deutsche Forschungsgemeinschaft (DFG - 469666862, DFG - CR 312/5-2); Italy: Istituto Nazionale di Fisica Nucleare (ICSC, NextGenerationEU), Ministero dell'Università e della Ricerca (PRIN - 20223N7F8K - PNRR M4.C2.1.1); Japan: Japan Society for the Promotion of Science (JSPS KAKENHI JP22H01227, JSPS KAKENHI JP22H04944, JSPS KAKENHI JP22KK0227, JSPS KAKENHI JP23KK0245); Netherlands: Netherlands Organisation for Scientific Research (NWO Veni 2020 - VI.Veni.202.179); Norway: Research Council of Norway (RCN-314472); Poland: Ministry of Science and Higher Education (IDUB AGH, POB8, D4 no 9722), Polish National Agency for Academic Exchange (PPN/PPO/2020/1/00002/U/00001), Polish National Science Centre (NCN 2021/42/E/ST2/00350, NCN OPUS nr 2022/47/B/ST2/03059, NCN UMO-2019/34/E/ST2/00393, UMO-2020/37/B/ST2/01043, UMO-2021/40/C/ST2/00187, UMO-2022/47/O/ST2/00148, UMO-2023/49/B/ST2/04085, UMO-2023/51/B/ST2/00920); Slovenia: Slovenian Research Agency (ARIS grant J1-3010); Spain: Generalitat Valenciana (Artemisa, FEDER, IDIFEDER/2018/048), Ministry of Science and Innovation (MCIN & NextGenEU PCI2022-135018-2, MICIN & FEDER PID2021-125273NB, RYC2019-028510-I, RYC2020-030254-I, RYC2021-031273-I, RYC2022-038164-I); Sweden: Swedish Research Council (Swedish Research Council 2023-04654, VR 2018-00482, VR 2022-03845, VR 2022-04683, VR 2023-03403, VR grant 2021-03651), Knut and Alice Wallenberg Foundation (KAW 2018.0458, KAW 2019.0447, KAW 2022.0358); Switzerland: Swiss National Science Foundation (SNSF - PCEFP2_194658); United Kingdom: Leverhulme Trust (Leverhulme Trust RPG-2020-004), Royal Society (NIF-R1-231091); United States of America: U.S. Department of Energy (ECA DE-AC02-76SF00515), Neubauer Family Foundation.

References

- [1] ATLAS Collaboration, *Observation of a new particle in the search for the Standard Model Higgs boson with the ATLAS detector at the LHC*, *Phys. Lett. B* **716** (2012) 1, arXiv: [1207.7214 \[hep-ex\]](#).
- [2] CMS Collaboration, *Observation of a new boson at a mass of 125 GeV with the CMS experiment at the LHC*, *Phys. Lett. B* **716** (2012) 30, arXiv: [1207.7235 \[hep-ex\]](#).
- [3] L. Evans and P. Bryant, *LHC Machine*, *JINST* **3** (2008) S08001.
- [4] ATLAS Collaboration, *A detailed map of Higgs boson interactions by the ATLAS experiment ten years after the discovery*, *Nature* **607** (2022) 52, arXiv: [2207.00092 \[hep-ex\]](#), Erratum: *Nature* **612** (2022) E24.
- [5] CMS Collaboration, *A portrait of the Higgs boson by the CMS experiment ten years after the discovery*, *Nature* **607** (2022) 60, arXiv: [2207.00043 \[hep-ex\]](#), Erratum: *Nature* **623** (2023) E4.
- [6] A. Djouadi, *The anatomy of electroweak symmetry breaking Tome II: The Higgs bosons in the Minimal Supersymmetric Model*, *Phys. Rept.* **459** (2008) 1, arXiv: [hep-ph/0503173 \[hep-ph\]](#).
- [7] G. Branco et al., *Theory and phenomenology of two-Higgs-doublet models*, *Phys. Rept.* **516** (2012) 1, arXiv: [1106.0034 \[hep-ph\]](#).
- [8] A. Pich and P. Tuzon, *Yukawa Alignment in the Two-Higgs-Doublet Model*, *Phys. Rev. D* **80** (2009) 091702, arXiv: [0908.1554 \[hep-ph\]](#).
- [9] T. Aoyama et al., *The anomalous magnetic moment of the muon in the Standard Model*, *Phys. Rept.* **887** (2020) 1, arXiv: [2006.04822 \[hep-ph\]](#).
- [10] Muon $g - 2$ Collaboration, *Measurement of the Positive Muon Anomalous Magnetic Moment to 0.46 ppm*, *Phys. Rev. Lett.* **126** (2021) 141801, arXiv: [2104.03281 \[hep-ex\]](#).
- [11] Muon $g - 2$ Collaboration, *Measurement of the Positive Muon Anomalous Magnetic Moment to 0.20 ppm*, *Phys. Rev. Lett.* **131** (2023) 161802, arXiv: [2308.06230 \[hep-ex\]](#).
- [12] G. Colangelo et al., *Prospects for precise predictions of a_μ in the Standard Model*, (2022), arXiv: [2203.15810 \[hep-ph\]](#).
- [13] S. Borsanyi et al., *Leading hadronic contribution to the muon magnetic moment from lattice QCD*, *Nature* **593** (2021) 51, arXiv: [2002.12347 \[hep-lat\]](#).
- [14] A. Boccaletti et al., *High precision calculation of the hadronic vacuum polarisation contribution to the muon anomaly*, (2024), arXiv: [2407.10913 \[hep-lat\]](#).
- [15] CMD-3 Collaboration, *Measurement of the $e^+e^- \rightarrow \pi^+\pi^-$ cross section from threshold to 1.2 GeV with the CMD-3 detector*, *Phys. Rev. D* **109** (2024) 112002, arXiv: [2302.08834 \[hep-ex\]](#).
- [16] A. Cherchiglia, D. Stöckinger and H. Stöckinger-Kim, *Muon $g - 2$ in the 2HDM: Maximum results and detailed phenomenology*, *Phys. Rev. D* **98** (2018) 035001, arXiv: [1711.11567 \[hep-ph\]](#).

- [17] S. M. Barr and A. Zee, *Electric Dipole Moment of the Electron and of the Neutron*, *Phys. Rev. Lett.* **65** (1990) 21, Erratum: *Phys. Rev. Lett.* **65** (1990) 2920.
- [18] V. Ilisie, *New Barr-Zee contributions to $(g - 2)_\mu$ in two-Higgs-doublet models*, *JHEP* **04** (2015) 077, arXiv: [1502.04199](https://arxiv.org/abs/1502.04199) [[hep-ph](#)].
- [19] D. Chang, W.-F. Chang, C.-H. Chou and W.-Y. Keung, *Large two loop contributions to $g - 2$ from a generic pseudoscalar boson*, *Phys. Rev. D* **63** (2001) 091301, arXiv: [hep-ph/0009292](https://arxiv.org/abs/hep-ph/0009292).
- [20] K.-m. Cheung, C.-H. Chou and O. C. W. Kong, *Muon anomalous magnetic moment, two Higgs doublet model, and supersymmetry*, *Phys. Rev. D* **64** (2001) 111301, arXiv: [hep-ph/0103183](https://arxiv.org/abs/hep-ph/0103183).
- [21] Y.-L. Wu and Y.-F. Zhou, *Muon anomalous magnetic moment in the standard model with two Higgs doublets*, *Phys. Rev. D* **64** (2001) 115018, arXiv: [hep-ph/0104056](https://arxiv.org/abs/hep-ph/0104056).
- [22] M. Krawczyk, *Precision muon $g - 2$ results and light Higgs bosons in the 2HDM(II)*, *Acta Phys. Polon. B* **33** (2002) 2621, arXiv: [hep-ph/0208076](https://arxiv.org/abs/hep-ph/0208076).
- [23] P. Athron et al., *New physics explanations of a_μ in light of the FNAL muon $g - 2$ measurement*, *JHEP* **09** (2021) 080, arXiv: [2104.03691](https://arxiv.org/abs/2104.03691) [[hep-ph](#)].
- [24] ATLAS Collaboration, *Search for neutral MSSM Higgs bosons decaying to $\tau^+\tau^-$ pairs in proton–proton collisions at $\sqrt{s} = 7$ TeV with the ATLAS detector*, *Phys. Lett. B* **705** (2011) 174, arXiv: [1107.5003](https://arxiv.org/abs/1107.5003) [[hep-ex](#)].
- [25] ATLAS Collaboration, *Search for neutral Higgs bosons of the minimal supersymmetric standard model in pp collisions at $\sqrt{s} = 8$ TeV with the ATLAS detector*, *JHEP* **11** (2014) 056, arXiv: [1409.6064](https://arxiv.org/abs/1409.6064) [[hep-ex](#)].
- [26] ATLAS Collaboration, *Search for Heavy Higgs Bosons Decaying into Two Tau Leptons with the ATLAS Detector Using pp Collisions at $\sqrt{s} = 13$ TeV*, *Phys. Rev. Lett.* **125** (2020) 051801, arXiv: [2002.12223](https://arxiv.org/abs/2002.12223) [[hep-ex](#)].
- [27] CMS Collaboration, *Search for additional neutral MSSM Higgs bosons in the $\tau\tau$ final state in proton–proton collisions at $\sqrt{s} = 13$ TeV*, *JHEP* **09** (2018) 007, arXiv: [1803.06553](https://arxiv.org/abs/1803.06553) [[hep-ex](#)].
- [28] CMS Collaboration, *Searches for additional Higgs bosons and for vector leptoquarks in $\tau\tau$ final states in proton–proton collisions at $\sqrt{s} = 13$ TeV*, *JHEP* **07** (2023) 073, arXiv: [2208.02717](https://arxiv.org/abs/2208.02717) [[hep-ex](#)].
- [29] Particle Data Group, R. L. Workman et al., *Review of Particle Physics*, *PTEP* **2022** (2022) 083C01.
- [30] ATLAS Collaboration, *The ATLAS Experiment at the CERN Large Hadron Collider*, *JINST* **3** (2008) S08003.
- [31] ATLAS Collaboration, *ATLAS Insertable B-Layer: Technical Design Report*, ATLAS-TDR-19; CERN-LHCC-2010-013, 2010, URL: <https://cds.cern.ch/record/1291633>, Addendum: ATLAS-TDR-19-ADD-1; CERN-LHCC-2012-009, 2012, URL: <https://cds.cern.ch/record/1451888>.
- [32] B. Abbott et al., *Production and integration of the ATLAS Insertable B-Layer*, *JINST* **13** (2018) T05008, arXiv: [1803.00844](https://arxiv.org/abs/1803.00844) [[physics.ins-det](#)].
- [33] G. Avoni et al., *The new LUCID-2 detector for luminosity measurement and monitoring in ATLAS*, *JINST* **13** (2018) P07017.

- [34] ATLAS Collaboration, *Performance of the ATLAS trigger system in 2015*, *Eur. Phys. J. C* **77** (2017) 317, arXiv: [1611.09661 \[hep-ex\]](#).
- [35] ATLAS Collaboration, *Software and computing for Run 3 of the ATLAS experiment at the LHC*, (2024), arXiv: [2404.06335 \[hep-ex\]](#).
- [36] ATLAS Collaboration, *Luminosity determination in pp collisions at $\sqrt{s} = 13$ TeV using the ATLAS detector at the LHC*, *Eur. Phys. J. C* **83** (2023) 982, arXiv: [2212.09379 \[hep-ex\]](#).
- [37] ATLAS Collaboration, *Performance of electron and photon triggers in ATLAS during LHC Run 2*, *Eur. Phys. J. C* **80** (2020) 47, arXiv: [1909.00761 \[hep-ex\]](#).
- [38] ATLAS Collaboration, *Performance of the ATLAS muon triggers in Run 2*, *JINST* **15** (2020) P09015, arXiv: [2004.13447 \[physics.ins-det\]](#).
- [39] S. Agostinelli et al., *GEANT4 – a simulation toolkit*, *Nucl. Instrum. Meth. A* **506** (2003) 250.
- [40] ATLAS Collaboration, *The ATLAS Simulation Infrastructure*, *Eur. Phys. J. C* **70** (2010) 823, arXiv: [1005.4568 \[physics.ins-det\]](#).
- [41] ATLAS Collaboration, *The simulation principle and performance of the ATLAS fast calorimeter simulation FastCaloSim*, ATL-PHYS-PUB-2010-013, 2010, URL: <https://cds.cern.ch/record/1300517>.
- [42] T. Sjöstrand et al., *An introduction to PYTHIA 8.2*, *Comput. Phys. Commun.* **191** (2015) 159, arXiv: [1410.3012 \[hep-ph\]](#).
- [43] NNPDF Collaboration, R. D. Ball et al., *Parton distributions with LHC data*, *Nucl. Phys. B* **867** (2013) 244, arXiv: [1207.1303 \[hep-ph\]](#).
- [44] R. D. Ball, M. Bonvini, S. Forte, S. Marzani and G. Ridolfi, *Higgs production in gluon fusion beyond NNLO*, *Nucl. Phys. B* **874** (2013) 746, arXiv: [1303.3590 \[hep-ph\]](#).
- [45] M. Bonvini, R. D. Ball, S. Forte, S. Marzani and G. Ridolfi, *Updated Higgs cross section at approximate N^3LO* , *J. Phys. G* **41** (2014) 095002, arXiv: [1404.3204 \[hep-ph\]](#).
- [46] M. Bonvini, S. Marzani, C. Muselli and L. Rottoli, *On the Higgs cross section at N^3LO+N^3LL and its uncertainty*, *JHEP* **08** (2016) 105, arXiv: [1603.08000 \[hep-ph\]](#).
- [47] T. Ahmed et al., *Pseudo-scalar Higgs boson production at $N^3LO_A + N^3LL$* , *Eur. Phys. J. C* **76** (2016) 663, arXiv: [1606.00837 \[hep-ph\]](#).
- [48] M. Bonvini and S. Marzani, *Double resummation for Higgs production*, *Phys. Rev. Lett.* **120** (2018) 202003, arXiv: [1802.07758 \[hep-ph\]](#).
- [49] M. Bonvini, *An approximate N^3LO cross section for Higgs production in gluon fusion*, *EPJ Web Conf.* **60** (2013) 12008, ed. by M. Bosman, A. Juste, M. Martinez and V. Sorin, arXiv: [1306.6633 \[hep-ph\]](#).
- [50] R. V. Harlander and W. B. Kilgore, *Next-to-next-to-leading order Higgs production at hadron colliders*, *Phys. Rev. Lett.* **88** (2002) 201801, arXiv: [hep-ph/0201206](#).

- [51] R. V. Harlander and K. J. Ozeren, *Finite top mass effects for hadronic Higgs production at next-to-next-to-leading order*, [JHEP **11** \(2009\) 088](#), arXiv: [0909.3420 \[hep-ph\]](#).
- [52] R. V. Harlander, H. Mantler, S. Marzani and K. J. Ozeren, *Higgs production in gluon fusion at next-to-next-to-leading order QCD for finite top mass*, [Eur. Phys. J. C **66** \(2010\) 359](#), arXiv: [0912.2104 \[hep-ph\]](#).
- [53] C. Anastasiou et al., *Higgs boson gluon-fusion production beyond threshold in N^3 LO QCD*, [JHEP **03** \(2015\) 091](#), arXiv: [1411.3584 \[hep-ph\]](#).
- [54] C. Anastasiou et al., *High precision determination of the gluon fusion Higgs boson cross-section at the LHC*, [JHEP **05** \(2016\) 058](#), arXiv: [1602.00695 \[hep-ph\]](#).
- [55] B. Mistlberger, *Higgs boson production at hadron colliders at N^3 LO in QCD*, [JHEP **05** \(2018\) 028](#), arXiv: [1802.00833 \[hep-ph\]](#).
- [56] E. Bothmann et al., *Event generation with Sherpa 2.2*, [SciPost Phys. **7** \(2019\) 034](#), arXiv: [1905.09127 \[hep-ph\]](#).
- [57] S. Frixione, G. Ridolfi and P. Nason, *A positive-weight next-to-leading-order Monte Carlo for heavy flavour hadroproduction*, [JHEP **09** \(2007\) 126](#), arXiv: [0707.3088 \[hep-ph\]](#).
- [58] P. Nason, *A new method for combining NLO QCD with shower Monte Carlo algorithms*, [JHEP **11** \(2004\) 040](#), arXiv: [hep-ph/0409146](#).
- [59] S. Frixione, P. Nason and C. Oleari, *Matching NLO QCD computations with parton shower simulations: the POWHEG method*, [JHEP **11** \(2007\) 070](#), arXiv: [0709.2092 \[hep-ph\]](#).
- [60] S. Alioli, P. Nason, C. Oleari and E. Re, *A general framework for implementing NLO calculations in shower Monte Carlo programs: the POWHEG BOX*, [JHEP **06** \(2010\) 043](#), arXiv: [1002.2581 \[hep-ph\]](#).
- [61] NNPDF Collaboration, R. D. Ball et al., *Parton distributions for the LHC run II*, [JHEP **04** \(2015\) 040](#), arXiv: [1410.8849 \[hep-ph\]](#).
- [62] ATLAS Collaboration, *ATLAS Pythia 8 tunes to 7 TeV data*, ATL-PHYS-PUB-2014-021, 2014, URL: <https://cds.cern.ch/record/1966419>.
- [63] S. Schumann and F. Krauss, *A parton shower algorithm based on Catani–Seymour dipole factorisation*, [JHEP **03** \(2008\) 038](#), arXiv: [0709.1027 \[hep-ph\]](#).
- [64] S. Höche, F. Krauss, M. Schönherr and F. Siegert, *A critical appraisal of NLO+PS matching methods*, [JHEP **09** \(2012\) 049](#), arXiv: [1111.1220 \[hep-ph\]](#).
- [65] S. Höche, F. Krauss, M. Schönherr and F. Siegert, *QCD matrix elements + parton showers. The NLO case*, [JHEP **04** \(2013\) 027](#), arXiv: [1207.5030 \[hep-ph\]](#).
- [66] S. Catani, F. Krauss, B. R. Webber and R. Kuhn, *QCD Matrix Elements + Parton Showers*, [JHEP **11** \(2001\) 063](#), arXiv: [hep-ph/0109231](#).

- [67] S. Höche, F. Krauss, S. Schumann and F. Siegert, *QCD matrix elements and truncated showers*, *JHEP* **05** (2009) 053, arXiv: [0903.1219](#) [[hep-ph](#)].
- [68] K. Hamilton, P. Nason, E. Re and G. Zanderighi, *NNLOPS simulation of Higgs boson production*, *JHEP* **10** (2013) 222, arXiv: [1309.0017](#) [[hep-ph](#)].
- [69] K. Hamilton, P. Nason and G. Zanderighi, *Finite quark-mass effects in the NNLOPS POWHEG+MiNLO Higgs generator*, *JHEP* **05** (2015) 140, arXiv: [1501.04637](#) [[hep-ph](#)].
- [70] J. Butterworth et al., *PDF4LHC recommendations for LHC Run II*, *J. Phys. G* **43** (2016) 023001, arXiv: [1510.03865](#) [[hep-ph](#)].
- [71] ATLAS Collaboration, *Measurement of the Z/γ^* boson transverse momentum distribution in pp collisions at $\sqrt{s} = 7$ TeV with the ATLAS detector*, *JHEP* **09** (2014) 145, arXiv: [1406.3660](#) [[hep-ex](#)].
- [72] A. Djouadi, J. Kalinowski and M. Spira, *HDECAY: a program for Higgs boson decays in the Standard Model and its supersymmetric extension*, *Comput. Phys. Commun.* **108** (1998) 56, arXiv: [hep-ph/9704448](#).
- [73] M. Spira, *QCD Effects in Higgs Physics*, *Fortsch. Phys.* **46** (1998) 203, arXiv: [hep-ph/9705337](#).
- [74] A. Djouadi, M. M. Mühlleitner and M. Spira, *Decays of Supersymmetric Particles: the Program SUSY-HIT (SUSpect-SdecaY-Hdecay-InTerface)*, *Acta Phys. Polon. B* **38** (2007) 635, arXiv: [hep-ph/0609292](#).
- [75] A. Bredenstein, A. Denner, S. Dittmaier and M. M. Weber, *Radiative corrections to the semileptonic and hadronic Higgs-boson decays $H \rightarrow WW/ZZ \rightarrow 4$ fermions*, *JHEP* **02** (2007) 080, arXiv: [hep-ph/0611234](#).
- [76] A. Bredenstein, A. Denner, S. Dittmaier and M. M. Weber, *Precise predictions for the Higgs-boson decay $H \rightarrow WW/ZZ \rightarrow 4$ leptons*, *Phys. Rev. D* **74** (2006) 013004, arXiv: [hep-ph/0604011](#) [[hep-ph](#)].
- [77] A. Bredenstein, A. Denner, S. Dittmaier and M. M. Weber, *Precision calculations for the Higgs decays $H \rightarrow ZZ/WW \rightarrow 4$ leptons*, *Nucl. Phys. B Proc. Suppl.* **160** (2006) 131, arXiv: [hep-ph/0607060](#) [[hep-ph](#)].
- [78] D. de Florian et al., *Handbook of LHC Higgs Cross Sections: 4. Deciphering the Nature of the Higgs Sector*, (2017), arXiv: [1610.07922](#) [[hep-ph](#)].
- [79] C. Anastasiou, C. Duhr, F. Dulat, F. Herzog and B. Mistlberger, *Higgs Boson Gluon-Fusion Production in QCD at Three Loops*, *Phys. Rev. Lett.* **114** (2015) 212001, arXiv: [1503.06056](#) [[hep-ph](#)].
- [80] F. Dulat, A. Lazopoulos and B. Mistlberger, *iHixs 2 – Inclusive Higgs cross sections*, *Comput. Phys. Commun.* **233** (2018) 243, arXiv: [1802.00827](#) [[hep-ph](#)].
- [81] R. V. Harlander and K. J. Ozeren, *Top mass effects in Higgs production at next-to-next-to-leading order QCD: Virtual corrections*, *Phys. Lett. B* **679** (2009) 467, arXiv: [0907.2997](#) [[hep-ph](#)].
- [82] A. Pak, M. Rogal and M. Steinhauser, *Finite top quark mass effects in NNLO Higgs boson production at LHC*, *JHEP* **02** (2010) 025, arXiv: [0911.4662](#) [[hep-ph](#)].

- [83] S. Actis, G. Passarino, C. Sturm and S. Uccirati, *NLO electroweak corrections to Higgs boson production at hadron colliders*, [Phys. Lett. B **670** \(2008\) 12](#), arXiv: [0809.1301 \[hep-ph\]](#).
- [84] S. Actis, G. Passarino, C. Sturm and S. Uccirati, *NNLO computational techniques: The cases $H \rightarrow \gamma\gamma$ and $H \rightarrow gg$* , [Nucl. Phys. B **811** \(2009\) 182](#), arXiv: [0809.3667 \[hep-ph\]](#).
- [85] M. Bonetti, K. Melnikov and L. Tancredi, *Higher order corrections to mixed QCD-EW contributions to Higgs boson production in gluon fusion*, [Phys. Rev. D **97** \(2018\) 056017](#), arXiv: [1801.10403 \[hep-ph\]](#), Erratum: [Phys. Rev. D **97** \(2018\) 099906\(E\)](#).
- [86] M. Ciccolini, A. Denner and S. Dittmaier, *Strong and Electroweak Corrections to the Production of a Higgs Boson + 2 Jets via Weak Interactions at the Large Hadron Collider*, [Phys. Rev. Lett. **99** \(2007\) 161803](#), arXiv: [0707.0381 \[hep-ph\]](#).
- [87] M. Ciccolini, A. Denner and S. Dittmaier, *Electroweak and QCD corrections to Higgs production via vector-boson fusion at the CERN LHC*, [Phys. Rev. D **77** \(2008\) 013002](#), arXiv: [0710.4749 \[hep-ph\]](#).
- [88] P. Bolzoni, F. Maltoni, S.-O. Moch and M. Zaro, *Higgs Boson Production via Vector-Boson Fusion at Next-to-Next-to-Leading Order in QCD*, [Phys. Rev. Lett. **105** \(2010\) 011801](#), arXiv: [1003.4451 \[hep-ph\]](#).
- [89] M. L. Ciccolini, S. Dittmaier and M. Krämer, *Electroweak radiative corrections to associated WH and ZH production at hadron colliders*, [Phys. Rev. D **68** \(2003\) 073003](#), arXiv: [hep-ph/0306234 \[hep-ph\]](#).
- [90] O. Brein, A. Djouadi and R. Harlander, *NNLO QCD corrections to the Higgs-strahlung processes at hadron colliders*, [Phys. Lett. B **579** \(2004\) 149](#), arXiv: [hep-ph/0307206](#).
- [91] O. Brein, R. V. Harlander, M. Wiesemann and T. Zirke, *Top-quark mediated effects in hadronic Higgs-Strahlung*, [Eur. Phys. J. C **72** \(2012\) 1868](#), arXiv: [1111.0761 \[hep-ph\]](#).
- [92] L. Altenkamp, S. Dittmaier, R. V. Harlander, H. Rzehak and T. J. E. Zirke, *Gluon-induced Higgs-strahlung at next-to-leading order QCD*, [JHEP **02** \(2013\) 078](#), arXiv: [1211.5015 \[hep-ph\]](#).
- [93] A. Denner, S. Dittmaier, S. Kallweit and A. Mück, *HAWK 2.0: A Monte Carlo program for Higgs production in vector-boson fusion and Higgs strahlung at hadron colliders*, [Comput. Phys. Commun. **195** \(2015\) 161](#), arXiv: [1412.5390 \[hep-ph\]](#).
- [94] O. Brein, R. V. Harlander and T. J. E. Zirke, *vh@nnlo – Higgs Strahlung at hadron colliders*, [Comput. Phys. Commun. **184** \(2013\) 998](#), arXiv: [1210.5347 \[hep-ph\]](#).
- [95] R. V. Harlander, A. Kulesza, V. Theeuwes and T. Zirke, *Soft gluon resummation for gluon-induced Higgs Strahlung*, [JHEP **11** \(2014\) 082](#), arXiv: [1410.0217 \[hep-ph\]](#).
- [96] T. Sjöstrand, S. Mrenna and P. Skands, *A brief introduction to PYTHIA 8.1*, [Comput. Phys. Commun. **178** \(2008\) 852](#), arXiv: [0710.3820 \[hep-ph\]](#).
- [97] ATLAS Collaboration, *The Pythia 8 A3 tune description of ATLAS minimum bias and inelastic measurements incorporating the Donnachie–Landshoff diffractive model*, ATL-PHYS-PUB-2016-017, 2016, URL: <https://cds.cern.ch/record/2206965>.

- [98] ATLAS Collaboration, *Vertex Reconstruction Performance of the ATLAS Detector at $\sqrt{s} = 13$ TeV*, ATL-PHYS-PUB-2015-026, 2015, URL: <https://cds.cern.ch/record/2037717>.
- [99] ATLAS Collaboration, *Electron and photon performance measurements with the ATLAS detector using the 2015–2017 LHC proton–proton collision data*, *JINST* **14** (2019) P12006, arXiv: [1908.00005](https://arxiv.org/abs/1908.00005) [hep-ex].
- [100] ATLAS Collaboration, *Muon reconstruction and identification efficiency in ATLAS using the full Run 2 pp collision data set at $\sqrt{s} = 13$ TeV*, *Eur. Phys. J. C* **81** (2021) 578, arXiv: [2012.00578](https://arxiv.org/abs/2012.00578) [hep-ex].
- [101] ATLAS Collaboration, *Jet reconstruction and performance using particle flow with the ATLAS Detector*, *Eur. Phys. J. C* **77** (2017) 466, arXiv: [1703.10485](https://arxiv.org/abs/1703.10485) [hep-ex].
- [102] ATLAS Collaboration, *Jet energy scale and resolution measured in proton–proton collisions at $\sqrt{s} = 13$ TeV with the ATLAS detector*, *Eur. Phys. J. C* **81** (2021) 689, arXiv: [2007.02645](https://arxiv.org/abs/2007.02645) [hep-ex].
- [103] ATLAS Collaboration, *Selection of jets produced in 13 TeV proton–proton collisions with the ATLAS detector*, ATL-CONF-2015-029, 2015, URL: <https://cds.cern.ch/record/2037702>.
- [104] ATLAS Collaboration, *Performance of pile-up mitigation techniques for jets in pp collisions at $\sqrt{s} = 8$ TeV using the ATLAS detector*, *Eur. Phys. J. C* **76** (2016) 581, arXiv: [1510.03823](https://arxiv.org/abs/1510.03823) [hep-ex].
- [105] ATLAS Collaboration, *Identification and rejection of pile-up jets at high pseudorapidity with the ATLAS detector*, *Eur. Phys. J. C* **77** (2017) 580, arXiv: [1705.02211](https://arxiv.org/abs/1705.02211) [hep-ex], Erratum: *Eur. Phys. J. C* **77** (2017) 712.
- [106] ATLAS Collaboration, *ATLAS flavour-tagging algorithms for the LHC Run 2 pp collision dataset*, *Eur. Phys. J. C* **83** (2023) 681, arXiv: [2211.16345](https://arxiv.org/abs/2211.16345) [physics.data-an].
- [107] ATLAS Collaboration, *Reconstruction, Energy Calibration, and Identification of Hadronically Decaying Tau Leptons in the ATLAS Experiment for Run-2 of the LHC*, ATL-PHYS-PUB-2015-045, 2015, URL: <https://cds.cern.ch/record/2064383>.
- [108] ATLAS Collaboration, *The performance of missing transverse momentum reconstruction and its significance with the ATLAS detector using 140fb^{-1} of $\sqrt{s} = 13$ TeV pp collisions*, (2024), arXiv: [2402.05858](https://arxiv.org/abs/2402.05858) [hep-ex].
- [109] A. Elagin, P. Murat, A. Pranko and A. Safonov, *A new mass reconstruction technique for resonances decaying to $\tau\tau$* , *Nucl. Instrum. Meth. A* **654** (2011) 481, arXiv: [1012.4686](https://arxiv.org/abs/1012.4686) [hep-ex].
- [110] ATLAS Collaboration, *Measurements of Higgs boson production cross-sections in the $H \rightarrow \tau^+\tau^-$ decay channel in pp collisions at $\sqrt{s} = 13$ TeV with the ATLAS detector*, *JHEP* **08** (2022) 175, arXiv: [2201.08269](https://arxiv.org/abs/2201.08269) [hep-ex].
- [111] ATLAS Collaboration, *Study of $Z \rightarrow l\bar{l}\gamma$ decays at $\sqrt{s} = 8$ TeV with the ATLAS detector*, *Eur. Phys. J. C* **84** (2023) 195, arXiv: [2310.11574](https://arxiv.org/abs/2310.11574) [hep-ex].
- [112] M. Czakon et al., *Top-pair production at the LHC through NNLO QCD and NLO EW*, *JHEP* **10** (2017) 186, arXiv: [1705.04105](https://arxiv.org/abs/1705.04105) [hep-ph].

- [113] ATLAS Collaboration, *Tools for estimating fake/non-prompt lepton backgrounds with the ATLAS detector at the LHC*, [JINST **18** \(2023\) T11004](#), arXiv: [2211.16178 \[hep-ex\]](#).
- [114] ATLAS Collaboration, *Measurements of b -jet tagging efficiency with the ATLAS detector using $t\bar{t}$ events at $\sqrt{s} = 13$ TeV*, [JHEP **08** \(2018\) 089](#), arXiv: [1805.01845 \[hep-ex\]](#).
- [115] ATLAS Collaboration, *Measurement of the c -jet mistagging efficiency in $t\bar{t}$ events using pp collision data at $\sqrt{s} = 13$ TeV collected with the ATLAS detector*, [Eur. Phys. J. C **82** \(2022\) 95](#), arXiv: [2109.10627 \[hep-ex\]](#).
- [116] ATLAS Collaboration, *Calibration of the light-flavour jet mistagging efficiency of the b -tagging algorithms with Z +jets events using 139 fb^{-1} of ATLAS proton–proton collision data at $\sqrt{s} = 13$ TeV*, [Eur. Phys. J. C **83** \(2023\) 728](#), arXiv: [2301.06319 \[hep-ex\]](#).
- [117] ATLAS Collaboration, *Measurement of W^\pm and Z -boson production cross sections in pp collisions at $\sqrt{s} = 13$ TeV with the ATLAS detector*, [Phys. Lett. B **759** \(2016\) 601](#), arXiv: [1603.09222 \[hep-ex\]](#).
- [118] M. Czakon and A. Mitov, *Top++: A program for the calculation of the top-pair cross-section at hadron colliders*, [Comput. Phys. Commun. **185** \(2014\) 2930](#), arXiv: [1112.5675 \[hep-ph\]](#).
- [119] M. Botje et al., *The PDF4LHC Working Group Interim Recommendations*, (2011), arXiv: [1101.0538 \[hep-ph\]](#).
- [120] A. D. Martin, W. J. Stirling, R. S. Thorne and G. Watt, *Uncertainties on α_S in global PDF analyses and implications for predicted hadronic cross sections*, [Eur. Phys. J. C **64** \(2009\) 653](#), arXiv: [0905.3531 \[hep-ph\]](#).
- [121] J. Gao et al., *CT10 next-to-next-to-leading order global analysis of QCD*, [Phys. Rev. D **89** \(2014\) 033009](#), arXiv: [1302.6246 \[hep-ph\]](#).
- [122] ATLAS Collaboration, *Measurement of fiducial and differential W^+W^- production cross-sections at $\sqrt{s} = 13$ TeV with the ATLAS detector*, [Eur. Phys. J. C **79** \(2019\) 884](#), arXiv: [1905.04242 \[hep-ex\]](#).
- [123] ATLAS Collaboration, *Measurement of ZZ production in the $\ell\ell\nu\nu$ final state with the ATLAS detector in pp collisions at $\sqrt{s} = 13$ TeV*, [JHEP **10** \(2019\) 127](#), arXiv: [1905.07163 \[hep-ex\]](#).
- [124] ATLAS Collaboration, *Measurement of $W^\pm Z$ production cross sections and gauge boson polarisation in pp collisions at $\sqrt{s} = 13$ TeV with the ATLAS detector*, [Eur. Phys. J. C **79** \(2019\) 535](#), arXiv: [1902.05759 \[hep-ex\]](#).
- [125] S. Dulat et al., *New parton distribution functions from a global analysis of quantum chromodynamics*, [Phys. Rev. D **93** \(2016\) 033006](#), arXiv: [1506.07443 \[hep-ph\]](#).
- [126] L. A. Harland-Lang, A. D. Martin, P. Motylinski and R. S. Thorne, *Parton distributions in the LHC era: MMHT 2014 PDFs*, [Eur. Phys. J. C **75** \(2015\) 204](#), arXiv: [1412.3989 \[hep-ph\]](#).
- [127] M. Bähr et al., *Herwig++ physics and manual*, [Eur. Phys. J. C **58** \(2008\) 639](#), arXiv: [0803.0883 \[hep-ph\]](#).

- [128] J. Bellm et al., *Herwig 7.0/Herwig++ 3.0 release note*, *Eur. Phys. J. C* **76** (2016) 196, arXiv: [1512.01178](https://arxiv.org/abs/1512.01178) [[hep-ph](#)].
- [129] J. Alwall et al., *The automated computation of tree-level and next-to-leading order differential cross sections, and their matching to parton shower simulations*, *JHEP* **07** (2014) 079, arXiv: [1405.0301](https://arxiv.org/abs/1405.0301) [[hep-ph](#)].
- [130] G. Cowan, K. Cranmer, E. Gross and O. Vitells, *Asymptotic formulae for likelihood-based tests of new physics*, *Eur. Phys. J. C* **71** (2011) 1554, arXiv: [1007.1727](https://arxiv.org/abs/1007.1727) [[physics.data-an](#)], Erratum: *Eur. Phys. J. C* **73** (2013) 2501.
- [131] A. L. Read, *Presentation of search results: the CL_S technique*, *J. Phys. G* **28** (2002) 2693.
- [132] ATLAS Collaboration, *ATLAS Computing Acknowledgements*, ATL-SOFT-PUB-2023-001, 2023, URL: <https://cds.cern.ch/record/2869272>.

The ATLAS Collaboration

G. Aad ¹⁰⁵, E. Aakvaag ¹⁷, B. Abbott ¹²⁴, S. Abdelhameed ^{120a}, K. Abeling ⁵⁷, N.J. Abicht ⁵¹, S.H. Abidi ³⁰, M. Aboeela ⁴⁶, A. Aboulhorma ^{36e}, H. Abramowicz ¹⁵⁵, H. Abreu ¹⁵⁴, Y. Abulaiti ¹²¹, B.S. Acharya ^{71a,71b,k}, A. Ackermann ^{65a}, C. Adam Bourdarios ⁴, L. Adamczyk ^{88a}, S.V. Addepalli ¹⁴⁷, M.J. Addison ¹⁰⁴, J. Adelman ¹¹⁹, A. Adiguzel ^{22c}, T. Adye ¹³⁸, A.A. Affolder ¹⁴⁰, Y. Afik ⁴¹, M.N. Agaras ¹³, A. Aggarwal ¹⁰³, C. Agheorghiesei ^{28c}, F. Ahmadov ^{40,z}, S. Ahuja ⁹⁸, X. Ai ^{64e}, G. Aielli ^{78a,78b}, A. Aikot ¹⁶⁸, M. Ait Tamliah ^{36e}, B. Aitbenkikh ^{36a}, M. Akbiyik ¹⁰³, T.P.A. Åkesson ¹⁰¹, A.V. Akimov ¹⁴⁹, D. Akiyama ¹⁷³, N.N. Akolkar ²⁵, S. Aktas ^{22a}, K. Al Houry ⁴³, G.L. Alberghi ^{24b}, J. Albert ¹⁷⁰, P. Albicocco ⁵⁵, G.L. Albouy ⁶², S. Alderweireldt ⁵⁴, Z.L. Alegria ¹²⁵, M. Aleksa ³⁷, I.N. Aleksandrov ⁴⁰, C. Alexa ^{28b}, T. Alexopoulos ¹⁰, F. Alfonsi ^{24b}, M. Algren ⁵⁸, M. Alhroob ¹⁷², B. Ali ¹³⁶, H.M.J. Ali ^{94,t}, S. Ali ³², S.W. Alibocus ⁹⁵, M. Aliev ^{34c}, G. Alimonti ^{73a}, W. Alkakh ⁵⁷, C. Allaire ⁶⁸, B.M.M. Allbrooke ¹⁵⁰, J.S. Allen ¹⁰⁴, J.F. Allen ⁵⁴, C.A. Allendes Flores ^{141f}, P.P. Allport ²¹, A. Aloisio ^{74a,74b}, F. Alonso ⁹³, C. Alpigiani ¹⁴², Z.M.K. Alsolami ⁹⁴, M. Alvarez Estevez ¹⁰², A. Alvarez Fernandez ¹⁰³, M. Alves Cardoso ⁵⁸, M.G. Alvigi ^{74a,74b}, M. Aly ¹⁰⁴, Y. Amaral Coutinho ^{85b}, A. Ambler ¹⁰⁷, C. Amelung ³⁷, M. Amerl ¹⁰⁴, C.G. Ames ¹¹², D. Amidei ¹⁰⁹, B. Amini ⁵⁶, K.J. Amirie ¹⁵⁹, S.P. Amor Dos Santos ^{134a}, K.R. Amos ¹⁶⁸, D. Amperiadou ¹⁵⁶, S. An ⁸⁶, V. Ananiev ¹²⁹, C. Anastopoulos ¹⁴³, T. Andeen ¹¹, J.K. Anders ³⁷, A.C. Anderson ⁶¹, A. Andreazza ^{73a,73b}, S. Angelidakis ⁹, A. Angerami ⁴³, A.V. Anisenkov ³⁹, A. Annovi ^{76a}, C. Antel ⁵⁸, E. Antipov ¹⁴⁹, M. Antonelli ⁵⁵, F. Anulli ^{77a}, M. Aoki ⁸⁶, T. Aoki ¹⁵⁷, M.A. Aparo ¹⁵⁰, L. Aperio Bella ⁵⁰, C. Appelt ¹⁵⁵, A. Apyan ²⁷, S.J. Arbiol Val ⁸⁹, C. Arcangeletti ⁵⁵, A.T.H. Arce ⁵³, J-F. Arguin ¹¹¹, S. Argyropoulos ¹⁵⁶, J.-H. Arling ⁵⁰, O. Arnaez ⁴, H. Arnold ¹⁴⁹, G. Artoni ^{77a,77b}, H. Asada ¹¹⁴, K. Asai ¹²², S. Asai ¹⁵⁷, N.A. Asbah ³⁷, R.A. Ashby Pickering ¹⁷², K. Assamagan ³⁰, R. Astalos ^{29a}, K.S.V. Astrand ¹⁰¹, S. Atashi ¹⁶³, R.J. Atkin ^{34a}, H. Atmani ^{36f}, P.A. Atlasiddha ¹³², K. Augsten ¹³⁶, A.D. Auriol ²¹, V.A. Austrup ¹⁰⁴, G. Avolio ³⁷, K. Axiotis ⁵⁸, G. Azuelos ^{111,ad}, D. Babal ^{29b}, H. Bachacou ¹³⁹, K. Bachas ^{156,o}, A. Bachiu ³⁵, E. Bachmann ⁵², A. Badea ⁴¹, T.M. Baer ¹⁰⁹, P. Bagnaia ^{77a,77b}, M. Bahmani ¹⁹, D. Bahner ⁵⁶, K. Bai ¹²⁷, J.T. Baines ¹³⁸, L. Baines ⁹⁷, O.K. Baker ¹⁷⁷, E. Bakos ¹⁶, D. Bakshi Gupta ⁸, L.E. Balabram Filho ^{85b}, V. Balakrishnan ¹²⁴, R. Balasubramanian ⁴, E.M. Baldin ³⁹, P. Balek ^{88a}, E. Ballabene ^{24b,24a}, F. Balli ¹³⁹, L.M. Baltes ^{65a}, W.K. Balunas ³³, J. Balz ¹⁰³, I. Bamwidhi ^{120b}, E. Banas ⁸⁹, M. Bandieramonte ¹³³, A. Bandyopadhyay ²⁵, S. Bansal ²⁵, L. Barak ¹⁵⁵, M. Barakat ⁵⁰, E.L. Barberio ¹⁰⁸, D. Barberis ^{59b,59a}, M. Barbero ¹⁰⁵, M.Z. Barel ¹¹⁸, T. Barillari ¹¹³, M-S. Barisits ³⁷, T. Barklow ¹⁴⁷, P. Baron ¹²⁶, D.A. Baron Moreno ¹⁰⁴, A. Baroncelli ^{64a}, A.J. Barr ¹³⁰, J.D. Barr ⁹⁹, F. Barreiro ¹⁰², J. Barreiro Guimarães da Costa ¹⁴, M.G. Barros Teixeira ^{134a}, S. Barsov ³⁹, F. Bartels ^{65a}, R. Bartoldus ¹⁴⁷, A.E. Barton ⁹⁴, P. Bartos ^{29a}, A. Basan ¹⁰³, M. Baselga ⁵¹, A. Bassalat ^{68,b}, M.J. Basso ^{160a}, S. Bataju ⁴⁶, R. Bate ¹⁶⁹, R.L. Bates ⁶¹, S. Batlamous ¹⁰², B. Batool ¹⁴⁵, M. Battaglia ¹⁴⁰, D. Battulga ¹⁹, M. Bauge ^{77a,77b}, M. Bauer ⁸¹, P. Bauer ²⁵, L.T. Bazzano Hurrell ³¹, J.B. Beacham ⁵³, T. Beau ¹³¹, J.Y. Beaucamp ⁹³, P.H. Beauchemin ¹⁶², P. Bechtel ²⁵, H.P. Beck ^{20,n}, K. Becker ¹⁷², A.J. Beddall ⁸⁴, V.A. Bednyakov ⁴⁰, C.P. Bee ¹⁴⁹, L.J. Beemster ¹⁶, T.A. Beermann ³⁷, M. Begalli ^{85d}, M. Begel ³⁰, A. Behera ¹⁴⁹, J.K. Behr ⁵⁰, J.F. Beirer ³⁷, F. Beisiegel ²⁵, M. Belfkir ^{120b}, G. Bella ¹⁵⁵, L. Bellagamba ^{24b}, A. Bellerive ³⁵, P. Bellos ²¹, K. Beloborodov ³⁹, D. Bencheikroun ^{36a}, F. Bendebba ^{36a}, Y. Benhammou ¹⁵⁵,

K.C. Benkendorfer ⁶³, L. Beresford ⁵⁰, M. Beretta ⁵⁵, E. Bergeaas Kuutmann ¹⁶⁶, N. Berger ⁴,
 B. Bergmann ¹³⁶, J. Beringer ^{18a}, G. Bernardi ⁵, C. Bernius ¹⁴⁷, F.U. Bernlochner ²⁵,
 F. Bernon ³⁷, A. Berrocal Guardia ¹³, T. Berry ⁹⁸, P. Berta ¹³⁷, A. Berthold ⁵², S. Bethke ¹¹³,
 A. Betti ^{77a,77b}, A.J. Bevan ⁹⁷, N.K. Bhalla ⁵⁶, S. Bhatta ¹⁴⁹, D.S. Bhattacharya ¹⁷¹,
 P. Bhattarai ¹⁴⁷, Z.M. Bhatti ¹²¹, K.D. Bhide ⁵⁶, V.S. Bhopatkar ¹²⁵, R.M. Bianchi ¹³³,
 G. Bianco ^{24b,24a}, O. Biebel ¹¹², M. Biglietti ^{79a}, C.S. Billingsley ⁴⁶, Y. Bimgdi ^{36f}, M. Bindi ⁵⁷,
 A. Bingul ^{22b}, C. Bini ^{77a,77b}, G.A. Bird ³³, M. Birman ¹⁷⁴, M. Biros ¹³⁷, S. Biryukov ¹⁵⁰,
 T. Bisanz ⁵¹, E. Bisceglie ^{45b,45a}, J.P. Biswal ¹³⁸, D. Biswas ¹⁴⁵, I. Bloch ⁵⁰, A. Blue ⁶¹,
 U. Blumenschein ⁹⁷, J. Blumenthal ¹⁰³, V.S. Bobrovnikov ³⁹, M. Boehler ⁵⁶, B. Boehm ¹⁷¹,
 D. Bogavac ³⁷, A.G. Bogdanchikov ³⁹, L.S. Boggia ¹³¹, C. Bohm ^{49a}, V. Boisvert ⁹⁸,
 P. Bokan ³⁷, T. Bold ^{88a}, M. Bomben ⁵, M. Bona ⁹⁷, M. Boonekamp ¹³⁹, A.G. Borbély ⁶¹,
 I.S. Bordulev ³⁹, G. Borissov ⁹⁴, D. Bortoletto ¹³⁰, D. Boscherini ^{24b}, M. Bosman ¹³,
 K. Bouaouda ^{36a}, N. Bouchhar ¹⁶⁸, L. Boudet ⁴, J. Boudreau ¹³³, E.V. Bouhova-Thacker ⁹⁴,
 D. Boumediene ⁴², R. Bouquet ^{59b,59a}, A. Boveia ¹²³, J. Boyd ³⁷, D. Boye ³⁰, I.R. Boyko ⁴⁰,
 L. Bozianu ⁵⁸, J. Bracinek ²¹, N. Brahimi ⁴, G. Brandt ¹⁷⁶, O. Brandt ³³, B. Brau ¹⁰⁶,
 J.E. Brau ¹²⁷, R. Brenner ¹⁷⁴, L. Brenner ¹¹⁸, R. Brenner ¹⁶⁶, S. Bressler ¹⁷⁴, G. Brianti ^{80a,80b},
 D. Britton ⁶¹, D. Britzger ¹¹³, I. Brock ²⁵, R. Brock ¹¹⁰, G. Brooijmans ⁴³, A.J. Brooks ⁷⁰,
 E.M. Brooks ^{160b}, E. Brost ³⁰, L.M. Brown ¹⁷⁰, L.E. Bruce ⁶³, T.L. Bruckler ¹³⁰,
 P.A. Bruckman de Renstrom ⁸⁹, B. Brüers ⁵⁰, A. Bruni ^{24b}, G. Bruni ^{24b}, D. Brunner ^{49a,49b},
 M. Bruschi ^{24b}, N. Bruscinò ^{77a,77b}, T. Buanes ¹⁷, Q. Buat ¹⁴², D. Buchin ¹¹³, A.G. Buckley ⁶¹,
 O. Bulekov ³⁹, B.A. Bullard ¹⁴⁷, S. Burdin ⁹⁵, C.D. Burgard ⁵¹, A.M. Burger ³⁷,
 B. Burghgrave ⁸, O. Burlayenko ⁵⁶, J. Burleson ¹⁶⁷, J.T.P. Burr ³³, J.C. Burzynski ¹⁴⁶,
 E.L. Busch ⁴³, V. Büscher ¹⁰³, P.J. Bussey ⁶¹, J.M. Butler ²⁶, C.M. Buttar ⁶¹,
 J.M. Butterworth ⁹⁹, W. Buttinger ¹³⁸, C.J. Buxo Vazquez ¹¹⁰, A.R. Buzykaev ³⁹,
 S. Cabrera Urbán ¹⁶⁸, L. Cadamuro ⁶⁸, D. Caforio ⁶⁰, H. Cai ¹³³, Y. Cai ^{14,115c}, Y. Cai ^{115a},
 V.M.M. Cairo ³⁷, O. Cakir ^{3a}, N. Calace ³⁷, P. Calafiura ^{18a}, G. Calderini ¹³¹, P. Calfayan ³⁵,
 G. Callea ⁶¹, L.P. Caloba ^{85b}, D. Calvet ⁴², S. Calvet ⁴², R. Camacho Toro ¹³¹, S. Camarda ³⁷,
 D. Camarero Munoz ²⁷, P. Camarri ^{78a,78b}, M.T. Camerlingo ^{74a,74b}, D. Cameron ³⁷,
 C. Camincher ¹⁷⁰, M. Campanelli ⁹⁹, A. Camplani ⁴⁴, V. Canale ^{74a,74b}, A.C. Canbay ^{3a},
 E. Canonero ⁹⁸, J. Cantero ¹⁶⁸, Y. Cao ¹⁶⁷, F. Capocasa ²⁷, M. Capua ^{45b,45a}, A. Carbone ^{73a,73b},
 R. Cardarelli ^{78a}, J.C.J. Cardenas ⁸, M.P. Cardiff ²⁷, G. Carducci ^{45b,45a}, T. Carli ³⁷,
 G. Carlino ^{74a}, J.I. Carlotto ¹³, B.T. Carlson ^{133,p}, E.M. Carlson ^{170,160a}, J. Carmignani ⁹⁵,
 L. Carminati ^{73a,73b}, A. Carnelli ¹³⁹, M. Carnesale ³⁷, S. Caron ¹¹⁷, E. Carquin ^{141f},
 I.B. Carr ¹⁰⁸, S. Carrá ^{73a}, G. Carratta ^{24b,24a}, A.M. Carroll ¹²⁷, M.P. Casado ^{13,h}, M. Caspar ⁵⁰,
 F.L. Castillo ⁴, L. Castillo Garcia ¹³, V. Castillo Gimenez ¹⁶⁸, N.F. Castro ^{134a,134e},
 A. Catinaccio ³⁷, J.R. Catmore ¹²⁹, T. Cavaliere ⁴, V. Cavaliere ³⁰, L.J. Caviedes Betancourt ^{23b},
 Y.C. Cekmecelioglu ⁵⁰, E. Celebi ⁸⁴, S. Cella ³⁷, V. Cepaitis ⁵⁸, K. Cerny ¹²⁶,
 A.S. Cerqueira ^{85a}, A. Cerri ¹⁵⁰, L. Cerrito ^{78a,78b}, F. Cerutti ^{18a}, B. Cervato ¹⁴⁵, A. Cervelli ^{24b},
 G. Cesarini ⁵⁵, S.A. Cetin ⁸⁴, P.M. Chabrilat ¹³¹, D. Chakraborty ¹¹⁹, J. Chan ^{18a},
 W.Y. Chan ¹⁵⁷, J.D. Chapman ³³, E. Chapon ¹³⁹, B. Chargeishvili ^{153b}, D.G. Charlton ²¹,
 M. Chatterjee ²⁰, C. Chauhan ¹³⁷, Y. Che ^{115a}, S. Chekanov ⁶, S.V. Chekulav ^{160a},
 G.A. Chelkov ^{40,a}, A. Chen ¹⁰⁹, B. Chen ¹⁵⁵, B. Chen ¹⁷⁰, H. Chen ^{115a}, H. Chen ³⁰,
 J. Chen ^{64c}, J. Chen ¹⁴⁶, M. Chen ¹³⁰, S. Chen ⁹⁰, S.J. Chen ^{115a}, X. Chen ^{64c}, X. Chen ^{15,ac},
 Y. Chen ^{64a}, C.L. Cheng ¹⁷⁵, H.C. Cheng ^{66a}, S. Cheong ¹⁴⁷, A. Cheplakov ⁴⁰,
 E. Cheremushkina ⁵⁰, E. Cherepanova ¹¹⁸, R. Cherkaoui El Moursli ^{36e}, E. Cheu ⁷, K. Cheung ⁶⁷,
 L. Chevalier ¹³⁹, V. Chiarella ⁵⁵, G. Chiarelli ^{76a}, N. Chiedde ¹⁰⁵, G. Chiodini ^{72a},
 A.S. Chisholm ²¹, A. Chitan ^{28b}, M. Chitishvili ¹⁶⁸, M.V. Chizhov ^{40,q}, K. Choi ¹¹, Y. Chou ¹⁴²,

E.Y.S. Chow ¹¹⁷, K.L. Chu ¹⁷⁴, M.C. Chu ^{66a}, X. Chu ^{14,115c}, Z. Chubinidze ⁵⁵, J. Chudoba ¹³⁵,
 J.J. Chwastowski ⁸⁹, D. Cieri ¹¹³, K.M. Ciesla ^{88a}, V. Cindro ⁹⁶, A. Ciocio ^{18a}, F. Ciroto ^{74a,74b},
 Z.H. Citron ¹⁷⁴, M. Citterio ^{73a}, D.A. Ciubotaru ^{28b}, A. Clark ⁵⁸, P.J. Clark ⁵⁴, N. Clarke Hall ⁹⁹,
 C. Clarry ¹⁵⁹, J.M. Clavijo Columbie ⁵⁰, S.E. Clawson ⁵⁰, C. Clement ^{49a,49b}, Y. Coadou ¹⁰⁵,
 M. Cobal ^{71a,71c}, A. Coccaro ^{59b}, R.F. Coelho Barrue ^{134a}, R. Coelho Lopes De Sa ¹⁰⁶,
 S. Coelli ^{73a}, L.S. Colangeli ¹⁵⁹, B. Cole ⁴³, J. Collot ⁶², P. Conde Muiño ^{134a,134g},
 M.P. Connell ^{34c}, S.H. Connell ^{34c}, E.I. Conroy ¹³⁰, F. Conventi ^{74a,ae}, H.G. Cooke ²¹,
 A.M. Cooper-Sarkar ¹³⁰, F.A. Corchia ^{24b,24a}, A. Cordeiro Oudot Choi ¹³¹, L.D. Corpe ⁴²,
 M. Corradi ^{77a,77b}, F. Corriveau ^{107,y}, A. Cortes-Gonzalez ¹⁹, M.J. Costa ¹⁶⁸, F. Costanza ⁴,
 D. Costanzo ¹⁴³, B.M. Cote ¹²³, J. Couthures ⁴, G. Cowan ⁹⁸, K. Cranmer ¹⁷⁵, L. Cremer ⁵¹,
 D. Cremonini ^{24b,24a}, S. Crépe-Renaudin ⁶², F. Crescioli ¹³¹, M. Cristinziani ¹⁴⁵,
 M. Cristoforetti ^{80a,80b}, V. Croft ¹¹⁸, J.E. Crosby ¹²⁵, G. Crosetti ^{45b,45a}, A. Cueto ¹⁰², H. Cui ⁹⁹,
 Z. Cui ⁷, W.R. Cunningham ⁶¹, F. Curcio ¹⁶⁸, J.R. Curran ⁵⁴, P. Czodrowski ³⁷,
 M.J. Da Cunha Sargedas De Sousa ^{59b,59a}, J.V. Da Fonseca Pinto ^{85b}, C. Da Via ¹⁰⁴,
 W. Dabrowski ^{88a}, T. Dado ³⁷, S. Dahbi ¹⁵², T. Dai ¹⁰⁹, D. Dal Santo ²⁰, C. Dallapiccola ¹⁰⁶,
 M. Dam ⁴⁴, G. D'amen ³⁰, V. D'Amico ¹¹², J. Damp ¹⁰³, J.R. Dandoy ³⁵, D. Dannheim ³⁷,
 M. Danninger ¹⁴⁶, V. Dao ¹⁴⁹, G. Darbo ^{59b}, S.J. Das ³⁰, F. Dattola ⁵⁰, S. D'Auria ^{73a,73b},
 A. D'Avanzo ^{74a,74b}, C. David ^{34a}, T. Davidek ¹³⁷, I. Dawson ⁹⁷, H.A. Day-hall ¹³⁶, K. De ⁸,
 C. De Almeida Rossi ¹⁵⁹, R. De Asmundis ^{74a}, N. De Biase ⁵⁰, S. De Castro ^{24b,24a},
 N. De Groot ¹¹⁷, P. de Jong ¹¹⁸, H. De la Torre ¹¹⁹, A. De Maria ^{115a}, A. De Salvo ^{77a},
 U. De Sanctis ^{78a,78b}, F. De Santis ^{72a,72b}, A. De Santo ¹⁵⁰, J.B. De Vivie De Regie ⁶²,
 J. Debevc ⁹⁶, D.V. Dedovich ⁴⁰, J. Degens ⁹⁵, A.M. Deiana ⁴⁶, F. Del Corso ^{24b,24a}, J. Del Peso ¹⁰²,
 L. Delagrangé ¹³¹, F. Deliot ¹³⁹, C.M. Delitzsch ⁵¹, M. Della Pietra ^{74a,74b}, D. Della Volpe ⁵⁸,
 A. Dell'Acqua ³⁷, L. Dell'Asta ^{73a,73b}, M. Delmastro ⁴, C.C. Delogu ¹⁰³, P.A. Delsart ⁶²,
 S. Demers ¹⁷⁷, M. Demichev ⁴⁰, S.P. Denisov ³⁹, L. D'Eramo ⁴², D. Derendarz ⁸⁹, F. Derue ¹³¹,
 P. Dervan ⁹⁵, K. Desch ²⁵, C. Deutsch ²⁵, F.A. Di Bello ^{59b,59a}, A. Di Ciaccio ^{78a,78b},
 L. Di Ciaccio ⁴, A. Di Domenico ^{77a,77b}, C. Di Donato ^{74a,74b}, A. Di Girolamo ³⁷,
 G. Di Gregorio ³⁷, A. Di Luca ^{80a,80b}, B. Di Micco ^{79a,79b}, R. Di Nardo ^{79a,79b}, K.F. Di Petrillo ⁴¹,
 M. Diamantopoulou ³⁵, F.A. Dias ¹¹⁸, T. Dias Do Vale ¹⁴⁶, M.A. Diaz ^{141a,141b}, A.R. Didenko ⁴⁰,
 M. Didenko ¹⁶⁸, E.B. Diehl ¹⁰⁹, S. Díez Cornell ⁵⁰, C. Díez Pardos ¹⁴⁵, C. Dimitriadi ¹⁶⁶,
 A. Dimitrievska ²¹, J. Dingfelder ²⁵, T. Dingley ¹³⁰, I-M. Dinu ^{28b}, S.J. Dittmeier ^{65b},
 F. Dittus ³⁷, M. Divisek ¹³⁷, B. Dixit ⁹⁵, F. Djama ¹⁰⁵, T. Djobava ^{153b}, C. Doglioni ^{104,101},
 A. Dohnalova ^{29a}, Z. Dolezal ¹³⁷, K. Domijan ^{88a}, K.M. Dona ⁴¹, M. Donadelli ^{85d},
 B. Dong ¹¹⁰, J. Donini ⁴², A. D'Onofrio ^{74a,74b}, M. D'Onofrio ⁹⁵, J. Dopke ¹³⁸, A. Doria ^{74a},
 N. Dos Santos Fernandes ^{134a}, P. Dougan ¹⁰⁴, M.T. Dova ⁹³, A.T. Doyle ⁶¹, M.A. Draguet ¹³⁰,
 M.P. Drescher ⁵⁷, E. Dreyer ¹⁷⁴, I. Drivas-koulouris ¹⁰, M. Drnevich ¹²¹, M. Drozdova ⁵⁸,
 D. Du ^{64a}, T.A. du Pree ¹¹⁸, F. Dubinin ³⁹, M. Dubovsky ^{29a}, E. Duchovni ¹⁷⁴, G. Duckeck ¹¹²,
 O.A. Ducu ^{28b}, D. Duda ⁵⁴, A. Dudarev ³⁷, E.R. Duden ²⁷, M. D'uffizi ¹⁰⁴, L. Duflot ⁶⁸,
 M. Dührssen ³⁷, I. Duminica ^{28g}, A.E. Dumitriu ^{28b}, M. Dunford ^{65a}, S. Dungs ⁵¹,
 K. Dunne ^{49a,49b}, A. Duperrin ¹⁰⁵, H. Duran Yildiz ^{3a}, M. Düren ⁶⁰, A. Durglishvili ^{153b},
 B.L. Dwyer ¹¹⁹, G.I. Dyckes ^{18a}, M. Dyndal ^{88a}, B.S. Dziedzic ³⁷, Z.O. Earnshaw ¹⁵⁰,
 G.H. Eberwein ¹³⁰, B. Eckerova ^{29a}, S. Eggebrecht ⁵⁷, E. Egidio Purcino De Souza ^{85e},
 L.F. Ehrke ⁵⁸, G. Eigen ¹⁷, K. Einsweiler ^{18a}, T. Ekelof ¹⁶⁶, P.A. Ekman ¹⁰¹, S. El Farkh ^{36b},
 Y. El Ghazali ^{64a}, H. El Jarrari ³⁷, A. El Moussaouy ^{36a}, V. Ellajosyula ¹⁶⁶, M. Ellert ¹⁶⁶,
 F. Ellinghaus ¹⁷⁶, N. Ellis ³⁷, J. Elmsheuser ³⁰, M. Elsayy ^{120a}, M. Elsing ³⁷,
 D. Emelianov ¹³⁸, Y. Enari ⁸⁶, I. Ene ^{18a}, S. Epari ¹³, P.A. Erland ⁸⁹,
 D. Ernani Martins Neto ⁸⁹, M. Errenst ¹⁷⁶, M. Escalier ⁶⁸, C. Escobar ¹⁶⁸, E. Etzion ¹⁵⁵,

G. Evans [id](#)^{134a}, H. Evans [id](#)⁷⁰, L.S. Evans [id](#)⁹⁸, A. Ezhilov [id](#)³⁹, S. Ezzarqtouni [id](#)^{36a}, F. Fabbri [id](#)^{24b,24a}, L. Fabbri [id](#)^{24b,24a}, G. Facini [id](#)⁹⁹, V. Fadeyev [id](#)¹⁴⁰, R.M. Fakhrutdinov [id](#)³⁹, D. Fakoudis [id](#)¹⁰³, S. Falciano [id](#)^{77a}, L.F. Falda Ulhoa Coelho [id](#)^{134a}, F. Fallavollita [id](#)¹¹³, G. Falsetti [id](#)^{45b,45a}, J. Faltova [id](#)¹³⁷, C. Fan [id](#)¹⁶⁷, K.Y. Fan [id](#)^{66b}, Y. Fan [id](#)¹⁴, Y. Fang [id](#)^{14,115c}, M. Fanti [id](#)^{73a,73b}, M. Faraj [id](#)^{71a,71b}, Z. Farazpay [id](#)¹⁰⁰, A. Farbin [id](#)⁸, A. Farilla [id](#)^{79a}, T. Farooque [id](#)¹¹⁰, J.N. Farr [id](#)¹⁷⁷, S.M. Farrington [id](#)^{138,54}, F. Fassi [id](#)^{36e}, D. Fassouliotis [id](#)⁹, M. Faucci Giannelli [id](#)^{78a,78b}, W.J. Fawcett [id](#)³³, L. Fayard [id](#)⁶⁸, P. Federic [id](#)¹³⁷, P. Federicova [id](#)¹³⁵, O.L. Fedin [id](#)^{39,a}, M. Feickert [id](#)¹⁷⁵, L. Feligioni [id](#)¹⁰⁵, D.E. Fellers [id](#)¹²⁷, C. Feng [id](#)^{64b}, Z. Feng [id](#)¹¹⁸, M.J. Fenton [id](#)¹⁶³, L. Ferencz [id](#)⁵⁰, R.A.M. Ferguson [id](#)⁹⁴, P. Fernandez Martinez [id](#)⁶⁹, M.J.V. Fernoux [id](#)¹⁰⁵, J. Ferrando [id](#)⁹⁴, A. Ferrari [id](#)¹⁶⁶, P. Ferrari [id](#)^{118,117}, R. Ferrari [id](#)^{75a}, D. Ferrere [id](#)⁵⁸, C. Ferretti [id](#)¹⁰⁹, M.P. Fewell [id](#)¹, D. Fiacco [id](#)^{77a,77b}, F. Fiedler [id](#)¹⁰³, P. Fiedler [id](#)¹³⁶, S. Filimonov [id](#)³⁹, A. Filipčič [id](#)⁹⁶, E.K. Filmer [id](#)^{160a}, F. Filthaut [id](#)¹¹⁷, M.C.N. Fiolhais [id](#)^{134a,134c,c}, L. Fiorini [id](#)¹⁶⁸, W.C. Fisher [id](#)¹¹⁰, T. Fitschen [id](#)¹⁰⁴, P.M. Fitzhugh [id](#)¹³⁹, I. Fleck [id](#)¹⁴⁵, P. Fleischmann [id](#)¹⁰⁹, T. Flick [id](#)¹⁷⁶, M. Flores [id](#)^{34d,aa}, L.R. Flores Castillo [id](#)^{66a}, L. Flores Sanz De Acedo [id](#)³⁷, F.M. Follega [id](#)^{80a,80b}, N. Fomin [id](#)³³, J.H. Foo [id](#)¹⁵⁹, A. Formica [id](#)¹³⁹, A.C. Forti [id](#)¹⁰⁴, E. Fortin [id](#)³⁷, A.W. Fortman [id](#)^{18a}, M.G. Foti [id](#)^{18a}, L. Fountas [id](#)^{9,i}, D. Fournier [id](#)⁶⁸, H. Fox [id](#)⁹⁴, P. Francavilla [id](#)^{76a,76b}, S. Francescato [id](#)⁶³, S. Franchellucci [id](#)⁵⁸, M. Franchini [id](#)^{24b,24a}, S. Franchino [id](#)^{65a}, D. Francis [id](#)³⁷, L. Franco [id](#)¹¹⁷, V. Franco Lima [id](#)³⁷, L. Franconi [id](#)⁵⁰, M. Franklin [id](#)⁶³, G. Frattari [id](#)²⁷, Y.Y. Frid [id](#)¹⁵⁵, J. Friend [id](#)⁶¹, N. Fritzsche [id](#)³⁷, A. Froch [id](#)⁵⁸, D. Froidevaux [id](#)³⁷, J.A. Frost [id](#)¹³⁰, Y. Fu [id](#)^{64a}, S. Fuenzalida Garrido [id](#)^{141f}, M. Fujimoto [id](#)¹⁰⁵, K.Y. Fung [id](#)^{66a}, E. Furtado De Simas Filho [id](#)^{85e}, M. Furukawa [id](#)¹⁵⁷, J. Fuster [id](#)¹⁶⁸, A. Gaa [id](#)⁵⁷, A. Gabrielli [id](#)^{24b,24a}, A. Gabrielli [id](#)¹⁵⁹, P. Gadow [id](#)³⁷, G. Gagliardi [id](#)^{59b,59a}, L.G. Gagnon [id](#)^{18a}, S. Gaid [id](#)¹⁶⁵, S. Galantzan [id](#)¹⁵⁵, J. Gallagher [id](#)¹, E.J. Gallas [id](#)¹³⁰, A.L. Gallen [id](#)¹⁶⁶, B.J. Gallop [id](#)¹³⁸, K.K. Gan [id](#)¹²³, S. Ganguly [id](#)¹⁵⁷, Y. Gao [id](#)⁵⁴, F.M. Garay Walls [id](#)^{141a,141b}, B. Garcia [id](#)³⁰, C. García [id](#)¹⁶⁸, A. Garcia Alonso [id](#)¹¹⁸, A.G. Garcia Caffaro [id](#)¹⁷⁷, J.E. García Navarro [id](#)¹⁶⁸, M. Garcia-Sciveres [id](#)^{18a}, G.L. Gardner [id](#)¹³², R.W. Gardner [id](#)⁴¹, N. Garelli [id](#)¹⁶², R.B. Garg [id](#)¹⁴⁷, J.M. Gargan [id](#)⁵⁴, C.A. Garner [id](#)¹⁵⁹, C.M. Garvey [id](#)^{34a}, V.K. Gassmann [id](#)¹⁶², G. Gaudio [id](#)^{75a}, V. Gautam [id](#)¹³, P. Gauzzi [id](#)^{77a,77b}, J. Gavranovic [id](#)⁹⁶, I.L. Gavrilenko [id](#)³⁹, A. Gavriluk [id](#)³⁹, C. Gay [id](#)¹⁶⁹, G. Gaycken [id](#)¹²⁷, E.N. Gazis [id](#)¹⁰, A.A. Geanta [id](#)^{28b}, A. Gekow [id](#)¹²³, C. Gemme [id](#)^{59b}, M.H. Genest [id](#)⁶², A.D. Gentry [id](#)¹¹⁶, S. George [id](#)⁹⁸, W.F. George [id](#)²¹, T. Geralis [id](#)⁴⁸, A.A. Gerwin [id](#)¹²⁴, P. Gessinger-Befurt [id](#)³⁷, M.E. Geyik [id](#)¹⁷⁶, M. Ghani [id](#)¹⁷², K. Ghorbanian [id](#)⁹⁷, A. Ghosal [id](#)¹⁴⁵, A. Ghosh [id](#)¹⁶³, A. Ghosh [id](#)⁷, B. Giacobbe [id](#)^{24b}, S. Giagu [id](#)^{77a,77b}, T. Giani [id](#)¹¹⁸, A. Giannini [id](#)^{64a}, S.M. Gibson [id](#)⁹⁸, M. Gignac [id](#)¹⁴⁰, D.T. Gil [id](#)^{88b}, A.K. Gilbert [id](#)^{88a}, B.J. Gilbert [id](#)⁴³, D. Gillberg [id](#)³⁵, G. Gilles [id](#)¹¹⁸, L. Ginabat [id](#)¹³¹, D.M. Gingrich [id](#)^{2,ad}, M.P. Giordani [id](#)^{71a,71c}, P.F. Giraud [id](#)¹³⁹, G. Giugliarelli [id](#)^{71a,71c}, D. Giugni [id](#)^{73a}, F. Giuli [id](#)^{78a,78b}, I. Gkialas [id](#)^{9,i}, L.K. Gladilin [id](#)³⁹, C. Glasman [id](#)¹⁰², G.R. Gledhill [id](#)¹²⁷, G. Glemža [id](#)⁵⁰, M. Glisic [id](#)¹²⁷, I. Gnesi [id](#)^{45b}, Y. Go [id](#)³⁰, M. Goblirsch-Kolb [id](#)³⁷, B. Gocke [id](#)⁵¹, D. Godin [id](#)¹¹¹, B. Gokturk [id](#)^{22a}, S. Goldfarb [id](#)¹⁰⁸, T. Golling [id](#)⁵⁸, M.G.D. Gololo [id](#)^{34g}, D. Golubkov [id](#)³⁹, J.P. Gombas [id](#)¹¹⁰, A. Gomes [id](#)^{134a,134b}, G. Gomes Da Silva [id](#)¹⁴⁵, A.J. Gomez Delegido [id](#)¹⁶⁸, R. Gonçalves [id](#)^{134a}, L. Gonella [id](#)²¹, A. Gongadze [id](#)^{153c}, F. Gonnella [id](#)²¹, J.L. Gonski [id](#)¹⁴⁷, R.Y. González Andana [id](#)⁵⁴, S. González de la Hoz [id](#)¹⁶⁸, R. Gonzalez Lopez [id](#)⁹⁵, C. Gonzalez Renteria [id](#)^{18a}, M.V. Gonzalez Rodrigues [id](#)⁵⁰, R. Gonzalez Suarez [id](#)¹⁶⁶, S. Gonzalez-Sevilla [id](#)⁵⁸, L. Goossens [id](#)³⁷, B. Gorini [id](#)³⁷, E. Gorini [id](#)^{72a,72b}, A. Gorišek [id](#)⁹⁶, T.C. Gosart [id](#)¹³², A.T. Goshaw [id](#)⁵³, M.I. Gostkin [id](#)⁴⁰, S. Goswami [id](#)¹²⁵, C.A. Gottardo [id](#)³⁷, S.A. Gotz [id](#)¹¹², M. Goughri [id](#)^{36b}, V. Goumarre [id](#)⁵⁰, A.G. Goussiou [id](#)¹⁴², N. Govender [id](#)^{34c}, R.P. Grabarczyk [id](#)¹³⁰, I. Grabowska-Bold [id](#)^{88a}, K. Graham [id](#)³⁵, E. Gramstad [id](#)¹²⁹, S. Grancagnolo [id](#)^{72a,72b}, C.M. Grant [id](#)^{1,139}, P.M. Gravila [id](#)^{28f}, F.G. Gravili [id](#)^{72a,72b}, H.M. Gray [id](#)^{18a}, M. Greco [id](#)^{72a,72b}, M.J. Green [id](#)¹, C. Grefe [id](#)²⁵, A.S. Grefsrud [id](#)¹⁷, I.M. Gregor [id](#)⁵⁰, K.T. Greif [id](#)¹⁶³, P. Grenier [id](#)¹⁴⁷, S.G. Grewe [id](#)¹¹³, A.A. Grillo [id](#)¹⁴⁰, K. Grimm [id](#)³², S. Grinstein [id](#)^{13,u}, J.-F. Grivaz [id](#)⁶⁸,

E. Gross ¹⁷⁴, J. Grosse-Knetter ⁵⁷, L. Guan ¹⁰⁹, J.G.R. Guerrero Rojas ¹⁶⁸, G. Guerrieri ³⁷,
 R. Gugel ¹⁰³, J.A.M. Guhit ¹⁰⁹, A. Guida ¹⁹, E. Guilloton ¹⁷², S. Guindon ³⁷, F. Guo ^{14,115c},
 J. Guo ^{64c}, L. Guo ⁵⁰, L. Guo ^{14,s}, Y. Guo ¹⁰⁹, A. Gupta ⁵¹, R. Gupta ¹³³, S. Gurbuz ²⁵,
 S.S. Gurdasani ⁵⁶, G. Gustavino ^{77a,77b}, P. Gutierrez ¹²⁴, L.F. Gutierrez Zagazeta ¹³²,
 M. Gutsche ⁵², C. Gutschow ⁹⁹, C. Gwenlan ¹³⁰, C.B. Gwilliam ⁹⁵, E.S. Haaland ¹²⁹,
 A. Haas ¹²¹, M. Habedank ⁶¹, C. Haber ^{18a}, H.K. Hadavand ⁸, A. Hadeef ⁵², A.I. Hagan ⁹⁴,
 J.J. Hahn ¹⁴⁵, E.H. Haines ⁹⁹, M. Haleem ¹⁷¹, J. Haley ¹²⁵, G.D. Hallewell ¹⁰⁵, L. Halser ²⁰,
 K. Hamano ¹⁷⁰, M. Hamer ²⁵, E.J. Hampshire ⁹⁸, J. Han ^{64b}, L. Han ^{115a}, L. Han ^{64a},
 S. Han ^{18a}, Y.F. Han ¹⁵⁹, K. Hanagaki ⁸⁶, M. Hance ¹⁴⁰, D.A. Hangal ⁴³, H. Hanif ¹⁴⁶,
 M.D. Hank ¹³², J.B. Hansen ⁴⁴, P.H. Hansen ⁴⁴, D. Harada ⁵⁸, T. Harenberg ¹⁷⁶,
 S. Harkusha ¹⁷⁸, M.L. Harris ¹⁰⁶, Y.T. Harris ²⁵, J. Harrison ¹³, N.M. Harrison ¹²³,
 P.F. Harrison ¹⁷², N.M. Hartman ¹¹³, N.M. Hartmann ¹¹², R.Z. Hasan ^{98,138}, Y. Hasegawa ¹⁴⁴,
 F. Haslbeck ¹³⁰, S. Hassan ¹⁷, R. Hauser ¹¹⁰, C.M. Hawkes ²¹, R.J. Hawkings ³⁷,
 Y. Hayashi ¹⁵⁷, D. Hayden ¹¹⁰, C. Hayes ¹⁰⁹, R.L. Hayes ¹¹⁸, C.P. Hays ¹³⁰, J.M. Hays ⁹⁷,
 H.S. Hayward ⁹⁵, F. He ^{64a}, M. He ^{14,115c}, Y. He ⁵⁰, Y. He ⁹⁹, N.B. Heatley ⁹⁷, V. Hedberg ¹⁰¹,
 A.L. Heggelund ¹²⁹, C. Heidegger ⁵⁶, K.K. Heidegger ⁵⁶, J. Heilman ³⁵, S. Heim ⁵⁰,
 T. Heim ^{18a}, J.G. Heinlein ¹³², J.J. Heinrich ¹²⁷, L. Heinrich ^{113,ab}, J. Hejbal ¹³⁵, A. Held ¹⁷⁵,
 S. Hellesund ¹⁷, C.M. Helling ¹⁶⁹, S. Hellman ^{49a,49b}, R.C.W. Henderson ⁹⁴, L. Henkelmann ³³,
 A.M. Henriques Correia ³⁷, H. Herde ¹⁰¹, Y. Hernández Jiménez ¹⁴⁹, L.M. Herrmann ²⁵,
 T. Herrmann ⁵², G. Herten ⁵⁶, R. Hertenberger ¹¹², L. Hervas ³⁷, M.E. Hespings ¹⁰³,
 N.P. Hessey ^{160a}, J. Hessler ¹¹³, M. Hidaoui ^{36b}, N. Hidic ¹³⁷, E. Hill ¹⁵⁹, S.J. Hillier ²¹,
 J.R. Hinds ¹¹⁰, F. Hinterkeuser ²⁵, M. Hirose ¹²⁸, S. Hirose ¹⁶¹, D. Hirschbuehl ¹⁷⁶,
 T.G. Hitchings ¹⁰⁴, B. Hiti ⁹⁶, J. Hobbs ¹⁴⁹, R. Hobincu ^{28e}, N. Hod ¹⁷⁴, M.C. Hodgkinson ¹⁴³,
 B.H. Hodgkinson ¹³⁰, A. Hoecker ³⁷, D.D. Hofer ¹⁰⁹, J. Hofer ¹⁶⁸, T. Holm ²⁵, M. Holzbock ³⁷,
 L.B.A.H. Hommels ³³, B.P. Honan ¹⁰⁴, J.J. Hong ⁷⁰, J. Hong ^{64c}, T.M. Hong ¹³³,
 B.H. Hooberman ¹⁶⁷, W.H. Hopkins ⁶, M.C. Hoppesch ¹⁶⁷, Y. Horii ¹¹⁴, M.E. Horstmann ¹¹³,
 S. Hou ¹⁵², M.R. Housenga ¹⁶⁷, A.S. Howard ⁹⁶, J. Howarth ⁶¹, J. Hoya ⁶, M. Hrabovsky ¹²⁶,
 A. Hrynevich ⁵⁰, T. Hryn'ova ⁴, P.J. Hsu ⁶⁷, S.-C. Hsu ¹⁴², T. Hsu ⁶⁸, M. Hu ^{18a}, Q. Hu ^{64a},
 S. Huang ³³, X. Huang ^{14,115c}, Y. Huang ¹⁴³, Y. Huang ¹⁰³, Y. Huang ¹⁴, Z. Huang ¹⁰⁴,
 Z. Hubacek ¹³⁶, M. Huebner ²⁵, F. Huegging ²⁵, T.B. Huffman ¹³⁰,
 M. Hufnagel Maranha De Faria ^{85a}, C.A. Hugli ⁵⁰, M. Huhtinen ³⁷, S.K. Huiberts ¹⁷,
 R. Hulsken ¹⁰⁷, N. Huseynov ^{12,f}, J. Huston ¹¹⁰, J. Huth ⁶³, R. Hyneman ⁷, G. Iacobucci ⁵⁸,
 G. Iakovidis ³⁰, L. Iconomidou-Fayard ⁶⁸, J.P. Iddon ³⁷, P. Iengo ^{74a,74b}, R. Iguchi ¹⁵⁷,
 Y. Iiyama ¹⁵⁷, T. Iizawa ¹³⁰, Y. Ikegami ⁸⁶, D. Iliadis ¹⁵⁶, N. Ilic ¹⁵⁹, H. Imam ^{85c},
 G. Inacio Goncalves ^{85d}, T. Ingebretsen Carlson ^{49a,49b}, J.M. Inglis ⁹⁷, G. Introzzi ^{75a,75b},
 M. Iodice ^{79a}, V. Ippolito ^{77a,77b}, R.K. Irwin ⁹⁵, M. Ishino ¹⁵⁷, W. Islam ¹⁷⁵, C. Issever ¹⁹,
 S. Istin ^{22a,ah}, H. Ito ¹⁷³, R. Iuppa ^{80a,80b}, A. Ivina ¹⁷⁴, J.M. Izen ⁴⁷, V. Izzo ^{74a}, P. Jacka ¹³⁵,
 P. Jackson ¹, C.S. Jagfeld ¹¹², G. Jain ^{160a}, P. Jain ⁵⁰, K. Jakobs ⁵⁶, T. Jakoubek ¹⁷⁴,
 J. Jamieson ⁶¹, W. Jang ¹⁵⁷, M. Javurkova ¹⁰⁶, P. Jawahar ¹⁰⁴, L. Jeanty ¹²⁷, J. Jejelava ^{153a},
 P. Jenni ^{56,e}, C.E. Jessiman ³⁵, C. Jia ^{64b}, H. Jia ¹⁶⁹, J. Jia ¹⁴⁹, X. Jia ^{14,115c}, Z. Jia ^{115a},
 C. Jiang ⁵⁴, S. Jiggins ⁵⁰, J. Jimenez Pena ¹³, S. Jin ^{115a}, A. Jinaru ^{28b}, O. Jinnouchi ¹⁵⁸,
 P. Johansson ¹⁴³, K.A. Johns ⁷, J.W. Johnson ¹⁴⁰, F.A. Jolly ⁵⁰, D.M. Jones ¹⁵⁰, E. Jones ⁵⁰,
 K.S. Jones ⁸, P. Jones ³³, R.W.L. Jones ⁹⁴, T.J. Jones ⁹⁵, H.L. Joos ^{57,37}, R. Joshi ¹²³,
 J. Jovicevic ¹⁶, X. Ju ^{18a}, J.J. Junggeburth ³⁷, T. Junkermann ^{65a}, A. Juste Rozas ^{13,u},
 M.K. Juzek ⁸⁹, S. Kabana ^{141e}, A. Kaczmarska ⁸⁹, M. Kado ¹¹³, H. Kagan ¹²³, M. Kagan ¹⁴⁷,
 A. Kahn ¹³², C. Kahra ¹⁰³, T. Kaji ¹⁵⁷, E. Kajomovitz ¹⁵⁴, N. Kakati ¹⁷⁴, I. Kalaitzidou ⁵⁶,
 C.W. Kalderon ³⁰, N.J. Kang ¹⁴⁰, D. Kar ^{34g}, K. Karava ¹³⁰, M.J. Kareem ^{160b}, E. Karentzos ²⁵,

O. Karkout ¹¹⁸, S.N. Karpov ⁴⁰, Z.M. Karpova ⁴⁰, V. Kartvelishvili ⁹⁴, A.N. Karyukhin ³⁹, E. Kasimi ¹⁵⁶, J. Katzy ⁵⁰, S. Kaur ³⁵, K. Kawade ¹⁴⁴, M.P. Kawale ¹²⁴, C. Kawamoto ⁹⁰, T. Kawamoto ^{64a}, E.F. Kay ³⁷, F.I. Kaya ¹⁶², S. Kazakos ¹¹⁰, V.F. Kazanin ³⁹, Y. Ke ¹⁴⁹, J.M. Keaveney ^{34a}, R. Keeler ¹⁷⁰, G.V. Kehris ⁶³, J.S. Keller ³⁵, J.J. Kempster ¹⁵⁰, O. Kepka ¹³⁵, J. Kerr ^{160b}, B.P. Kerridge ¹³⁸, S. Kersten ¹⁷⁶, B.P. Kerševan ⁹⁶, L. Keszeghova ^{29a}, S. Ketabchi Haghghat ¹⁵⁹, R.A. Khan ¹³³, A. Khanov ¹²⁵, A.G. Kharlamov ³⁹, T. Kharlamova ³⁹, E.E. Khoda ¹⁴², M. Kholodenko ^{134a}, T.J. Khoo ¹⁹, G. Khoriauli ¹⁷¹, J. Khubua ^{153b,*}, Y.A.R. Khwaira ¹³¹, B. Kibirige ^{34g}, D. Kim ⁶, D.W. Kim ^{49a,49b}, Y.K. Kim ⁴¹, N. Kimura ⁹⁹, M.K. Kingston ⁵⁷, A. Kirchhoff ⁵⁷, C. Kirfel ²⁵, F. Kirfel ²⁵, J. Kirk ¹³⁸, A.E. Kiryunin ¹¹³, S. Kita ¹⁶¹, C. Kitsaki ¹⁰, O. Kivernyk ²⁵, M. Klassen ¹⁶², C. Klein ³⁵, L. Klein ¹⁷¹, M.H. Klein ⁴⁶, S.B. Klein ⁵⁸, U. Klein ⁹⁵, A. Klimentov ³⁰, T. Klioutchnikova ³⁷, P. Kluit ¹¹⁸, S. Kluth ¹¹³, E. Kneringer ⁸¹, T.M. Knight ¹⁵⁹, A. Knue ⁵¹, D. Kobylanskii ¹⁷⁴, S.F. Koch ¹³⁰, M. Kocian ¹⁴⁷, P. Kodyš ¹³⁷, D.M. Koeck ¹²⁷, P.T. Koenig ²⁵, T. Koffas ³⁵, O. Kolay ⁵², I. Koletsou ⁴, T. Komarek ⁸⁹, K. Köneke ⁵⁷, A.X.Y. Kong ¹, T. Kono ¹²², N. Konstantinidis ⁹⁹, P. Kontaxakis ⁵⁸, B. Konya ¹⁰¹, R. Kopeliansky ⁴³, S. Koperny ^{88a}, K. Korcyl ⁸⁹, K. Kordas ^{156,d}, A. Korn ⁹⁹, S. Korn ⁵⁷, I. Korolkov ¹³, N. Korotkova ³⁹, B. Kortman ¹¹⁸, O. Kortner ¹¹³, S. Kortner ¹¹³, W.H. Kostecka ¹¹⁹, V.V. Kostyukhin ¹⁴⁵, A. Kotsokechagia ³⁷, A. Kotwal ⁵³, A. Koulouris ³⁷, A. Kourkoumeli-Charalampidi ^{75a,75b}, C. Kourkoumelis ⁹, E. Kourlitis ^{113,ab}, O. Kovanda ¹²⁷, R. Kowalewski ¹⁷⁰, W. Kozanecki ¹²⁷, A.S. Kozhin ³⁹, V.A. Kramarenko ³⁹, G. Kramberger ⁹⁶, P. Kramer ²⁵, M.W. Krasny ¹³¹, A. Krasznahorkay ³⁷, A.C. Kraus ¹¹⁹, J.W. Kraus ¹⁷⁶, J.A. Kremer ⁵⁰, T. Kresse ⁵², L. Kretschmann ¹⁷⁶, J. Kretschmar ⁹⁵, K. Kreul ¹⁹, P. Krieger ¹⁵⁹, K. Krizka ²¹, K. Kroeninger ⁵¹, H. Kroha ¹¹³, J. Kroll ¹³⁵, J. Kroll ¹³², K.S. Krowpman ¹¹⁰, U. Kruchonak ⁴⁰, H. Krüger ²⁵, N. Krumnack ⁸³, M.C. Kruse ⁵³, O. Kuchinskaja ³⁹, S. Kuday ^{3a}, S. Kuehn ³⁷, R. Kuesters ⁵⁶, T. Kuhl ⁵⁰, V. Kukhtin ⁴⁰, Y. Kulchitsky ⁴⁰, S. Kuleshov ^{141d,141b}, M. Kumar ^{34g}, N. Kumari ⁵⁰, P. Kumari ^{160b}, A. Kupco ¹³⁵, T. Kupfer ⁵¹, A. Kupich ³⁹, O. Kuprash ⁵⁶, H. Kurashige ⁸⁷, L.L. Kurchaninov ^{160a}, O. Kurdysh ⁶⁸, Y.A. Kurochkin ³⁸, A. Kurova ³⁹, M. Kuze ¹⁵⁸, A.K. Kvam ¹⁰⁶, J. Kvita ¹²⁶, T. Kwan ¹⁰⁷, N.G. Kyriacou ¹⁰⁹, L.A.O. Laatu ¹⁰⁵, C. Lacasta ¹⁶⁸, F. Lacava ^{77a,77b}, H. Lacker ¹⁹, D. Lacour ¹³¹, N.N. Lad ⁹⁹, E. Ladygin ⁴⁰, A. Lafarge ⁴², B. Laforge ¹³¹, T. Lagouri ¹⁷⁷, F.Z. Lahbabi ^{36a}, S. Lai ⁵⁷, J.E. Lambert ¹⁷⁰, S. Lammers ⁷⁰, W. Lampl ⁷, C. Lampoudis ^{156,d}, G. Lamprinoudis ¹⁰³, A.N. Lancaster ¹¹⁹, E. Lançon ³⁰, U. Landgraf ⁵⁶, M.P.J. Landon ⁹⁷, V.S. Lang ⁵⁶, O.K.B. Langrekken ¹²⁹, A.J. Lankford ¹⁶³, F. Lanni ³⁷, K. Lantzsch ²⁵, A. Lanza ^{75a}, M. Lanzac Berrocal ¹⁶⁸, J.F. Laporte ¹³⁹, T. Lari ^{73a}, F. Lasagni Manghi ^{24b}, M. Lassnig ³⁷, V. Latonova ¹³⁵, S.D. Lawlor ¹⁴³, Z. Lawrence ¹⁰⁴, R. Lazaridou ¹⁷², M. Lazzaroni ^{73a,73b}, H.D.M. Le ¹¹⁰, E.M. Le Boulicaut ¹⁷⁷, L.T. Le Pottier ^{18a}, B. Leban ^{24b,24a}, A. Lebedev ⁸³, M. LeBlanc ¹⁰⁴, F. Ledroit-Guillon ⁶², S.C. Lee ¹⁵², S. Lee ^{49a,49b}, T.F. Lee ⁹⁵, L.L. Leeuw ^{34c}, M. Lefebvre ¹⁷⁰, C. Leggett ^{18a}, G. Lehmann Miotto ³⁷, M. Leigh ⁵⁸, W.A. Leight ¹⁰⁶, W. Leinonen ¹¹⁷, A. Leisos ^{156,r}, M.A.L. Leite ^{85c}, C.E. Leitgeb ¹⁹, R. Leitner ¹³⁷, K.J.C. Leney ⁴⁶, T. Lenz ²⁵, S. Leone ^{76a}, C. Leonidopoulos ⁵⁴, A. Leopold ¹⁴⁸, R. Les ¹¹⁰, C.G. Lester ³³, M. Levchenko ³⁹, J. Levêque ⁴, L.J. Levinson ¹⁷⁴, G. Levrini ^{24b,24a}, M.P. Lewicki ⁸⁹, C. Lewis ¹⁴², D.J. Lewis ⁴, L. Lewitt ¹⁴³, A. Li ³⁰, B. Li ^{64b}, C. Li ^{64a}, C-Q. Li ¹¹³, H. Li ^{64a}, H. Li ^{64b}, H. Li ^{115a}, H. Li ¹⁵, H. Li ^{64b}, J. Li ^{64c}, K. Li ¹⁴, L. Li ^{64c}, M. Li ^{14,115c}, R. Li ¹⁷⁷, S. Li ^{14,115c}, S. Li ^{64d,64c}, T. Li ⁵, X. Li ¹⁰⁷, Z. Li ¹⁵⁷, Z. Li ^{14,115c}, Z. Li ^{64a}, S. Liang ^{14,115c}, Z. Liang ¹⁴, M. Liberatore ¹³⁹, B. Liberti ^{78a}, K. Lie ^{66c}, J. Lieber Marin ^{85e}, H. Lien ⁷⁰, H. Lin ¹⁰⁹, K. Lin ¹¹⁰, L. Linden ¹¹², R.E. Lindley ⁷, J.H. Lindon ², J. Ling ⁶³, E. Lipeles ¹³², A. Lipniacka ¹⁷, A. Lister ¹⁶⁹, J.D. Little ⁷⁰, B. Liu ¹⁴, B.X. Liu ^{115b}, D. Liu ^{64d,64c},

E.H.L. Liu ²¹, J.B. Liu ^{64a}, J.K.K. Liu ³³, K. Liu ^{64d}, K. Liu ^{64d,64c}, M. Liu ^{64a}, M.Y. Liu ^{64a}, P. Liu ¹⁴, Q. Liu ^{64d,142,64c}, X. Liu ^{64a}, X. Liu ^{64b}, Y. Liu ^{115b,115c}, Y.L. Liu ^{64b}, Y.W. Liu ^{64a}, S.L. Lloyd ⁹⁷, E.M. Lobodzinska ⁵⁰, P. Loch ⁷, E. Lodhi ¹⁵⁹, T. Lohse ¹⁹, K. Lohwasser ¹⁴³, E. Loiacono ⁵⁰, J.D. Lomas ²¹, J.D. Long ⁴³, I. Longarini ¹⁶³, R. Longo ¹⁶⁷, I. Lopez Paz ⁶⁹, A. Lopez Solis ⁵⁰, N.A. Lopez-canelas ⁷, N. Lorenzo Martinez ⁴, A.M. Lory ¹¹², M. Losada ^{120a}, G. Löschcke Centeno ¹⁵⁰, O. Loseva ³⁹, X. Lou ^{49a,49b}, X. Lou ^{14,115c}, A. Lounis ⁶⁸, P.A. Love ⁹⁴, G. Lu ^{14,115c}, M. Lu ⁶⁸, S. Lu ¹³², Y.J. Lu ¹⁵², H.J. Lubatti ¹⁴², C. Luci ^{77a,77b}, F.L. Lucio Alves ^{115a}, F. Luehring ⁷⁰, O. Lukianchuk ⁶⁸, B.S. Lunday ¹³², O. Lundberg ¹⁴⁸, B. Lund-Jensen ^{148,*}, N.A. Luongo ⁶, M.S. Lutz ³⁷, A.B. Lux ²⁶, D. Lynn ³⁰, R. Lysak ¹³⁵, E. Lytken ¹⁰¹, V. Lyubushkin ⁴⁰, T. Lyubushkina ⁴⁰, M.M. Lyukova ¹⁴⁹, M.Firdaus M. Soberi ⁵⁴, H. Ma ³⁰, K. Ma ^{64a}, L.L. Ma ^{64b}, W. Ma ^{64a}, Y. Ma ¹²⁵, J.C. MacDonald ¹⁰³, P.C. Machado De Abreu Farias ^{85e}, R. Madar ⁴², T. Madula ⁹⁹, J. Maeda ⁸⁷, T. Maeno ³⁰, P.T. Mafa ^{34c}, H. Maguire ¹⁴³, V. Maiboroda ¹³⁹, A. Maio ^{134a,134b,134d}, K. Maj ^{88a}, O. Majersky ⁵⁰, S. Majewski ¹²⁷, N. Makovec ⁶⁸, V. Maksimovic ¹⁶, B. Malaescu ¹³¹, Pa. Malecki ⁸⁹, V.P. Maleev ³⁹, F. Malek ^{62,m}, M. Mali ⁹⁶, D. Malito ⁹⁸, U. Mallik ^{82,*}, S. Maltezos ¹⁰, S. Malyukov ⁴⁰, J. Mamuzic ¹³, G. Mancini ⁵⁵, M.N. Mancini ²⁷, G. Manco ^{75a,75b}, J.P. Mandalia ⁹⁷, S.S. Mandarray ¹⁵⁰, I. Mandić ⁹⁶, L. Manhaes de Andrade Filho ^{85a}, I.M. Maniatis ¹⁷⁴, J. Manjarres Ramos ⁹², D.C. Mankad ¹⁷⁴, A. Mann ¹¹², S. Manzoni ³⁷, L. Mao ^{64c}, X. Mapekula ^{34c}, A. Marantis ^{156,r}, G. Marchiori ⁵, M. Marcisovsky ¹³⁵, C. Marcon ^{73a}, M. Marinescu ²¹, S. Marium ⁵⁰, M. Marjanovic ¹²⁴, A. Markhoos ⁵⁶, M. Markovitch ⁶⁸, M.K. Maroun ¹⁰⁶, E.J. Marshall ⁹⁴, Z. Marshall ^{18a}, S. Marti-Garcia ¹⁶⁸, J. Martin ⁹⁹, T.A. Martin ¹³⁸, V.J. Martin ⁵⁴, B. Martin dit Latour ¹⁷, L. Martinelli ^{77a,77b}, M. Martinez ^{13,u}, P. Martinez Agullo ¹⁶⁸, V.I. Martinez Outschoorn ¹⁰⁶, P. Martinez Suarez ¹³, S. Martin-Haugh ¹³⁸, G. Martinovicova ¹³⁷, V.S. Martoiu ^{28b}, A.C. Martyniuk ⁹⁹, A. Marzin ³⁷, D. Mascione ^{80a,80b}, L. Masetti ¹⁰³, J. Masik ¹⁰⁴, A.L. Maslennikov ³⁹, S.L. Mason ⁴³, P. Massarotti ^{74a,74b}, P. Mastrandrea ^{76a,76b}, A. Mastroberardino ^{45b,45a}, T. Masubuchi ¹²⁸, T.T. Mathew ¹²⁷, T. Mathisen ¹⁶⁶, J. Matousek ¹³⁷, D.M. Mattern ⁵¹, J. Maurer ^{28b}, T. Maurin ⁶¹, A.J. Maury ⁶⁸, B. Maček ⁹⁶, D.A. Maximov ³⁹, A.E. May ¹⁰⁴, R. Mazini ^{34g}, I. Maznas ¹¹⁹, M. Mazza ¹¹⁰, S.M. Mazza ¹⁴⁰, E. Mazzeo ^{73a,73b}, J.P. Mc Gowan ¹⁷⁰, S.P. Mc Kee ¹⁰⁹, C.A. Mc Lean ⁶, C.C. McCracken ¹⁶⁹, E.F. McDonald ¹⁰⁸, A.E. McDougall ¹¹⁸, L.F. Mcelhinney ⁹⁴, J.A. Mcfayden ¹⁵⁰, R.P. McGovern ¹³², R.P. Mckenzie ^{34g}, T.C. Mclachlan ⁵⁰, D.J. McLaughlin ⁹⁹, S.J. McMahon ¹³⁸, C.M. Mcpartland ⁹⁵, R.A. McPherson ^{170,y}, S. Mehlhase ¹¹², A. Mehta ⁹⁵, D. Melini ¹⁶⁸, B.R. Mellado Garcia ^{34g}, A.H. Melo ⁵⁷, F. Meloni ⁵⁰, A.M. Mendes Jacques Da Costa ¹⁰⁴, H.Y. Meng ¹⁵⁹, L. Meng ⁹⁴, S. Menke ¹¹³, M. Mentink ³⁷, E. Meoni ^{45b,45a}, G. Mercado ¹¹⁹, S. Merianos ¹⁵⁶, C. Merlassino ^{71a,71c}, L. Merola ^{74a,74b}, C. Meroni ^{73a,73b}, J. Metcalfe ⁶, A.S. Mete ⁶, E. Meuser ¹⁰³, C. Meyer ⁷⁰, J-P. Meyer ¹³⁹, R.P. Middleton ¹³⁸, L. Mijović ⁵⁴, G. Mikenberg ¹⁷⁴, M. Mikestikova ¹³⁵, M. Mikuž ⁹⁶, H. Mildner ¹⁰³, A. Milic ³⁷, D.W. Miller ⁴¹, E.H. Miller ¹⁴⁷, L.S. Miller ³⁵, A. Milov ¹⁷⁴, D.A. Milstead ^{49a,49b}, T. Min ^{115a}, A.A. Minaenko ³⁹, I.A. Minashvili ^{153b}, A.I. Mincer ¹²¹, B. Mindur ^{88a}, M. Mineev ⁴⁰, Y. Mino ⁹⁰, L.M. Mir ¹³, M. Miralles Lopez ⁶¹, M. Mironova ^{18a}, M.C. Missio ¹¹⁷, A. Mitra ¹⁷², V.A. Mitsou ¹⁶⁸, Y. Mitsumori ¹¹⁴, O. Miu ¹⁵⁹, P.S. Miyagawa ⁹⁷, T. Mkrtchyan ^{65a}, M. Mlinarevic ⁹⁹, T. Mlinarevic ⁹⁹, M. Mlynarikova ³⁷, S. Mobius ²⁰, P. Mogg ¹¹², M.H. Mohamed Farook ¹¹⁶, A.F. Mohammed ^{14,115c}, S. Mohapatra ⁴³, G. Mokgatitwane ^{34g}, L. Moleri ¹⁷⁴, B. Mondal ¹⁴⁵, S. Mondal ¹³⁶, K. Mönig ⁵⁰, E. Monnier ¹⁰⁵, L. Monsonis Romero ¹⁶⁸, J. Montejo Berlingen ¹³, A. Montella ^{49a,49b}, M. Montella ¹²³, F. Montekali ^{79a,79b}, F. Monticelli ⁹³, S. Monzani ^{71a,71c}, A. Morancho Tarda ⁴⁴, N. Morange ⁶⁸, A.L. Moreira De Carvalho ⁵⁰, M. Moreno Llácer ¹⁶⁸, C. Moreno Martinez ⁵⁸,

J.M. Moreno Perez^{23b}, P. Morettini^{59b}, S. Morgenstern³⁷, M. Morii⁶³, M. Morinaga¹⁵⁷, M. Moritsu⁹¹, F. Morodei^{77a,77b}, P. Moschovakos³⁷, B. Moser¹³⁰, M. Mosidze^{153b}, T. Moskalets⁴⁶, P. Moskvitina¹¹⁷, J. Moss^{32j}, P. Moszkowicz^{88a}, A. Moussa^{36d}, Y. Moyal¹⁷⁴, E.J.W. Moyse¹⁰⁶, O. Mtintsilana^{34g}, S. Muanza¹⁰⁵, J. Mueller¹³³, D. Muenstermann⁹⁴, R. Müller³⁷, G.A. Mullier¹⁶⁶, A.J. Mullin³³, J.J. Mullin¹³², A.E. Mulski⁶³, D.P. Mungo¹⁵⁹, D. Munoz Perez¹⁶⁸, F.J. Munoz Sanchez¹⁰⁴, M. Murin¹⁰⁴, W.J. Murray^{172,138}, M. Muškinja⁹⁶, C. Mwewa³⁰, A.G. Myagkov^{39,a}, A.J. Myers⁸, G. Myers¹⁰⁹, M. Myska¹³⁶, B.P. Nachman^{18a}, K. Nagai¹³⁰, K. Nagano⁸⁶, R. Nagasaka¹⁵⁷, J.L. Nagle^{30,af}, E. Nagy¹⁰⁵, A.M. Nairz³⁷, Y. Nakahama⁸⁶, K. Nakamura⁸⁶, K. Nakkalil⁵, H. Nanjo¹²⁸, E.A. Narayanan⁴⁶, Y. Narukawa¹⁵⁷, I. Naryshkin³⁹, L. Nasella^{73a,73b}, S. Nasri^{120b}, C. Nass²⁵, G. Navarro^{23a}, J. Navarro-Gonzalez¹⁶⁸, A. Nayaz¹⁹, P.Y. Nechaeva³⁹, S. Nechaeva^{24b,24a}, F. Nechansky¹³⁵, L. Nedic¹³⁰, T.J. Neep²¹, A. Negri^{75a,75b}, M. Negrini^{24b}, C. Nellist¹¹⁸, C. Nelson¹⁰⁷, K. Nelson¹⁰⁹, S. Nemecek¹³⁵, M. Nessi^{37,g}, M.S. Neubauer¹⁶⁷, F. Neuhaus¹⁰³, J. Neundorff⁵⁰, J. Newell⁹⁵, P.R. Newman²¹, C.W. Ng¹³³, Y.W.Y. Ng⁵⁰, B. Ngair^{120a}, H.D.N. Nguyen¹¹¹, R.B. Nickerson¹³⁰, R. Nicolaidou¹³⁹, J. Nielsen¹⁴⁰, M. Niemeyer⁵⁷, J. Niermann³⁷, N. Nikiforou³⁷, V. Nikolaenko^{39,a}, I. Nikolic-Audit¹³¹, K. Nikolopoulos²¹, P. Nilsson³⁰, I. Ninca⁵⁰, G. Ninio¹⁵⁵, A. Nisati^{77a}, N. Nishu², R. Nisius¹¹³, N. Nitika^{71a,71c}, J-E. Nitschke⁵², E.K. Nkadimeng^{34g}, T. Nobe¹⁵⁷, T. Nommensen¹⁵¹, M.B. Norfolk¹⁴³, B.J. Norman³⁵, M. Noury^{36a}, J. Novak⁹⁶, T. Novak⁹⁶, L. Novotny¹³⁶, R. Novotny¹¹⁶, L. Nozka¹²⁶, K. Ntekas¹⁶³, N.M.J. Nunes De Moura Junior^{85b}, J. Ocariz¹³¹, A. Ochi⁸⁷, I. Ochoa^{134a}, S. Oerdek^{50,v}, J.T. Offermann⁴¹, A. Ogrodnik¹³⁷, A. Oh¹⁰⁴, C.C. Ohm¹⁴⁸, H. Oide⁸⁶, R. Oishi¹⁵⁷, M.L. Ojeda³⁷, Y. Okumura¹⁵⁷, L.F. Oleiro Seabra^{134a}, I. Oleksiyuk⁵⁸, S.A. Olivares Pino^{141d}, G. Oliveira Correa¹³, D. Oliveira Damazio³⁰, J.L. Oliver¹⁶³, Ö.O. Öncel⁵⁶, A.P. O'Neill²⁰, A. Onofre^{134a,134e}, P.U.E. Onyisi¹¹, M.J. Oreglia⁴¹, D. Orestano^{79a,79b}, N. Orlando¹³, R.S. Orr¹⁵⁹, L.M. Osojnak¹³², Y. Osumi¹¹⁴, G. Otero y Garzon³¹, H. Otono⁹¹, P.S. Ott^{65a}, G.J. Ottino^{18a}, M. Ouchrif^{36d}, F. Ould-Saada¹²⁹, T. Ovsiannikova¹⁴², M. Owen⁶¹, R.E. Owen¹³⁸, V.E. Ozcan^{22a}, F. Ozturk⁸⁹, N. Ozturk⁸, S. Ozturk⁸⁴, H.A. Pacey¹³⁰, A. Pacheco Pages¹³, C. Padilla Aranda¹³, G. Padovano^{77a,77b}, S. Pagan Griso^{18a}, G. Palacino⁷⁰, A. Palazzo^{72a,72b}, J. Pampel²⁵, J. Pan¹⁷⁷, T. Pan^{66a}, D.K. Panchal¹¹, C.E. Pandini¹¹⁸, J.G. Panduro Vazquez¹³⁸, H.D. Pandya¹, H. Pang¹⁵, P. Pani⁵⁰, G. Panizzo^{71a,71c}, L. Panwar¹³¹, L. Paolozzi⁵⁸, S. Parajuli¹⁶⁷, A. Paramonov⁶, C. Paraskevopoulos⁵⁵, D. Paredes Hernandez^{66b}, A. Pareti^{75a,75b}, K.R. Park⁴³, T.H. Park¹⁵⁹, M.A. Parker³³, F. Parodi^{59b,59a}, V.A. Parrish⁵⁴, J.A. Parsons⁴³, U. Parzefall⁵⁶, B. Pascual Dias¹¹¹, L. Pascual Dominguez¹⁰², E. Pasqualucci^{77a}, S. Passaggio^{59b}, F. Pastore⁹⁸, P. Patel⁸⁹, U.M. Patel⁵³, J.R. Pater¹⁰⁴, T. Pauly³⁷, F. Pauwels¹³⁷, C.I. Pazos¹⁶², M. Pedersen¹²⁹, R. Pedro^{134a}, S.V. Peleganchuk³⁹, O. Penc³⁷, E.A. Pender⁵⁴, S. Peng¹⁵, G.D. Penn¹⁷⁷, K.E. Pensi¹¹², M. Penzin³⁹, B.S. Peralva^{85d}, A.P. Pereira Peixoto¹⁴², L. Pereira Sanchez¹⁴⁷, D.V. Perepelitsa^{30,af}, G. Perera¹⁰⁶, E. Perez Codina^{160a}, M. Perganti¹⁰, H. Pernegger³⁷, S. Perrella^{77a,77b}, O. Perrin⁴², K. Peters⁵⁰, R.F.Y. Peters¹⁰⁴, B.A. Petersen³⁷, T.C. Petersen⁴⁴, E. Petit¹⁰⁵, V. Petousis¹³⁶, C. Petridou^{156,d}, T. Petru¹³⁷, A. Petrukhin¹⁴⁵, M. Pettee^{18a}, A. Petukhov⁸⁴, K. Petukhova³⁷, R. Pezoa^{141f}, L. Pezzotti³⁷, G. Pezzullo¹⁷⁷, A.J. Pflieger³⁷, T.M. Pham¹⁷⁵, T. Pham¹⁰⁸, P.W. Phillips¹³⁸, G. Piacquadio¹⁴⁹, E. Pianori^{18a}, F. Piazza¹²⁷, R. Piegaia³¹, D. Pietreanu^{28b}, A.D. Pilkington¹⁰⁴, M. Pinamonti^{71a,71c}, J.L. Pinfold², B.C. Pinheiro Pereira^{134a}, J. Pinol Bel¹³, A.E. Pinto Pinoargote^{139,139}, L. Pintucci^{71a,71c}, K.M. Piper¹⁵⁰, A. Pirttikoski⁵⁸, D.A. Pizzi³⁵, L. Pizzimento^{66b}, A. Pizzini¹¹⁸, M.-A. Pleier³⁰, V. Pleskot¹³⁷, E. Plotnikova⁴⁰, G. Poddar⁹⁷, R. Poettgen¹⁰¹,

L. Poggioli ¹³¹, S. Polacek ¹³⁷, G. Polesello ^{75a}, A. Poley ^{146,160a}, A. Polini ^{24b}, C.S. Pollard ¹⁷²,
 Z.B. Pollock ¹²³, E. Pompa Pacchi ¹²⁴, N.I. Pond ⁹⁹, D. Ponomarenko ⁷⁰, L. Pontecorvo ³⁷,
 S. Popa ^{28a}, G.A. Popeneciu ^{28d}, A. Poreba ³⁷, D.M. Portillo Quintero ^{160a}, S. Pospisil ¹³⁶,
 M.A. Postill ¹⁴³, P. Postolache ^{28c}, K. Potamianos ¹⁷², P.A. Potepa ^{88a}, I.N. Potrap ⁴⁰,
 C.J. Potter ³³, H. Potti ¹⁵¹, J. Poveda ¹⁶⁸, M.E. Pozo Astigarraga ³⁷, A. Prades Ibanez ^{78a,78b},
 J. Pretel ¹⁷⁰, D. Price ¹⁰⁴, M. Primavera ^{72a}, L. Primomo ^{71a,71c}, M.A. Principe Martin ¹⁰²,
 R. Privara ¹²⁶, T. Procter ⁶¹, M.L. Proffitt ¹⁴², N. Proklova ¹³², K. Prokofiev ^{66c}, G. Proto ¹¹³,
 J. Proudfoot ⁶, M. Przybycien ^{88a}, W.W. Przygoda ^{88b}, A. Psallidas ⁴⁸, J.E. Puddefoot ¹⁴³,
 D. Pudzha ⁵⁶, D. Pyatiizbyantseva ³⁹, J. Qian ¹⁰⁹, R. Qian ¹¹⁰, D. Qichen ¹⁰⁴, Y. Qin ¹³,
 T. Qiu ⁵⁴, A. Quadt ⁵⁷, M. Queitsch-Maitland ¹⁰⁴, G. Quetant ⁵⁸, R.P. Quinn ¹⁶⁹,
 G. Rabanal Bolanos ⁶³, D. Rafanoharana ⁵⁶, F. Raffaelli ^{78a,78b}, F. Ragusa ^{73a,73b}, J.L. Rainbolt ⁴¹,
 J.A. Raine ⁵⁸, S. Rajagopalan ³⁰, E. Ramakoti ³⁹, L. Rambelli ^{59b,59a}, I.A. Ramirez-Berend ³⁵,
 K. Ran ^{50,115c}, D.S. Rankin ¹³², N.P. Rapheeha ^{34g}, H. Rasheed ^{28b}, V. Raskina ¹³¹,
 D.F. Rassloff ^{65a}, A. Rastogi ^{18a}, S. Rave ¹⁰³, S. Ravera ^{59b,59a}, B. Ravina ⁵⁷, I. Ravinovich ¹⁷⁴,
 M. Raymond ³⁷, A.L. Read ¹²⁹, N.P. Readioff ¹⁴³, D.M. Rebuzzi ^{75a,75b}, G. Redlinger ³⁰,
 A.S. Reed ¹¹³, K. Reeves ²⁷, J.A. Reidelsturz ¹⁷⁶, D. Reikher ¹²⁷, A. Rej ⁵¹, C. Rembser ³⁷,
 M. Renda ^{28b}, F. Renner ⁵⁰, A.G. Rennie ¹⁶³, A.L. Rescia ⁵⁰, S. Resconi ^{73a},
 M. Ressegotti ^{59b,59a}, S. Rettie ³⁷, J.G. Reyes Rivera ¹¹⁰, E. Reynolds ^{18a}, O.L. Rezanova ³⁹,
 P. Reznicek ¹³⁷, H. Riani ^{36d}, N. Ribaric ⁵³, E. Ricci ^{80a,80b}, R. Richter ¹¹³, S. Richter ^{49a,49b},
 E. Richter-Was ^{88b}, M. Ridel ¹³¹, S. Ridouani ^{36d}, P. Rieck ¹²¹, P. Riedler ³⁷, E.M. Riefel ^{49a,49b},
 J.O. Rieger ¹¹⁸, M. Rijssenbeek ¹⁴⁹, M. Rimoldi ³⁷, L. Rinaldi ^{24b,24a}, P. Rincke ^{57,166},
 T.T. Rinn ³⁰, M.P. Rinnagel ¹¹², G. Ripellino ¹⁶⁶, I. Riu ¹³, J.C. Rivera Vergara ¹⁷⁰,
 F. Rizatdinova ¹²⁵, E. Rizvi ⁹⁷, B.R. Roberts ^{18a}, S.S. Roberts ¹⁴⁰, S.H. Robertson ^{107,y},
 D. Robinson ³³, M. Robles Manzano ¹⁰³, A. Robson ⁶¹, A. Rocchi ^{78a,78b}, C. Roda ^{76a,76b},
 S. Rodriguez Bosca ³⁷, Y. Rodriguez Garcia ^{23a}, A.M. Rodríguez Vera ¹¹⁹, S. Roe ³⁷,
 J.T. Roemer ³⁷, O. Røhne ¹²⁹, R.A. Rojas ¹⁰⁶, C.P.A. Roland ¹³¹, J. Roloff ³⁰, A. Romaniouk ⁸¹,
 E. Romano ^{75a,75b}, M. Romano ^{24b}, A.C. Romero Hernandez ¹⁶⁷, N. Rompotis ⁹⁵, L. Roos ¹³¹,
 S. Rosati ^{77a}, B.J. Rosser ⁴¹, E. Rossi ¹³⁰, E. Rossi ^{74a,74b}, L.P. Rossi ⁶³, L. Rossini ⁵⁶,
 R. Rosten ¹²³, M. Rotaru ^{28b}, B. Rottler ⁵⁶, C. Rougier ⁹², D. Rousseau ⁶⁸, D. Rousso ⁵⁰,
 A. Roy ¹⁶⁷, S. Roy-Garand ¹⁵⁹, A. Rozanov ¹⁰⁵, Z.M.A. Rozario ⁶¹, Y. Rozen ¹⁵⁴,
 A. Rubio Jimenez ¹⁶⁸, V.H. Ruelas Rivera ¹⁹, T.A. Ruggeri ¹, A. Ruggiero ¹³⁰,
 A. Ruiz-Martinez ¹⁶⁸, A. Rummler ³⁷, Z. Rurikova ⁵⁶, N.A. Rusakovich ⁴⁰, H.L. Russell ¹⁷⁰,
 G. Russo ^{77a,77b}, J.P. Rutherford ⁷, S. Rutherford Colmenares ³³, M. Rybar ¹³⁷, E.B. Rye ¹²⁹,
 A. Ryzhov ⁴⁶, J.A. Sabater Iglesias ⁵⁸, H.F.W. Sadrozinski ¹⁴⁰, F. Safai Tehrani ^{77a},
 B. Safarzadeh Samani ¹³⁸, S. Saha ¹, M. Sahinsoy ⁸⁴, A. Saibel ¹⁶⁸, M. Saimpert ¹³⁹,
 M. Saito ¹⁵⁷, T. Saito ¹⁵⁷, A. Sala ^{73a,73b}, D. Salamani ³⁷, A. Salnikov ¹⁴⁷, J. Salt ¹⁶⁸,
 A. Salvador Salas ¹⁵⁵, D. Salvatore ^{45b,45a}, F. Salvatore ¹⁵⁰, A. Salzburger ³⁷, D. Sammel ⁵⁶,
 E. Sampson ⁹⁴, D. Sampsonidis ^{156,d}, D. Sampsonidou ¹²⁷, J. Sánchez ¹⁶⁸,
 V. Sanchez Sebastian ¹⁶⁸, H. Sandaker ¹²⁹, C.O. Sander ⁵⁰, J.A. Sandesara ¹⁰⁶, M. Sandhoff ¹⁷⁶,
 C. Sandoval ^{23b}, L. Sanfilippo ^{65a}, D.P.C. Sankey ¹³⁸, T. Sano ⁹⁰, A. Sansoni ⁵⁵, L. Santi ^{37,77b},
 C. Santoni ⁴², H. Santos ^{134a,134b}, A. Santra ¹⁷⁴, E. Sanzani ^{24b,24a}, K.A. Saoucha ¹⁶⁵,
 J.G. Saraiva ^{134a,134d}, J. Sardain ⁷, O. Sasaki ⁸⁶, K. Sato ¹⁶¹, C. Sauer ³⁷, E. Sauvan ⁴,
 P. Savard ^{159,ad}, R. Sawada ¹⁵⁷, C. Sawyer ¹³⁸, L. Sawyer ¹⁰⁰, C. Sbarra ^{24b}, A. Sbrizzi ^{24b,24a},
 T. Scanlon ⁹⁹, J. Schaarschmidt ¹⁴², U. Schäfer ¹⁰³, A.C. Schaffer ^{68,46}, D. Schaile ¹¹²,
 R.D. Schamberger ¹⁴⁹, C. Scharf ¹⁹, M.M. Schefer ²⁰, V.A. Schegelsky ³⁹, D. Scheirich ¹³⁷,
 M. Schernau ^{141e}, C. Scheulen ⁵⁸, C. Schiavi ^{59b,59a}, M. Schioppa ^{45b,45a}, B. Schlag ¹⁴⁷,
 S. Schlenker ³⁷, J. Schmeing ¹⁷⁶, C.R. Schmidt ⁵², M.A. Schmidt ¹⁷⁶, K. Schmieden ¹⁰³,

C. Schmitt ¹⁰³, N. Schmitt ¹⁰³, S. Schmitt ⁵⁰, L. Schoeffel ¹³⁹, A. Schoening ^{65b},
 P.G. Scholer ³⁵, E. Schopf ¹³⁰, M. Schott ²⁵, J. Schovancova ³⁷, S. Schramm ⁵⁸, T. Schroer ⁵⁸,
 H-C. Schultz-Coulon ^{65a}, M. Schumacher ⁵⁶, B.A. Schumm ¹⁴⁰, Ph. Schune ¹³⁹, A.J. Schuy ¹⁴²,
 H.R. Schwartz ¹⁴⁰, A. Schwartzman ¹⁴⁷, T.A. Schwarz ¹⁰⁹, Ph. Schwemling ¹³⁹,
 R. Schwienhorst ¹¹⁰, F.G. Sciacca ²⁰, A. Sciandra ³⁰, G. Sciolla ²⁷, F. Scuri ^{76a},
 C.D. Sebastiani ⁹⁵, K. Sedlaczek ¹¹⁹, S.C. Seidel ¹¹⁶, A. Seiden ¹⁴⁰, B.D. Seidlitz ⁴³, C. Seitz ⁵⁰,
 J.M. Seixas ^{85b}, G. Sekhniaidze ^{74a}, L. Selem ⁶², N. Semprini-Cesari ^{24b,24a}, A. Semushin ^{178,39},
 D. Sengupta ⁵⁸, V. Senthilkumar ¹⁶⁸, L. Serin ⁶⁸, M. Sessa ^{78a,78b}, H. Severini ¹²⁴,
 F. Sforza ^{59b,59a}, A. Sfyrila ⁵⁸, Q. Sha ¹⁴, E. Shabalina ⁵⁷, A.H. Shah ³³, R. Shaheen ¹⁴⁸,
 J.D. Shahinian ¹³², D. Shaked Renous ¹⁷⁴, L.Y. Shan ¹⁴, M. Shapiro ^{18a}, A. Sharma ³⁷,
 A.S. Sharma ¹⁶⁹, P. Sharma ³⁰, P.B. Shatalov ³⁹, K. Shaw ¹⁵⁰, S.M. Shaw ¹⁰⁴, Q. Shen ^{64c},
 D.J. Sheppard ¹⁴⁶, P. Sherwood ⁹⁹, L. Shi ⁹⁹, X. Shi ¹⁴, S. Shimizu ⁸⁶, C.O. Shimmin ¹⁷⁷,
 I.P.J. Shipsey ¹³⁰, S. Shirabe ⁹¹, M. Shiyakova ^{40,w}, M.J. Shochet ⁴¹, D.R. Shope ¹²⁹,
 B. Shrestha ¹²⁴, S. Shrestha ^{123,ag}, I. Shreyber ³⁹, M.J. Shroff ¹⁷⁰, P. Sicho ¹³⁵, A.M. Sickles ¹⁶⁷,
 E. Sideras Haddad ^{34g,164}, A.C. Sidley ¹¹⁸, A. Sidoti ^{24b}, F. Siegert ⁵², Dj. Sijacki ¹⁶, F. Sili ⁹³,
 J.M. Silva ⁵⁴, I. Silva Ferreira ^{85b}, M.V. Silva Oliveira ³⁰, S.B. Silverstein ^{49a}, S. Simion ⁶⁸,
 R. Simoniello ³⁷, E.L. Simpson ¹⁰⁴, H. Simpson ¹⁵⁰, L.R. Simpson ¹⁰⁹, S. Simsek ⁸⁴,
 S. Sindhu ⁵⁷, P. Sinervo ¹⁵⁹, S. Singh ³⁰, S. Sinha ⁵⁰, S. Sinha ¹⁰⁴, M. Sioli ^{24b,24a}, I. Siral ³⁷,
 E. Sitnikova ⁵⁰, J. Sjölin ^{49a,49b}, A. Skaf ⁵⁷, E. Skorda ²¹, P. Skubic ¹²⁴, M. Slawinska ⁸⁹,
 I. Slazyk ¹⁷, V. Smakhtin ¹⁷⁴, B.H. Smart ¹³⁸, S.Yu. Smirnov ³⁹, Y. Smirnov ³⁹, L.N. Smirnova ^{39,a},
 O. Smirnova ¹⁰¹, A.C. Smith ⁴³, D.R. Smith ¹⁶³, E.A. Smith ⁴¹, J.L. Smith ¹⁰⁴, R. Smith ¹⁴⁷,
 H. Smitmanns ¹⁰³, M. Smizanska ⁹⁴, K. Smolek ¹³⁶, A.A. Snesarev ³⁹, H.L. Snoek ¹¹⁸,
 S. Snyder ³⁰, R. Sobie ^{170,y}, A. Soffer ¹⁵⁵, C.A. Solans Sanchez ³⁷, E.Yu. Soldatov ³⁹,
 U. Soldevila ¹⁶⁸, A.A. Solodkov ³⁹, S. Solomon ²⁷, A. Soloshenko ⁴⁰, K. Solovieva ⁵⁶,
 O.V. Solovyanov ⁴², P. Sommer ⁵², A. Sonay ¹³, W.Y. Song ^{160b}, A. Sopczak ¹³⁶, A.L. Sopio ⁵⁴,
 F. Sopkova ^{29b}, J.D. Sorenson ¹¹⁶, I.R. Sotarriva Alvarez ¹⁵⁸, V. Sothilingam ^{65a},
 O.J. Soto Sandoval ^{141c,141b}, S. Sottocornola ⁷⁰, R. Soualah ¹⁶⁵, Z. Soumami ^{36e}, D. South ⁵⁰,
 N. Soybelman ¹⁷⁴, S. Spagnolo ^{72a,72b}, M. Spalla ¹¹³, D. Sperlich ⁵⁶, G. Spigo ³⁷,
 B. Spisso ^{74a,74b}, D.P. Spiteri ⁶¹, M. Spousta ¹³⁷, E.J. Staats ³⁵, R. Stamen ^{65a}, A. Stampekis ²¹,
 E. Stanecka ⁸⁹, W. Stanek-Maslouska ⁵⁰, M.V. Stange ⁵², B. Stanislaus ^{18a}, M.M. Stanitzki ⁵⁰,
 B. Stapf ⁵⁰, E.A. Starchenko ³⁹, G.H. Stark ¹⁴⁰, J. Stark ⁹², P. Staroba ¹³⁵, P. Starovoitov ^{65a},
 S. Stärz ¹⁰⁷, R. Staszewski ⁸⁹, G. Stavropoulos ⁴⁸, A. Steff ³⁷, P. Steinberg ³⁰, B. Stelzer ^{146,160a},
 H.J. Stelzer ¹³³, O. Stelzer-Chilton ^{160a}, H. Stenzel ⁶⁰, T.J. Stevenson ¹⁵⁰, G.A. Stewart ³⁷,
 J.R. Stewart ¹²⁵, M.C. Stockton ³⁷, G. Stoicea ^{28b}, M. Stolarski ^{134a}, S. Stonjek ¹¹³,
 A. Straessner ⁵², J. Strandberg ¹⁴⁸, S. Strandberg ^{49a,49b}, M. Stratmann ¹⁷⁶, M. Strauss ¹²⁴,
 T. Strebler ¹⁰⁵, P. Strizenec ^{29b}, R. Ströhmer ¹⁷¹, D.M. Strom ¹²⁷, R. Stroynowski ⁴⁶,
 A. Strubig ^{49a,49b}, S.A. Stucci ³⁰, B. Stugu ¹⁷, J. Stupak ¹²⁴, N.A. Styles ⁵⁰, D. Su ¹⁴⁷,
 S. Su ^{64a}, W. Su ^{64d}, X. Su ^{64a}, D. Suchy ^{29a}, K. Sugizaki ¹⁵⁷, V.V. Sulin ³⁹, M.J. Sullivan ⁹⁵,
 D.M.S. Sultan ¹³⁰, L. Sultanaliyeva ³⁹, S. Sultansoy ^{3b}, T. Sumida ⁹⁰, S. Sun ¹⁷⁵, W. Sun ¹⁴,
 O. Sunneborn Gudnadottir ¹⁶⁶, N. Sur ¹⁰⁵, M.R. Sutton ¹⁵⁰, H. Suzuki ¹⁶¹, M. Svatos ¹³⁵,
 M. Swiatlowski ^{160a}, T. Swirski ¹⁷¹, I. Sykora ^{29a}, M. Sykora ¹³⁷, T. Sykora ¹³⁷, D. Ta ¹⁰³,
 K. Tackmann ^{50,v}, A. Taffard ¹⁶³, R. Tafirout ^{160a}, J.S. Tafoya Vargas ⁶⁸, Y. Takubo ⁸⁶,
 M. Talby ¹⁰⁵, A.A. Talyshev ³⁹, K.C. Tam ^{66b}, N.M. Tamir ¹⁵⁵, A. Tanaka ¹⁵⁷, J. Tanaka ¹⁵⁷,
 R. Tanaka ⁶⁸, M. Tanasini ¹⁴⁹, Z. Tao ¹⁶⁹, S. Tapia Araya ^{141f}, S. Tapprogge ¹⁰³,
 A. Tarek Abouelfadl Mohamed ¹¹⁰, S. Tarem ¹⁵⁴, K. Tariq ¹⁴, G. Tarna ^{28b}, G.F. Tartarelli ^{73a},
 M.J. Tartarin ⁹², P. Tas ¹³⁷, M. Tasevsky ¹³⁵, E. Tassi ^{45b,45a}, A.C. Tate ¹⁶⁷, G. Tateno ¹⁵⁷,
 Y. Tayalati ^{36e,x}, G.N. Taylor ¹⁰⁸, W. Taylor ^{160b}, P. Teixeira-Dias ⁹⁸, J.J. Teoh ¹⁵⁹,

K. Terashi ¹⁵⁷, J. Terron ¹⁰², S. Terzo ¹³, M. Testa ⁵⁵, R.J. Teuscher ^{159,y}, A. Thaler ⁸¹,
 O. Theiner ⁵⁸, T. Thevenaux-Pelzer ¹⁰⁵, O. Thielmann ¹⁷⁶, D.W. Thomas ⁹⁸, J.P. Thomas ²¹,
 E.A. Thompson ^{18a}, P.D. Thompson ²¹, E. Thomson ¹³², R.E. Thornberry ⁴⁶, C. Tian ^{64a},
 Y. Tian ⁵⁸, V. Tikhomirov ^{39,a}, Yu.A. Tikhonov ³⁹, S. Timoshenko ³⁹, D. Timoshyn ¹³⁷,
 E.X.L. Ting ¹, P. Tipton ¹⁷⁷, A. Tishelman-Charny ³⁰, S.H. Tlou ^{34g}, K. Todome ¹⁵⁸,
 S. Todorova-Nova ¹³⁷, S. Todt ⁵², L. Toffolin ^{71a,71c}, M. Togawa ⁸⁶, J. Tojo ⁹¹, S. Tokár ^{29a},
 K. Tokushuku ⁸⁶, O. Toldaiev ⁷⁰, G. Tolkachev ¹⁰⁵, M. Tomoto ^{86,114}, L. Tompkins ^{147,1},
 E. Torrence ¹²⁷, H. Torres ⁹², E. Torró Pastor ¹⁶⁸, M. Toscani ³¹, C. Tosciri ⁴¹, M. Tost ¹¹,
 D.R. Tovey ¹⁴³, I.S. Trandafir ^{28b}, T. Trefzger ¹⁷¹, A. Tricoli ³⁰, I.M. Trigger ^{160a},
 S. Trincaz-Duvoid ¹³¹, D.A. Trischuk ²⁷, B. Trocmé ⁶², A. Tropina ⁴⁰, L. Truong ^{34c},
 M. Trzebinski ⁸⁹, A. Trzuppek ⁸⁹, F. Tsai ¹⁴⁹, M. Tsai ¹⁰⁹, A. Tsiamis ¹⁵⁶, P.V. Tsiarehka ⁴⁰,
 S. Tsigaridas ^{160a}, A. Tsigigotis ^{156,r}, V. Tsiskaridze ¹⁵⁹, E.G. Tskhadadze ^{153a}, M. Tsopoulou ¹⁵⁶,
 Y. Tsujikawa ⁹⁰, I.I. Tsukerman ³⁹, V. Tsulaia ^{18a}, S. Tsuno ⁸⁶, K. Tsuru ¹²², D. Tsybychev ¹⁴⁹,
 Y. Tu ^{66b}, A. Tudorache ^{28b}, V. Tudorache ^{28b}, A.N. Tuna ⁶³, S. Turchikhin ^{59b,59a},
 I. Turk Cakir ^{3a}, R. Turra ^{73a}, T. Turtuvshin ⁴⁰, P.M. Tuts ⁴³, S. Tzamarias ^{156,d}, E. Tzovara ¹⁰³,
 F. Ukegawa ¹⁶¹, P.A. Ulloa Poblete ^{141c,141b}, E.N. Umaka ³⁰, G. Unal ³⁷, A. Undrus ³⁰,
 G. Unel ¹⁶³, J. Urban ^{29b}, P. Urrejola ^{141a}, G. Usai ⁸, R. Ushioda ¹⁵⁸, M. Usman ¹¹¹,
 F. Ustuner ⁵⁴, Z. Uysal ⁸⁴, V. Vacek ¹³⁶, B. Vachon ¹⁰⁷, T. Vafeiadis ³⁷, A. Vaitkus ⁹⁹,
 C. Valderanis ¹¹², E. Valdes Santurio ^{49a,49b}, M. Valente ^{160a}, S. Valentinetti ^{24b,24a}, A. Valero ¹⁶⁸,
 E. Valiente Moreno ¹⁶⁸, A. Vallier ⁹², J.A. Valls Ferrer ¹⁶⁸, D.R. Van Arneman ¹¹⁸,
 T.R. Van Daalen ¹⁴², A. Van Der Graaf ⁵¹, P. Van Gemmeren ⁶, M. Van Rijnbach ³⁷,
 S. Van Stroud ⁹⁹, I. Van Vulpen ¹¹⁸, P. Vana ¹³⁷, M. Vanadia ^{78a,78b}, U.M. Vande Voorde ¹⁴⁸,
 W. Vandelli ³⁷, E.R. Vandewall ¹²⁵, D. Vannicola ¹⁵⁵, L. Vannoli ⁵⁵, R. Vari ^{77a}, E.W. Varnes ⁷,
 C. Varni ^{18b}, D. Varouchas ⁶⁸, L. Varriale ¹⁶⁸, K.E. Varvell ¹⁵¹, M.E. Vasile ^{28b}, L. Vaslin ⁸⁶,
 A. Vasyukov ⁴⁰, L.M. Vaughan ¹²⁵, R. Vavricka ¹⁰³, T. Vazquez Schroeder ³⁷, J. Veatch ³²,
 V. Vecchio ¹⁰⁴, M.J. Veen ¹⁰⁶, I. Veliscek ³⁰, L.M. Veloce ¹⁵⁹, F. Veloso ^{134a,134c},
 S. Veneziano ^{77a}, A. Ventura ^{72a,72b}, S. Ventura Gonzalez ¹³⁹, A. Verbytskyi ¹¹³,
 M. Verducci ^{76a,76b}, C. Vergis ⁹⁷, M. Verissimo De Araujo ^{85b}, W. Verkerke ¹¹⁸,
 J.C. Vermeulen ¹¹⁸, C. Vernieri ¹⁴⁷, M. Vessella ¹⁶³, M.C. Vetterli ^{146,ad}, A. Vgenopoulos ¹⁰³,
 N. Viaux Maira ^{141f}, T. Vickey ¹⁴³, O.E. Vickey Boeriu ¹⁴³, G.H.A. Viehhauser ¹³⁰, L. Vignani ^{65b},
 M. Vigl ¹¹³, M. Villa ^{24b,24a}, M. Villaplana Perez ¹⁶⁸, E.M. Villhauer ⁵⁴, E. Vilucchi ⁵⁵,
 M.G. Vincter ³⁵, A. Visible ¹¹⁸, C. Vittori ³⁷, I. Vivarelli ^{24b,24a}, E. Voevodina ¹¹³, F. Vogel ¹¹²,
 J.C. Voigt ⁵², P. Vokac ¹³⁶, Yu. Volkotrub ^{88b}, E. Von Toerne ²⁵, A. Vorlander ¹⁷⁶,
 B. Vormwald ³⁷, V. Vorobel ¹³⁷, K. Vorobev ³⁹, M. Vos ¹⁶⁸, K. Voss ¹⁴⁵, M. Vozak ¹¹⁸,
 L. Vozdecky ¹²⁴, N. Vranjes ¹⁶, M. Vranjes Milosavljevic ¹⁶, M. Vreeswijk ¹¹⁸, N.K. Vu ^{64d},
 R. Vuillermet ³⁷, O. Vujinovic ¹⁰³, I. Vukotic ⁴¹, I.K. Vyas ³⁵, S. Wada ¹⁶¹, C. Wagner ¹⁴⁷,
 J.M. Wagner ^{18a}, W. Wagner ¹⁷⁶, S. Wahdan ¹⁷⁶, H. Wahlberg ⁹³, C.H. Waits ¹²⁴, J. Walder ¹³⁸,
 R. Walker ¹¹², W. Walkowiak ¹⁴⁵, A. Wall ¹³², E.J. Wallin ¹⁰¹, T. Wamorkar ⁶, A.Z. Wang ¹⁴⁰,
 C. Wang ¹⁰³, C. Wang ¹¹, H. Wang ^{18a}, J. Wang ^{66c}, P. Wang ¹⁰⁴, P. Wang ⁹⁹, R. Wang ⁶³,
 R. Wang ⁶, S.M. Wang ¹⁵², S. Wang ¹⁴, T. Wang ^{64a}, W.T. Wang ⁸², W. Wang ¹⁴,
 X. Wang ¹⁶⁷, X. Wang ^{64c}, Y. Wang ^{64d}, Y. Wang ^{115a}, Y. Wang ^{64a}, Z. Wang ¹⁰⁹,
 Z. Wang ^{64d,53,64c}, Z. Wang ¹⁰⁹, A. Warburton ¹⁰⁷, R.J. Ward ²¹, N. Warrack ⁶¹,
 S. Waterhouse ⁹⁸, A.T. Watson ²¹, H. Watson ⁵⁴, M.F. Watson ²¹, E. Watton ^{61,138}, G. Watts ¹⁴²,
 B.M. Waugh ⁹⁹, J.M. Webb ⁵⁶, C. Weber ³⁰, H.A. Weber ¹⁹, M.S. Weber ²⁰, S.M. Weber ^{65a},
 C. Wei ^{64a}, Y. Wei ⁵⁶, A.R. Weidberg ¹³⁰, E.J. Weik ¹²¹, J. Weingarten ⁵¹, C. Weiser ⁵⁶,
 C.J. Wells ⁵⁰, T. Wenaus ³⁰, B. Wendland ⁵¹, T. Wengler ³⁷, N.S. Wenke ¹¹³, N. Wermes ²⁵,
 M. Wessels ^{65a}, A.M. Wharton ⁹⁴, A.S. White ⁶³, A. White ⁸, M.J. White ¹, D. Whiteson ¹⁶³,

L. Wickremasinghe ¹²⁸, W. Wiedenmann ¹⁷⁵, M. Wielers ¹³⁸, C. Wiglesworth ⁴⁴, D.J. Wilbern ¹²⁴, H.G. Wilkens ³⁷, J.J.H. Wilkinson ³³, D.M. Williams ⁴³, H.H. Williams ¹³², S. Williams ³³, S. Willocq ¹⁰⁶, B.J. Wilson ¹⁰⁴, D.J. Wilson ¹⁰⁴, P.J. Windischhofer ⁴¹, F.I. Winkel ³¹, F. Winklmeier ¹²⁷, B.T. Winter ⁵⁶, J.K. Winter ¹⁰⁴, M. Wittgen ¹⁴⁷, M. Wobisch ¹⁰⁰, T. Wojtkowski ⁶², Z. Wolffs ¹¹⁸, J. Wollrath ³⁷, M.W. Wolter ⁸⁹, H. Wolters ^{134a,134c}, M.C. Wong ¹⁴⁰, E.L. Woodward ⁴³, S.D. Worm ⁵⁰, B.K. Wosiek ⁸⁹, K.W. Woźniak ⁸⁹, S. Wozniowski ⁵⁷, K. Wraight ⁶¹, C. Wu ²¹, M. Wu ^{115b}, M. Wu ¹¹⁷, S.L. Wu ¹⁷⁵, X. Wu ⁵⁸, X. Wu ^{64a}, Y. Wu ^{64a}, Z. Wu ⁴, J. Wuerzinger ^{113,ab}, T.R. Wyatt ¹⁰⁴, B.M. Wynne ⁵⁴, S. Xella ⁴⁴, L. Xia ^{115a}, M. Xia ¹⁵, M. Xie ^{64a}, A. Xiong ¹²⁷, J. Xiong ^{18a}, D. Xu ¹⁴, H. Xu ^{64a}, L. Xu ^{64a}, R. Xu ¹³², T. Xu ¹⁰⁹, Y. Xu ¹⁴², Z. Xu ⁵⁴, Z. Xu ^{115a}, B. Yabsley ¹⁵¹, S. Yacoob ^{34a}, Y. Yamaguchi ⁸⁶, E. Yamashita ¹⁵⁷, H. Yamauchi ¹⁶¹, T. Yamazaki ^{18a}, Y. Yamazaki ⁸⁷, S. Yan ⁶¹, Z. Yan ¹⁰⁶, H.J. Yang ^{64c,64d}, H.T. Yang ^{64a}, S. Yang ^{64a}, T. Yang ^{66c}, X. Yang ³⁷, X. Yang ¹⁴, Y. Yang ⁴⁶, Y. Yang ^{64a}, W-M. Yao ^{18a}, H. Ye ⁵⁷, J. Ye ¹⁴, S. Ye ³⁰, X. Ye ^{64a}, Y. Yeh ⁹⁹, I. Yeletsikh ⁴⁰, B. Yeo ^{18b}, M.R. Yexley ⁹⁹, T.P. Yildirim ¹³⁰, P. Yin ⁴³, K. Yorita ¹⁷³, S. Younas ^{28b}, C.J.S. Young ³⁷, C. Young ¹⁴⁷, C. Yu ^{14,115c}, Y. Yu ^{64a}, J. Yuan ^{14,115c}, M. Yuan ¹⁰⁹, R. Yuan ^{64d,64c}, L. Yue ⁹⁹, M. Zaazoua ^{64a}, B. Zabinski ⁸⁹, I. Zahir ^{36a}, E. Zaid ⁵⁴, Z.K. Zak ⁸⁹, T. Zakareishvili ¹⁶⁸, S. Zambito ⁵⁸, J.A. Zamora Saa ^{141d,141b}, J. Zang ¹⁵⁷, D. Zanzi ⁵⁶, R. Zanzottera ^{73a,73b}, O. Zaplatilek ¹³⁶, C. Zeitnitz ¹⁷⁶, H. Zeng ¹⁴, J.C. Zeng ¹⁶⁷, D.T. Zenger Jr ²⁷, O. Zenin ³⁹, T. Ženiš ^{29a}, S. Zenz ⁹⁷, S. Zerradi ^{36a}, D. Zerwas ⁶⁸, M. Zhai ^{14,115c}, D.F. Zhang ¹⁴³, J. Zhang ^{64b}, J. Zhang ⁶, K. Zhang ^{14,115c}, L. Zhang ^{64a}, L. Zhang ^{115a}, P. Zhang ^{14,115c}, R. Zhang ¹⁷⁵, S. Zhang ¹⁰⁹, S. Zhang ⁹², T. Zhang ¹⁵⁷, X. Zhang ^{64c}, Y. Zhang ¹⁴², Y. Zhang ⁹⁹, Y. Zhang ^{115a}, Z. Zhang ^{18a}, Z. Zhang ^{64b}, Z. Zhang ⁶⁸, H. Zhao ¹⁴², T. Zhao ^{64b}, Y. Zhao ¹⁴⁰, Z. Zhao ^{64a}, Z. Zhao ^{64a}, A. Zhemchugov ⁴⁰, J. Zheng ^{115a}, K. Zheng ¹⁶⁷, X. Zheng ^{64a}, Z. Zheng ¹⁴⁷, D. Zhong ¹⁶⁷, B. Zhou ¹⁰⁹, H. Zhou ⁷, N. Zhou ^{64c}, Y. Zhou ¹⁵, Y. Zhou ^{115a}, Y. Zhou ⁷, C.G. Zhu ^{64b}, J. Zhu ¹⁰⁹, X. Zhu ^{64d}, Y. Zhu ^{64c}, Y. Zhu ^{64a}, X. Zhuang ¹⁴, K. Zhukov ⁷⁰, N.I. Zimine ⁴⁰, J. Zinsser ^{65b}, M. Ziolkowski ¹⁴⁵, L. Živković ¹⁶, A. Zoccoli ^{24b,24a}, K. Zoch ⁶³, T.G. Zorbas ¹⁴³, O. Zormpa ⁴⁸, W. Zou ⁴³, L. Zwalinski ³⁷.

¹Department of Physics, University of Adelaide, Adelaide; Australia.

²Department of Physics, University of Alberta, Edmonton AB; Canada.

³(^a)Department of Physics, Ankara University, Ankara; (^b)Division of Physics, TOBB University of Economics and Technology, Ankara; Türkiye.

⁴LAPP, Université Savoie Mont Blanc, CNRS/IN2P3, Annecy; France.

⁵APC, Université Paris Cité, CNRS/IN2P3, Paris; France.

⁶High Energy Physics Division, Argonne National Laboratory, Argonne IL; United States of America.

⁷Department of Physics, University of Arizona, Tucson AZ; United States of America.

⁸Department of Physics, University of Texas at Arlington, Arlington TX; United States of America.

⁹Physics Department, National and Kapodistrian University of Athens, Athens; Greece.

¹⁰Physics Department, National Technical University of Athens, Zografou; Greece.

¹¹Department of Physics, University of Texas at Austin, Austin TX; United States of America.

¹²Institute of Physics, Azerbaijan Academy of Sciences, Baku; Azerbaijan.

¹³Institut de Física d'Altes Energies (IFAE), Barcelona Institute of Science and Technology, Barcelona; Spain.

¹⁴Institute of High Energy Physics, Chinese Academy of Sciences, Beijing; China.

¹⁵Physics Department, Tsinghua University, Beijing; China.

¹⁶Institute of Physics, University of Belgrade, Belgrade; Serbia.

- ¹⁷Department for Physics and Technology, University of Bergen, Bergen; Norway.
- ¹⁸(^a)Physics Division, Lawrence Berkeley National Laboratory, Berkeley CA; (^b)University of California, Berkeley CA; United States of America.
- ¹⁹Institut für Physik, Humboldt Universität zu Berlin, Berlin; Germany.
- ²⁰Albert Einstein Center for Fundamental Physics and Laboratory for High Energy Physics, University of Bern, Bern; Switzerland.
- ²¹School of Physics and Astronomy, University of Birmingham, Birmingham; United Kingdom.
- ²²(^a)Department of Physics, Bogazici University, Istanbul; (^b)Department of Physics Engineering, Gaziantep University, Gaziantep; (^c)Department of Physics, Istanbul University, Istanbul; Türkiye.
- ²³(^a)Facultad de Ciencias y Centro de Investigaciones, Universidad Antonio Nariño, Bogotá; (^b)Departamento de Física, Universidad Nacional de Colombia, Bogotá; Colombia.
- ²⁴(^a)Dipartimento di Fisica e Astronomia A. Righi, Università di Bologna, Bologna; (^b)INFN Sezione di Bologna; Italy.
- ²⁵Physikalisches Institut, Universität Bonn, Bonn; Germany.
- ²⁶Department of Physics, Boston University, Boston MA; United States of America.
- ²⁷Department of Physics, Brandeis University, Waltham MA; United States of America.
- ²⁸(^a)Transilvania University of Brasov, Brasov; (^b)Horia Hulubei National Institute of Physics and Nuclear Engineering, Bucharest; (^c)Department of Physics, Alexandru Ioan Cuza University of Iasi, Iasi; (^d)National Institute for Research and Development of Isotopic and Molecular Technologies, Physics Department, Cluj-Napoca; (^e)National University of Science and Technology Politehnica, Bucharest; (^f)West University in Timisoara, Timisoara; (^g)Faculty of Physics, University of Bucharest, Bucharest; Romania.
- ²⁹(^a)Faculty of Mathematics, Physics and Informatics, Comenius University, Bratislava; (^b)Department of Subnuclear Physics, Institute of Experimental Physics of the Slovak Academy of Sciences, Kosice; Slovak Republic.
- ³⁰Physics Department, Brookhaven National Laboratory, Upton NY; United States of America.
- ³¹Universidad de Buenos Aires, Facultad de Ciencias Exactas y Naturales, Departamento de Física, y CONICET, Instituto de Física de Buenos Aires (IFIBA), Buenos Aires; Argentina.
- ³²California State University, CA; United States of America.
- ³³Cavendish Laboratory, University of Cambridge, Cambridge; United Kingdom.
- ³⁴(^a)Department of Physics, University of Cape Town, Cape Town; (^b)iThemba Labs, Western Cape; (^c)Department of Mechanical Engineering Science, University of Johannesburg, Johannesburg; (^d)National Institute of Physics, University of the Philippines Diliman (Philippines); (^e)University of South Africa, Department of Physics, Pretoria; (^f)University of Zululand, KwaDlangezwa; (^g)School of Physics, University of the Witwatersrand, Johannesburg; South Africa.
- ³⁵Department of Physics, Carleton University, Ottawa ON; Canada.
- ³⁶(^a)Faculté des Sciences Ain Chock, Université Hassan II de Casablanca; (^b)Faculté des Sciences, Université Ibn-Tofail, Kénitra; (^c)Faculté des Sciences Semlalia, Université Cadi Ayyad, LPHEA-Marrakech; (^d)LPMR, Faculté des Sciences, Université Mohamed Premier, Oujda; (^e)Faculté des sciences, Université Mohammed V, Rabat; (^f)Institute of Applied Physics, Mohammed VI Polytechnic University, Ben Guerir; Morocco.
- ³⁷CERN, Geneva; Switzerland.
- ³⁸Affiliated with an institute formerly covered by a cooperation agreement with CERN.
- ³⁹Affiliated with an institute covered by a cooperation agreement with CERN.
- ⁴⁰Affiliated with an international laboratory covered by a cooperation agreement with CERN.
- ⁴¹Enrico Fermi Institute, University of Chicago, Chicago IL; United States of America.
- ⁴²LPC, Université Clermont Auvergne, CNRS/IN2P3, Clermont-Ferrand; France.
- ⁴³Nevis Laboratory, Columbia University, Irvington NY; United States of America.

- ⁴⁴Niels Bohr Institute, University of Copenhagen, Copenhagen; Denmark.
- ⁴⁵(^a)Dipartimento di Fisica, Università della Calabria, Rende; (^b)INFN Gruppo Collegato di Cosenza, Laboratori Nazionali di Frascati; Italy.
- ⁴⁶Physics Department, Southern Methodist University, Dallas TX; United States of America.
- ⁴⁷Physics Department, University of Texas at Dallas, Richardson TX; United States of America.
- ⁴⁸National Centre for Scientific Research "Demokritos", Agia Paraskevi; Greece.
- ⁴⁹(^a)Department of Physics, Stockholm University; (^b)Oskar Klein Centre, Stockholm; Sweden.
- ⁵⁰Deutsches Elektronen-Synchrotron DESY, Hamburg and Zeuthen; Germany.
- ⁵¹Fakultät Physik, Technische Universität Dortmund, Dortmund; Germany.
- ⁵²Institut für Kern- und Teilchenphysik, Technische Universität Dresden, Dresden; Germany.
- ⁵³Department of Physics, Duke University, Durham NC; United States of America.
- ⁵⁴SUPA - School of Physics and Astronomy, University of Edinburgh, Edinburgh; United Kingdom.
- ⁵⁵INFN e Laboratori Nazionali di Frascati, Frascati; Italy.
- ⁵⁶Physikalisches Institut, Albert-Ludwigs-Universität Freiburg, Freiburg; Germany.
- ⁵⁷II. Physikalisches Institut, Georg-August-Universität Göttingen, Göttingen; Germany.
- ⁵⁸Département de Physique Nucléaire et Corpusculaire, Université de Genève, Genève; Switzerland.
- ⁵⁹(^a)Dipartimento di Fisica, Università di Genova, Genova; (^b)INFN Sezione di Genova; Italy.
- ⁶⁰II. Physikalisches Institut, Justus-Liebig-Universität Giessen, Giessen; Germany.
- ⁶¹SUPA - School of Physics and Astronomy, University of Glasgow, Glasgow; United Kingdom.
- ⁶²LPSC, Université Grenoble Alpes, CNRS/IN2P3, Grenoble INP, Grenoble; France.
- ⁶³Laboratory for Particle Physics and Cosmology, Harvard University, Cambridge MA; United States of America.
- ⁶⁴(^a)Department of Modern Physics and State Key Laboratory of Particle Detection and Electronics, University of Science and Technology of China, Hefei; (^b)Institute of Frontier and Interdisciplinary Science and Key Laboratory of Particle Physics and Particle Irradiation (MOE), Shandong University, Qingdao; (^c)School of Physics and Astronomy, Shanghai Jiao Tong University, Key Laboratory for Particle Astrophysics and Cosmology (MOE), SKLPPC, Shanghai; (^d)Tsung-Dao Lee Institute, Shanghai; (^e)School of Physics and Microelectronics, Zhengzhou University; China.
- ⁶⁵(^a)Kirchhoff-Institut für Physik, Ruprecht-Karls-Universität Heidelberg, Heidelberg; (^b)Physikalisches Institut, Ruprecht-Karls-Universität Heidelberg, Heidelberg; Germany.
- ⁶⁶(^a)Department of Physics, Chinese University of Hong Kong, Shatin, N.T., Hong Kong; (^b)Department of Physics, University of Hong Kong, Hong Kong; (^c)Department of Physics and Institute for Advanced Study, Hong Kong University of Science and Technology, Clear Water Bay, Kowloon, Hong Kong; China.
- ⁶⁷Department of Physics, National Tsing Hua University, Hsinchu; Taiwan.
- ⁶⁸IJCLab, Université Paris-Saclay, CNRS/IN2P3, 91405, Orsay; France.
- ⁶⁹Centro Nacional de Microelectrónica (IMB-CNM-CSIC), Barcelona; Spain.
- ⁷⁰Department of Physics, Indiana University, Bloomington IN; United States of America.
- ⁷¹(^a)INFN Gruppo Collegato di Udine, Sezione di Trieste, Udine; (^b)ICTP, Trieste; (^c)Dipartimento Politecnico di Ingegneria e Architettura, Università di Udine, Udine; Italy.
- ⁷²(^a)INFN Sezione di Lecce; (^b)Dipartimento di Matematica e Fisica, Università del Salento, Lecce; Italy.
- ⁷³(^a)INFN Sezione di Milano; (^b)Dipartimento di Fisica, Università di Milano, Milano; Italy.
- ⁷⁴(^a)INFN Sezione di Napoli; (^b)Dipartimento di Fisica, Università di Napoli, Napoli; Italy.
- ⁷⁵(^a)INFN Sezione di Pavia; (^b)Dipartimento di Fisica, Università di Pavia, Pavia; Italy.
- ⁷⁶(^a)INFN Sezione di Pisa; (^b)Dipartimento di Fisica E. Fermi, Università di Pisa, Pisa; Italy.
- ⁷⁷(^a)INFN Sezione di Roma; (^b)Dipartimento di Fisica, Sapienza Università di Roma, Roma; Italy.
- ⁷⁸(^a)INFN Sezione di Roma Tor Vergata; (^b)Dipartimento di Fisica, Università di Roma Tor Vergata, Roma; Italy.

- ^{79(a)}INFN Sezione di Roma Tre;^(b)Dipartimento di Matematica e Fisica, Università Roma Tre, Roma; Italy.
- ^{80(a)}INFN-TIFPA;^(b)Università degli Studi di Trento, Trento; Italy.
- ⁸¹Universität Innsbruck, Department of Astro and Particle Physics, Innsbruck; Austria.
- ⁸²University of Iowa, Iowa City IA; United States of America.
- ⁸³Department of Physics and Astronomy, Iowa State University, Ames IA; United States of America.
- ⁸⁴Istinye University, Sariyer, Istanbul; Türkiye.
- ^{85(a)}Departamento de Engenharia Elétrica, Universidade Federal de Juiz de Fora (UFJF), Juiz de Fora;^(b)Universidade Federal do Rio De Janeiro COPPE/EE/IF, Rio de Janeiro;^(c)Instituto de Física, Universidade de São Paulo, São Paulo;^(d)Rio de Janeiro State University, Rio de Janeiro;^(e)Federal University of Bahia, Bahia; Brazil.
- ⁸⁶KEK, High Energy Accelerator Research Organization, Tsukuba; Japan.
- ⁸⁷Graduate School of Science, Kobe University, Kobe; Japan.
- ^{88(a)}AGH University of Krakow, Faculty of Physics and Applied Computer Science, Krakow;^(b)Marian Smoluchowski Institute of Physics, Jagiellonian University, Krakow; Poland.
- ⁸⁹Institute of Nuclear Physics Polish Academy of Sciences, Krakow; Poland.
- ⁹⁰Faculty of Science, Kyoto University, Kyoto; Japan.
- ⁹¹Research Center for Advanced Particle Physics and Department of Physics, Kyushu University, Fukuoka ; Japan.
- ⁹²L2IT, Université de Toulouse, CNRS/IN2P3, UPS, Toulouse; France.
- ⁹³Instituto de Física La Plata, Universidad Nacional de La Plata and CONICET, La Plata; Argentina.
- ⁹⁴Physics Department, Lancaster University, Lancaster; United Kingdom.
- ⁹⁵Oliver Lodge Laboratory, University of Liverpool, Liverpool; United Kingdom.
- ⁹⁶Department of Experimental Particle Physics, Jožef Stefan Institute and Department of Physics, University of Ljubljana, Ljubljana; Slovenia.
- ⁹⁷School of Physics and Astronomy, Queen Mary University of London, London; United Kingdom.
- ⁹⁸Department of Physics, Royal Holloway University of London, Egham; United Kingdom.
- ⁹⁹Department of Physics and Astronomy, University College London, London; United Kingdom.
- ¹⁰⁰Louisiana Tech University, Ruston LA; United States of America.
- ¹⁰¹Fysiska institutionen, Lunds universitet, Lund; Sweden.
- ¹⁰²Departamento de Física Teórica C-15 and CIAFF, Universidad Autónoma de Madrid, Madrid; Spain.
- ¹⁰³Institut für Physik, Universität Mainz, Mainz; Germany.
- ¹⁰⁴School of Physics and Astronomy, University of Manchester, Manchester; United Kingdom.
- ¹⁰⁵CPPM, Aix-Marseille Université, CNRS/IN2P3, Marseille; France.
- ¹⁰⁶Department of Physics, University of Massachusetts, Amherst MA; United States of America.
- ¹⁰⁷Department of Physics, McGill University, Montreal QC; Canada.
- ¹⁰⁸School of Physics, University of Melbourne, Victoria; Australia.
- ¹⁰⁹Department of Physics, University of Michigan, Ann Arbor MI; United States of America.
- ¹¹⁰Department of Physics and Astronomy, Michigan State University, East Lansing MI; United States of America.
- ¹¹¹Group of Particle Physics, University of Montreal, Montreal QC; Canada.
- ¹¹²Fakultät für Physik, Ludwig-Maximilians-Universität München, München; Germany.
- ¹¹³Max-Planck-Institut für Physik (Werner-Heisenberg-Institut), München; Germany.
- ¹¹⁴Graduate School of Science and Kobayashi-Maskawa Institute, Nagoya University, Nagoya; Japan.
- ^{115(a)}Department of Physics, Nanjing University, Nanjing;^(b)School of Science, Shenzhen Campus of Sun Yat-sen University;^(c)University of Chinese Academy of Science (UCAS), Beijing; China.
- ¹¹⁶Department of Physics and Astronomy, University of New Mexico, Albuquerque NM; United States of

America.

¹¹⁷Institute for Mathematics, Astrophysics and Particle Physics, Radboud University/Nikhef, Nijmegen; Netherlands.

¹¹⁸Nikhef National Institute for Subatomic Physics and University of Amsterdam, Amsterdam; Netherlands.

¹¹⁹Department of Physics, Northern Illinois University, DeKalb IL; United States of America.

¹²⁰(^a)New York University Abu Dhabi, Abu Dhabi;(^b)United Arab Emirates University, Al Ain; United Arab Emirates.

¹²¹Department of Physics, New York University, New York NY; United States of America.

¹²²Ochanomizu University, Otsuka, Bunkyo-ku, Tokyo; Japan.

¹²³Ohio State University, Columbus OH; United States of America.

¹²⁴Homer L. Dodge Department of Physics and Astronomy, University of Oklahoma, Norman OK; United States of America.

¹²⁵Department of Physics, Oklahoma State University, Stillwater OK; United States of America.

¹²⁶Palacký University, Joint Laboratory of Optics, Olomouc; Czech Republic.

¹²⁷Institute for Fundamental Science, University of Oregon, Eugene, OR; United States of America.

¹²⁸Graduate School of Science, Osaka University, Osaka; Japan.

¹²⁹Department of Physics, University of Oslo, Oslo; Norway.

¹³⁰Department of Physics, Oxford University, Oxford; United Kingdom.

¹³¹LPNHE, Sorbonne Université, Université Paris Cité, CNRS/IN2P3, Paris; France.

¹³²Department of Physics, University of Pennsylvania, Philadelphia PA; United States of America.

¹³³Department of Physics and Astronomy, University of Pittsburgh, Pittsburgh PA; United States of America.

¹³⁴(^a)Laboratório de Instrumentação e Física Experimental de Partículas - LIP, Lisboa;(^b)Departamento de Física, Faculdade de Ciências, Universidade de Lisboa, Lisboa;(^c)Departamento de Física, Universidade de Coimbra, Coimbra;(^d)Centro de Física Nuclear da Universidade de Lisboa, Lisboa;(^e)Departamento de Física, Universidade do Minho, Braga;(^f)Departamento de Física Teórica y del Cosmos, Universidad de Granada, Granada (Spain);(^g)Departamento de Física, Instituto Superior Técnico, Universidade de Lisboa, Lisboa; Portugal.

¹³⁵Institute of Physics of the Czech Academy of Sciences, Prague; Czech Republic.

¹³⁶Czech Technical University in Prague, Prague; Czech Republic.

¹³⁷Charles University, Faculty of Mathematics and Physics, Prague; Czech Republic.

¹³⁸Particle Physics Department, Rutherford Appleton Laboratory, Didcot; United Kingdom.

¹³⁹IRFU, CEA, Université Paris-Saclay, Gif-sur-Yvette; France.

¹⁴⁰Santa Cruz Institute for Particle Physics, University of California Santa Cruz, Santa Cruz CA; United States of America.

¹⁴¹(^a)Departamento de Física, Pontificia Universidad Católica de Chile, Santiago;(^b)Millennium Institute for Subatomic physics at high energy frontier (SAPHIR), Santiago;(^c)Instituto de Investigación Multidisciplinario en Ciencia y Tecnología, y Departamento de Física, Universidad de La Serena;(^d)Universidad Andres Bello, Department of Physics, Santiago;(^e)Instituto de Alta Investigación, Universidad de Tarapacá, Arica;(^f)Departamento de Física, Universidad Técnica Federico Santa María, Valparaíso; Chile.

¹⁴²Department of Physics, University of Washington, Seattle WA; United States of America.

¹⁴³Department of Physics and Astronomy, University of Sheffield, Sheffield; United Kingdom.

¹⁴⁴Department of Physics, Shinshu University, Nagano; Japan.

¹⁴⁵Department Physik, Universität Siegen, Siegen; Germany.

¹⁴⁶Department of Physics, Simon Fraser University, Burnaby BC; Canada.

- ¹⁴⁷SLAC National Accelerator Laboratory, Stanford CA; United States of America.
- ¹⁴⁸Department of Physics, Royal Institute of Technology, Stockholm; Sweden.
- ¹⁴⁹Departments of Physics and Astronomy, Stony Brook University, Stony Brook NY; United States of America.
- ¹⁵⁰Department of Physics and Astronomy, University of Sussex, Brighton; United Kingdom.
- ¹⁵¹School of Physics, University of Sydney, Sydney; Australia.
- ¹⁵²Institute of Physics, Academia Sinica, Taipei; Taiwan.
- ¹⁵³^(a)E. Andronikashvili Institute of Physics, Iv. Javakhishvili Tbilisi State University, Tbilisi; ^(b)High Energy Physics Institute, Tbilisi State University, Tbilisi; ^(c)University of Georgia, Tbilisi; Georgia.
- ¹⁵⁴Department of Physics, Technion, Israel Institute of Technology, Haifa; Israel.
- ¹⁵⁵Raymond and Beverly Sackler School of Physics and Astronomy, Tel Aviv University, Tel Aviv; Israel.
- ¹⁵⁶Department of Physics, Aristotle University of Thessaloniki, Thessaloniki; Greece.
- ¹⁵⁷International Center for Elementary Particle Physics and Department of Physics, University of Tokyo, Tokyo; Japan.
- ¹⁵⁸Department of Physics, Tokyo Institute of Technology, Tokyo; Japan.
- ¹⁵⁹Department of Physics, University of Toronto, Toronto ON; Canada.
- ¹⁶⁰^(a)TRIUMF, Vancouver BC; ^(b)Department of Physics and Astronomy, York University, Toronto ON; Canada.
- ¹⁶¹Division of Physics and Tomonaga Center for the History of the Universe, Faculty of Pure and Applied Sciences, University of Tsukuba, Tsukuba; Japan.
- ¹⁶²Department of Physics and Astronomy, Tufts University, Medford MA; United States of America.
- ¹⁶³Department of Physics and Astronomy, University of California Irvine, Irvine CA; United States of America.
- ¹⁶⁴University of West Attica, Athens; Greece.
- ¹⁶⁵University of Sharjah, Sharjah; United Arab Emirates.
- ¹⁶⁶Department of Physics and Astronomy, University of Uppsala, Uppsala; Sweden.
- ¹⁶⁷Department of Physics, University of Illinois, Urbana IL; United States of America.
- ¹⁶⁸Instituto de Física Corpuscular (IFIC), Centro Mixto Universidad de Valencia - CSIC, Valencia; Spain.
- ¹⁶⁹Department of Physics, University of British Columbia, Vancouver BC; Canada.
- ¹⁷⁰Department of Physics and Astronomy, University of Victoria, Victoria BC; Canada.
- ¹⁷¹Fakultät für Physik und Astronomie, Julius-Maximilians-Universität Würzburg, Würzburg; Germany.
- ¹⁷²Department of Physics, University of Warwick, Coventry; United Kingdom.
- ¹⁷³Waseda University, Tokyo; Japan.
- ¹⁷⁴Department of Particle Physics and Astrophysics, Weizmann Institute of Science, Rehovot; Israel.
- ¹⁷⁵Department of Physics, University of Wisconsin, Madison WI; United States of America.
- ¹⁷⁶Fakultät für Mathematik und Naturwissenschaften, Fachgruppe Physik, Bergische Universität Wuppertal, Wuppertal; Germany.
- ¹⁷⁷Department of Physics, Yale University, New Haven CT; United States of America.
- ¹⁷⁸Yerevan Physics Institute, Yerevan; Armenia.
- ^a Also Affiliated with an institute covered by a cooperation agreement with CERN.
- ^b Also at An-Najah National University, Nablus; Palestine.
- ^c Also at Borough of Manhattan Community College, City University of New York, New York NY; United States of America.
- ^d Also at Center for Interdisciplinary Research and Innovation (CIRI-AUTH), Thessaloniki; Greece.
- ^e Also at CERN, Geneva; Switzerland.
- ^f Also at CMD-AC UNEC Research Center, Azerbaijan State University of Economics (UNEC); Azerbaijan.

- ^g Also at Département de Physique Nucléaire et Corpusculaire, Université de Genève, Genève; Switzerland.
- ^h Also at Departament de Física de la Universitat Autònoma de Barcelona, Barcelona; Spain.
- ⁱ Also at Department of Financial and Management Engineering, University of the Aegean, Chios; Greece.
- ^j Also at Department of Physics, California State University, Sacramento; United States of America.
- ^k Also at Department of Physics, King's College London, London; United Kingdom.
- ^l Also at Department of Physics, Stanford University, Stanford CA; United States of America.
- ^m Also at Department of Physics, Stellenbosch University; South Africa.
- ⁿ Also at Department of Physics, University of Fribourg, Fribourg; Switzerland.
- ^o Also at Department of Physics, University of Thessaly; Greece.
- ^p Also at Department of Physics, Westmont College, Santa Barbara; United States of America.
- ^q Also at Faculty of Physics, Sofia University, 'St. Kliment Ohridski', Sofia; Bulgaria.
- ^r Also at Hellenic Open University, Patras; Greece.
- ^s Also at Henan University; China.
- ^t Also at Imam Mohammad Ibn Saud Islamic University; Saudi Arabia.
- ^u Also at Institutio Catalana de Recerca i Estudis Avancats, ICREA, Barcelona; Spain.
- ^v Also at Institut für Experimentalphysik, Universität Hamburg, Hamburg; Germany.
- ^w Also at Institute for Nuclear Research and Nuclear Energy (INRNE) of the Bulgarian Academy of Sciences, Sofia; Bulgaria.
- ^x Also at Institute of Applied Physics, Mohammed VI Polytechnic University, Ben Guerir; Morocco.
- ^y Also at Institute of Particle Physics (IPP); Canada.
- ^z Also at Institute of Physics, Azerbaijan Academy of Sciences, Baku; Azerbaijan.
- ^{aa} Also at National Institute of Physics, University of the Philippines Diliman (Philippines); Philippines.
- ^{ab} Also at Technical University of Munich, Munich; Germany.
- ^{ac} Also at The Collaborative Innovation Center of Quantum Matter (CICQM), Beijing; China.
- ^{ad} Also at TRIUMF, Vancouver BC; Canada.
- ^{ae} Also at Università di Napoli Parthenope, Napoli; Italy.
- ^{af} Also at University of Colorado Boulder, Department of Physics, Colorado; United States of America.
- ^{ag} Also at Washington College, Chestertown, MD; United States of America.
- ^{ah} Also at Yeditepe University, Physics Department, Istanbul; Türkiye.
- * Deceased